ALFRED-WEGENER-INSTITUT
HELMHOLTZ-ZENTRUM FÜR POLAR- UND MEERESFORSCHUNG

695
2016

Berichte
zur Polar- und Meeresforschung

Reports on Polar and Marine Research

The Expedition PS93.1

of the Research Vessel POLARSTERN to the Greenland Sea and the Fram Strait in 2015

Edited by

Ruediger Stein

with contributions of the participants

HELMHOLTZ GEMEINSCHAFT

Die Berichte zur Polar- und Meeresforschung werden vom Alfred-Wegener-Institut, Helmholtz-Zentrum für Polar- und Meeresforschung (AWI) in Bremerhaven, Deutschland, in Fortsetzung der vormaligen Berichte zur Polarforschung herausgegeben. Sie erscheinen in unregelmäßiger Abfolge.

Die Berichte zur Polar- und Meeresforschung enthalten Darstellungen und Ergebnisse der vom AWI selbst oder mit seiner Unterstützung durchgeführten Forschungsarbeiten in den Polargebieten und in den Meeren.

Die Publikationen umfassen Expeditionsberichte der vom AWI betriebenen Schiffe, Flugzeuge und Stationen, Forschungsergebnisse (inkl. Dissertationen) des Instituts und des Archivs für deutsche Polarforschung, sowie Abstracts und Proceedings von nationalen und internationalen Tagungen und Workshops des AWI.

Die Beiträge geben nicht notwendigerweise die Auffassung des AWI wider.

Herausgeber
Dr. Horst Bornemann

Redaktionelle Bearbeitung und Layout
Birgit Reimann

Alfred-Wegener-Institut
Helmholtz-Zentrum für Polar- und Meeresforschung
Am Handeshafen 12
27570 Bremerhaven
Germany

www.awi.de
www.reports.awi.de

The Reports on Polar and Marine Research are issued by the Alfred Wegener Institute, Helmholtz Centre for Polar and Marine Research (AWI) in Bremerhaven, Germany, succeeding the former Reports on Polar Research. They are published at irregular intervals.

The Reports on Polar and Marine Research contain presentations and results of research activities in polar regions and in the seas either carried out by the AWI or with its support.

Publications comprise expedition reports of the ships, aircrafts, and stations operated by the AWI, research results (incl. dissertations) of the Institute and the Archiv für deutsche Polarforschung, as well as abstracts and proceedings of national and international conferences and workshops of the AWI.

The papers contained in the Reports do not necessarily reflect the opinion of the AWI.

Editor
Dr. Horst Bornemann

Editorial editing and layout
Birgit Reimann

Alfred-Wegener-Institut
Helmholtz-Zentrum für Polar- und Meeresforschung
Am Handeshafen 12
27570 Bremerhaven
Germany

www.awi.de
www.reports.awi.de

Titel: Station PS93/006-1 (Framstrasse, 79°12.22'N, 04°40.13'O, Wassertiefe 1.593 m):Ein erfolgreich gefahrenes Kastenlot mit intakter „Zipfelmütze" am Ende des Kastens kommt an Deck (Foto R. Stein/AWI).

Cover: Station PS93/006-1 (Fram Strait, 79°12.22'N, 04°40.13'E, water depth 1,593 m): A successful kastenlot with the core catcher displaying a perfect "zipfelmütze" comes on deck (Photo R. Stein/AWI).

The Expedition PS93.1 of the Research Vessel POLARSTERN to the Greenland Sea and the Fram Strait in 2015

Edited by

Ruediger Stein

with contributions of the participants

Please cite or link this publication using the identifiers
hdl:10013/epic.46907 or http://hdl.handle.net/10013/epic.46907 and
doi:10.2312/BzPM_0695_2016 or http://doi.org/10.2312/BzPM_0695_2016

ISSN 1866-3192

PS93.1

29 June 2015 – 18 July 2015

Longyearbyen - Tromsø

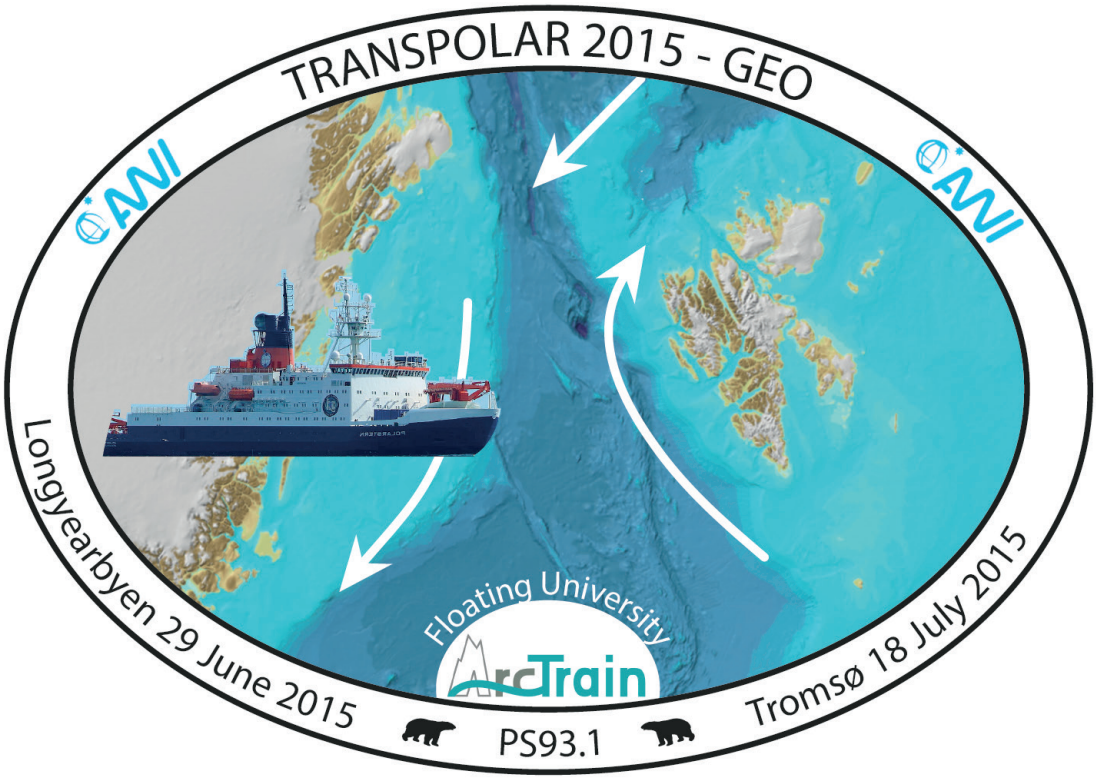

Chief Scientist
Ruediger Stein

Coordinator
Rainer Knust

Contents

1. ZUSAMMENFASSUNG UND FAHRTVERLAUF

Ruediger Stein (AWI)

Grant-No. AWI-PS93.1_01

Zusammenfassung

Geographisches Zielgebiet der Expedition war der nördlichste Nordatlantik zwischen NE Grönland und W Svalbard (Abb. 1.1). Das wissenschaftliche Ziel des marin-geologischen Schwerpunktprogramms ist die Rekonstruktion vergangener Klimaverhältnisse, wobei die letzte Warmzeit (Eem, ca. 130-120000 Jahre v. Heute) und das Holozän (die letzten 12000) von besonderem Interesse sind. Für die Untersuchungen sollten lange Sedimentkerne aus Gebieten mit potenziell hohen Sedimentakkumulationsraten gewonnen werden. Neben dem Geologie-Programm wurden in begrenztem Rahmen ozeanographische, biologische und atmosphären-chemische Untersuchungen durchgeführt sowie eine “Floating University” abgehalten.

Zusammenfassend lässt sich festhalten:

- Umfangreiche geologische Beprobungen (4 x Kastenlot, 22 x Schwerelot, 29 x Großkastengreifer, 11 x Multicorer) wurden in der Framstraße, der Grönlandsee und auf dem ostgrönländischen Schelf durchgeführt (Abb. 1.2). Das gewonnene, z.T. einmalige Kernmaterial wird uns in die Lage versetzen, detaillierte Rekonstruktionen der Vereisungsgeschichte Grönlands, der Meereisvariabilität und der Wassermassenzirkulation im Holozän, aber auch älteren Zeitabschnitten (z.B. Eem) zu machen.

- Während Transitstrecken und der gesamten Arbeiten in den Untersuchungsgebieten wurden durchgehend Hydrosweep- und Parasound-Daten aufgezeichnet. Insgesamt konnten so ca. 4.000 km neue Hydrosweep- und Parasound-Profile gewonnen werden, die Grundlage für die präzise Auswahl der Kernstationen waren.

- Neben dem geowissenschaftlichen Schwerpunktprogramm erfolgten umfangreiche Untersuchungen zur Ozeanographie (Bergen bzw. Aussetzen von fünf Verankerungsketten, Aussetzen von zwei Gliedern und Messprofile mit der „Underway CTD“) (Abb. 1.2), Biologie (Gewinnung von 123 Phytoplanktonproben, die am AWI weiter vereinzelt und analysiert werden, um die Biodiversität und Biogeographie von arktischen Phytoplanktonarten zu erfassen) und Atmosphärenchemie (kontinuierliche und automatische Messungen der Isotopenzusammensetzung von Wasserdampf über dem Arktischen Ozean).

- Ein weiterer besonderer Aspekt war die „Floating University ArcTrain“, für die 20 Studenten/innen aus Kanada und Deutschland zu Ausbildungszwecken mit an Bord waren. Die „ArcTrainler“, die aus ganz unterschiedlichen Fachrichtungen kamen (Biologie, Geologie, Ozeanographie, Modellierung), waren für alle unsere Arbeitsgruppen eine enorme Hilfe und Bereicherung. Mit großem Einsatz und Interesse und zu jeder Tag- und Nachtzeit waren sie einsatzbereit und voll in das Forschungsprogramm mit integriert.

Fahrtverlauf

Leinen los! *Polarstern* lief am 29.06.2015 gegen Mittag aus Longyearbyen aus. An Bord waren 44 Besatzungsmitglieder sowie 50 Wissenschaftler, Hubschrauberpiloten und Techniker aus 12 Ländern. Erstes Ziel waren Stationen, an denen in der zentralen Framstraße Verankerungsketten aufgrund der extremen Eisverhältnisse und fehlender Schiffszeit im Sommer 2014 nicht geborgen werden konnten (Abb. 1.2). Die erste Station erreichten wir am 30.06.15. Trotz intensiver Bemühungen konnte die Verankerungskette nicht gefunden werden. Dafür wurde an selbiger Stelle eine neue Verankerung ausgebracht. An weiteren Stationen, nur 12-20 Meilen weiter nach Westen, war die Suche erfolgreicher, so dass gegen Abend drei der vier für den Tag geplanten Verankerungsketten geborgen werden konnten. Gegen Mitternacht wurde die erste Geostation auf dem Vestnesa Rückens (Abb. 1.2; Station PS93/006; 79°12.2´N, 04°40.0'W; Wassertiefe 1,570 m) gefahren und dabei erfolgreich ein 7.5 m langer Kastenlotkern gezogen.

Auf erstes Meereis trafen wir am 01.07.15 um 03:00 Uhr bei 79°14'N, 04°30'O, vier Stunden später hatten wir einen ersten direkten Eiskontakt (Abb. 1.3). Profilfahrten mit Hydrosweep und Parasound Richtung Westen folgten, am 03.07.15 erreichten wir den ostgrönländischen Schelf. Nach Parasound-Daten, die während der letztjährigen *Polarstern*-Expedition PS87 aufgezeichnet wurden, wählten wir Kernstationen aus, an denen eventuell alte (präquartäre) Sediment- oder Gesteinspakete beprobt werden könnten. Die vier Schwereloteinsätze blieben allerdings leider ohne Erfolg. Am 04.07.15 erreichten wir die Polynya, ein großes fast eisfreies Gebiet, an der Nordostspitze Grönlands (Abb. 1.3), wo gezielt mehrere Stationen abgearbeitet und geologische, biologische und ozeanographische Beprobungen bzw. Arbeiten durchgeführt wurden.

Am 05.07.15 näherten wir uns dem Nordrand der Polynya, unserem nördlichsten Arbeitsgebiet. Hier trafen wir auf „alte Bekannte": Yngve Kristoffersen und Audun Tholfsen, zwei norwegische Kollegen, die wir mit ihrem Hovercraft *Sabvabaa* und Eiscamp am 30.08.14 während der *Polarstern* PS87-Expedition zurückgelassen hatten und die dann in den 10 Folgemonate fast quer durch den gesamten Arktischen Ozean gedriftet sind (Abb. 1.4). Nach intensiver Diskussion zwischen allen Beteiligten und Rücksprache mit der *Polarstern*-Schiffskoordination in Bremerhaven beschlossen wir, alle Gefahrgüter des Eiscamps zu bergen und an Bord von *Polarstern* zu bringen. Das FRAM-2014/15 Eisdrift-Experiment wurde dann von Yngve Kristoffersen allein weitergeführt (und am 18.08.15 erfolgreich beendet; siehe Abb. 1.4), während sich Audun Tholfsen an Bord von *Polarstern* begab.

Vom 07. - 09.07.15 bestimmten intensive geologische Beprobungen mittels Kastenlot, Schwerelot, Großkastengreifer und Multicorer entlang des ostgrönländischen Kontinentalrands zwischen 81 und 79°N die Aktivitäten an Bord von *Polarstern* (Abb. 1.2). Der 10.07.15 stand dann wieder ganz im Zeichen der Ozeanographie, d.h., es konnten weitere Verankerungsketten in der zentralen Framstraße geborgen bzw. ausgebracht werden (Abb. 1.2; Stationen PS93/033 bis /035). Auf dem Weg zu den Verankerungen und auf dem anschließenden Weg zurück Richtung Westen ins Meereis wurde erfolgreich die „Underway CTD" eingesetzt, um kontinuierliche Temperatur- und Salzgehaltdaten entlang von O-W-Schnitten zu gewinnen.

Parasound- und Hydrosweep-Profilfahrten auf dem ostgrönländischen Schelf ermöglichten das Auffinden von Kernstationen für eine Beprobung ungestörter mächtiger Abfolgen von jungen (holozänen) Sedimenten. Mit diesen am 12.07.15 durchgeführten geologischen Beprobungen wurde unser Arbeitsprogamm auf dem eisbedeckten NO-grönländischen Schelf erfolgreich abgeschlossen.

In der Nacht vom 13./14.07.15 verließen wir endgültig das Eis. Es folgten ein paar letzte biologische, ozeanographische und geologische Stationen, an denen alle Geräte noch einmal

erfolgreich zum Einsatz kamen. Unter anderem wurden bei diesen Aktivitäten am 14.07.15 auch zwei „Sea Glider“, von Bremerhaven aus ferngesteuerte Messinstrumente zur Bestimmung von Temperatur, Druck und Salzgehalt, ausgesetzt. Der letzte Stationstag (15.07.15) wurde dann mit einer multidisziplinären Beprobungsaktion (Abb. 1.2, Station PS93/046) und einer 12-stündigen Hydrosweep-Profilfahrt abgeschlossen.

Am 18.07. gegen 10:30 Uhr lief *Polarstern* wieder in Tromsø ein.

Abschließend möchten wir uns ganz herzlich bei Kapitän Wunderlich und seiner Besatzung für die große Unterstützung und Hilfsbereitschaft in allen Situationen bedanken.

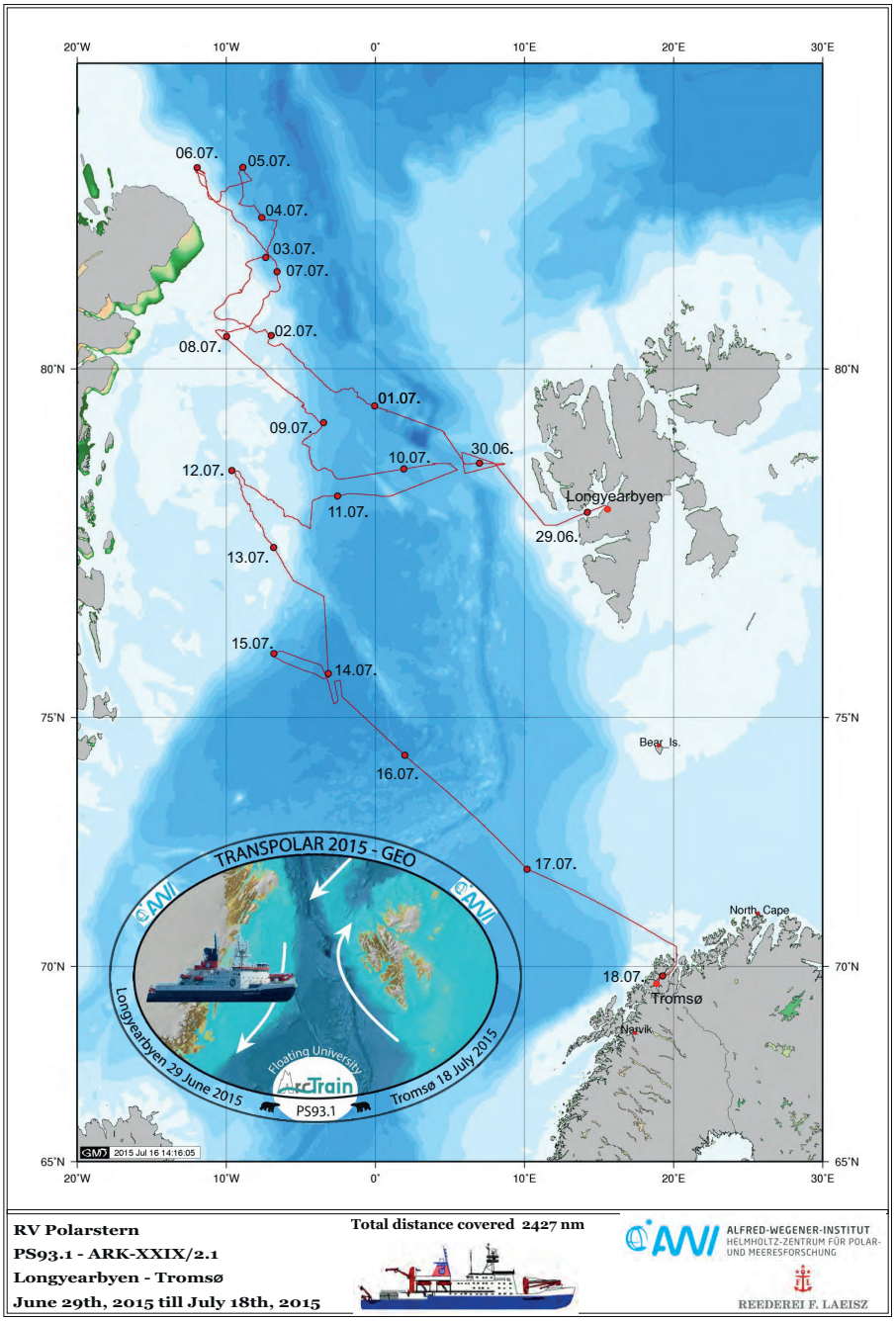

Abb. 1.1: Fahrtroute der PS93.1-Expedition
Fig. 1.1: Cruise track of Expedition PS93.1

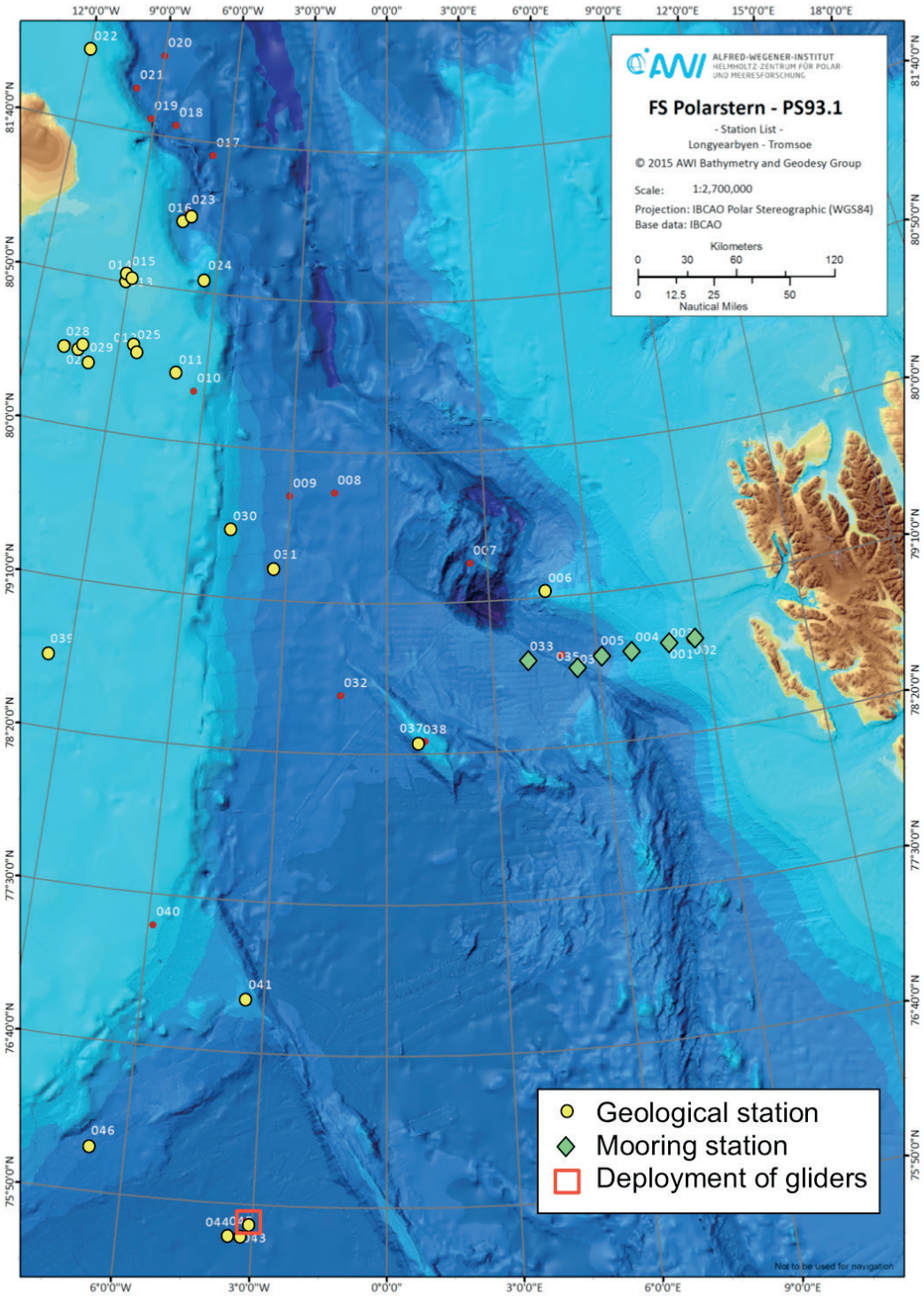

Abb. 1.2: Stationen der PS93.1-Expedition. Geologie-Stationen und Ozeanographie-Stationen (Einholen bzw. Aussetzen von Verankerungsketten; Aussetzen der „Sea glider“) sind angegeben. Weiterhin wurden an zahlreichen Stationen biologische und weitere ozeanographische Arbeiten durchgeführt, die hier nicht weiter gekennzeichnet worden sind (siehe Kapitel 4 und 5).

Fig. 1.2: Stations of Expedition PS93.1. Geological stations, moorings stations and the area of deployment of the sea gliders are indicated. In addition, biological and oceanographic stations were carried-out that are not indicated here (For details and station numbers see Chapters 4 and 5).

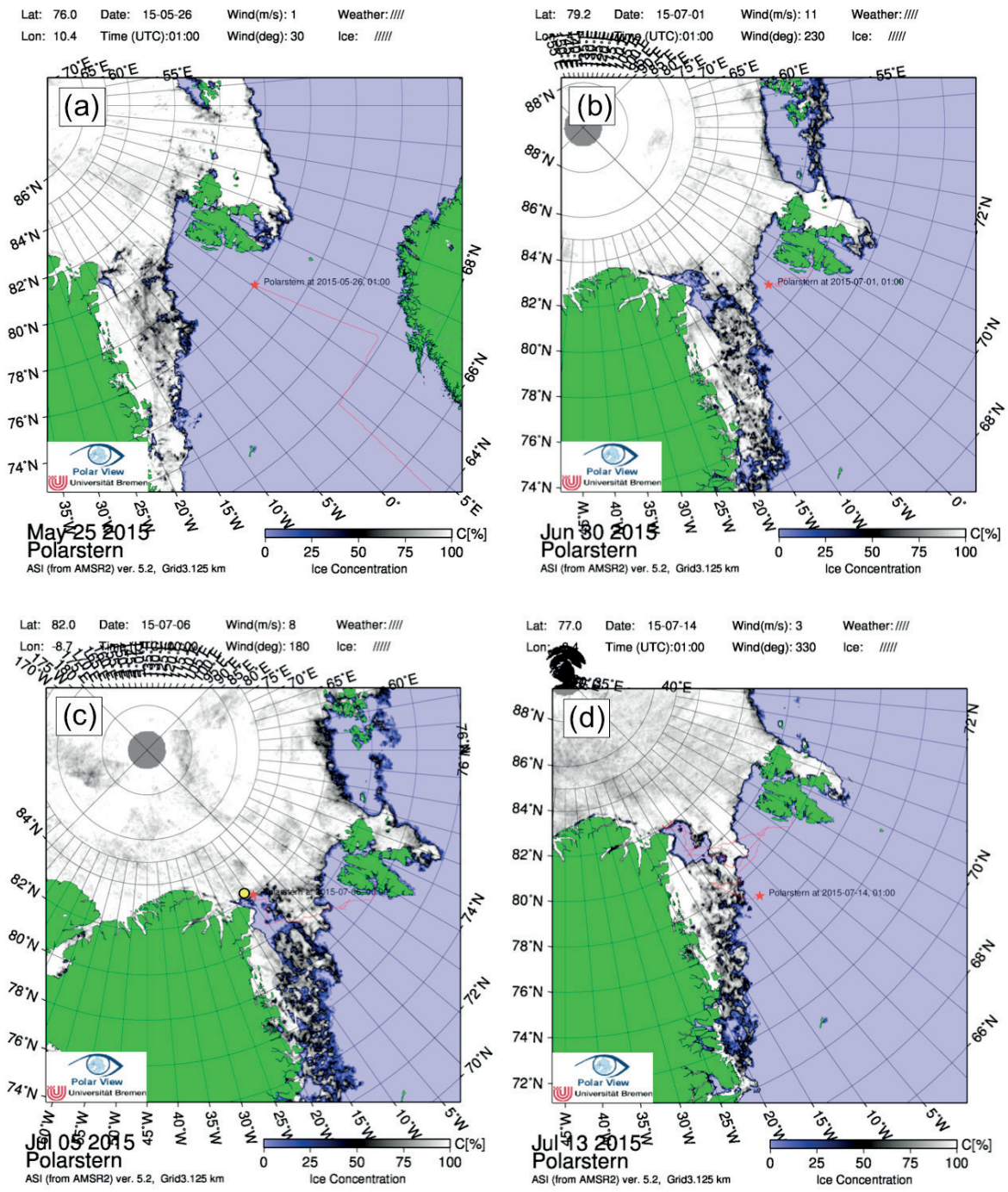

Abb. 1.3: Meereisverbreitung am (a) 25.05.15, (b) 30.06.15, (c) 05.07.15 und (d) 13.07.15. Die Position von Polarstern (roter Stern) am jeweiligen Tag ist eingezeichnet. Der gelbe Kreis in (c) zeigt die Position der FRAM-2014/15 Eis-Drift-Station.

Fig. 1.3: Sea-ice concentration on (a) 25 May, (b) 30 June, (c) 05 July, and (d) 13 July 2015. The position of Polarstern (red star) at the specific day is indicated. Yellow circle in (c) indiactes position of the FRAM-2014/15 Ice Drift Station.

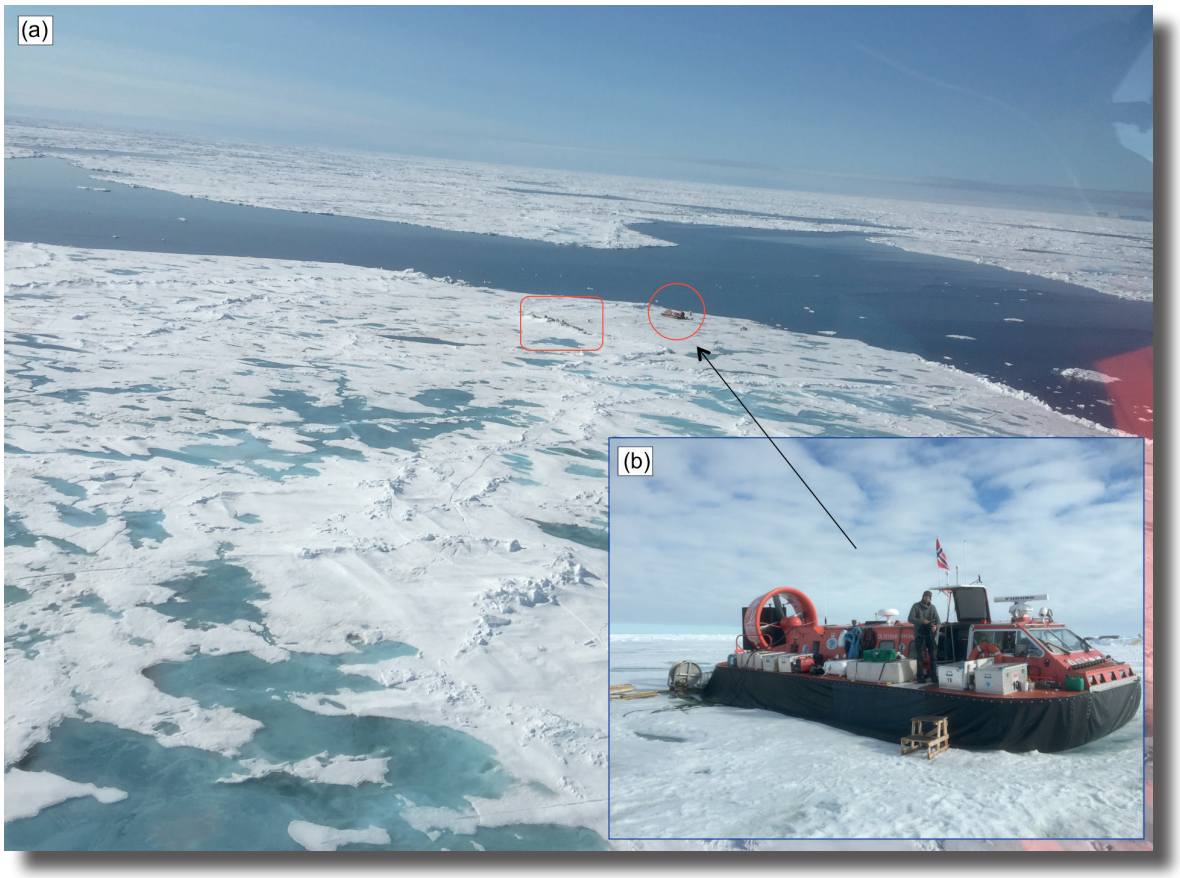

30 August 2014 (Start of FRAM-2014/15)
Deployment of drift station by
Polarstern during Expedition PS87

05/06 July 2015
Rendezvous of *Polarstern* and drift station
during Expedition PS93.1

18 August 2015 (End of FRAM-2014/15)
Recovery of the drift ice station
by the sealer *Havsel* and start
of transit back to Longyearbyen

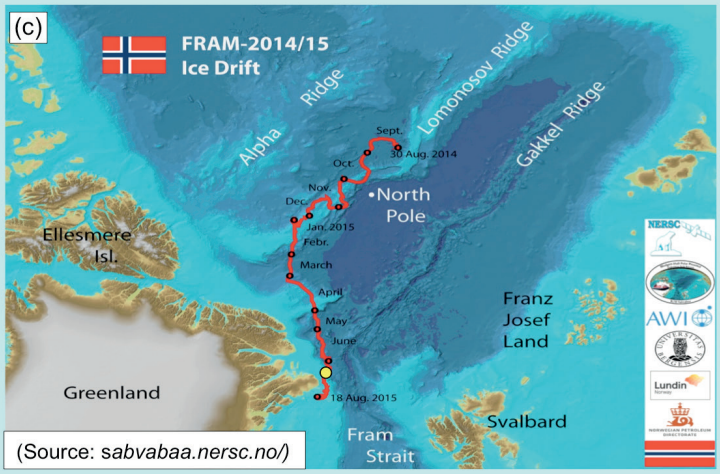

Abb. 1.4: FRAM-2014/15 Eis-Drift-Experiment. (a) Helicopter-Anflug auf FRAM-2014/15 Eis-Drift-Station am 05.07.15. Roter Kreis markiert Hovercraft (Luftkissenboot) Sabvabaa, rotes Rechteck die Eisstation (Foto: R. Stein/AWI); (b) Hovercraft Sabvabaa (Foto: R. Stein/AWI); (c) Drift-Route der FRAM-2014/15 Eis-Drift-Station vom 30.08.2014 – 18.08.2015 (sabvabaa.nersc.no).

Fig. 1.4: FRAM-2014/15 Ice Drift Experiment. Arrival/landing of helicopter at the FRAM-2014/15 Ice Drift Station on 05 July 2015. Red circle marks hovercraft, red rectangle the ice camp (Photo: R. Stein/AWI); (b) Hovercraft Sabvabaa (Photo: R. Stein/AWI); (c) Drift track of FRAM-2014/15 Ice Drift Station from 30 August 2014 to 18 August 2015 (sabvabaa.nersc.no).

SUMMARY AND ITINERARY

Summary

Target areas of expedition PS93.1 were the NE Greenland continental margin, the central Fram Strait and the western Svalbard margin (Fig. 1.1). The overall scientific goal of the marine-geological research programme is to investigate the variability of key environmental parameters during warm periods (interglacials) of the geological past. Of special interest are the last interglacial (Eemian, ca. 130-120 ka) and the Holocene (last ca. 12 ka). For this purpose, long sediment cores from potential areas with high sediment accumulation are needed. Besides the main geological programme, some complementary oceanographic, biological and air-chemical programmes as well as a “Floating University” were carried out.

Key activities of the expedition can be summarized as follows:

- A detailed geological coring programme (4 x Kastenlot corer, 22 x gravity corer, 29 x Giant Box Corer, 11 x Multicorer) was carried out in Fram Strait, Greenland Sea and East Greenland continental shelf (Fig. 1.2). High-quality long sediment cores were recovered that will allow detailed reconstructions of the Greenland ice sheet history, the sea-ice variability and changes in water mass circulation on different time scales including the Holocene and the Eemian.
- During transit and within the main working areas, Hydrosweep and Parasound were running continuously, resulting in about 4,000 km of high-quality profiles that were the basis for the precise selection of coring stations.
- The geoscientific programme was supplemented by additional activities related to oceanography (recovery and deployment of moorings systems, deployment of sea gliders and underway CTD) (Fig. 1.2), biology (collecting 123 phytoplankton samples that will be further isolated and analysed at the AWI to assess the biodiversity and biogeography of Arctic phytoplankton species), and atmosphere-chemistry (continuous and automatic measurements of isotopic signatures of water vapour over the Arctic Ocean).
- As major part of expedition PS93.1, a “Floating University” was held onboard *Polarstern* under the umbrella of the International Research Training Group “Processes and impacts of climate change in the North Atlantic Ocean and the Canadian Arctic - ArcTrain”. Within this programme, 20 Canadian and German PhD students were introduced to all technical aspects of field work in marine sciences as well as to the concepts of teamwork, interdisciplinary and international collaboration. All the ArcTrain students have done an excellent job and significantly contributed to the success of this expedition.

Itinerary

Polarstern left Longyearbyen on June 29 around noon, onboard 44 crew members and 50 scientists, helicopter pilots, and technicians from twelve different countries. First target area was the central Fram Strait where several oceanographic mooring systems were left behind last summer because of extreme sea-ice conditions and lack of ship time. We reached the

first station on June 30. The search for the first mooring system remained unsuccessful, however, a new mooring was deployed at the same location. 10-20 miles towards the west, the search activities were more successful, and at the end of the day three mooring systems were recovered. Around midnight, the first geological coring station was carried-out, and a 7.5 m long Kastenlot core was recovered (Fig. 1.2; Station PS93/006: 79°12.2'N, 04°40.0'W; water depth 1,570 m).
In the early morning of July 01, we sighted the first sea ice at 79°14'N, 04°30'E, four hours later we encountered the first sea ice directly (Fig. 1.3). Steaming towards the west we carried out a Hydrosweep and Parasound site survey. On July 03 we reached the East Greenland continental shelf. Based on Parasound data from last year's cruise we selected some locations where very old sediments or rocks might outcrop at the seafloor. Coring activities by means of a gravity corer, however, remained unsuccessful. Thus, we steamed further towards the north, and reached the polynya east of NE Greenland on July 04, where several geological, biological and oceanographic stations were carried-out.

On July 05, we reached the northern edge of the polynia, the northernmost part of our study area, where we met "old friends: Yngve Kristoffersen and Audun Tholfson, two Norwegian colleagues, who - along with their hovercraft - we took to the central Arctic Ocean where we had left them on 30 August 2014 on a large ice floe near the Lomonosov Ridge (Fig. 1.4). Within the last ten months – during the winter in complete darkness – the ice floe with the camp, hovercraft and its two passengers on board had drifted through the entire Arctic Ocean (Fig. 1.4). After intense discussions, phone calls, etc. we agreed to recover all the dangerous goods and that Yngve Kristoffersen and the hovercraft would continue the drift experiment, and Audun Tholfson would come onboard *Polarstern* (Yngve Kristoffersen ended the FRAM-2014/15 Ice Drift Experiment successfully on August 18; Fig. 1.4).

July 07 to July 09 were dominated by intense coring and sampling activities of the geologists along the East Greenland continental margin between 81° and 79°N. On July 10, we were steaming towards the east, the central Fram Strait, to recover and deploy, respectively, three mooring systems (Fig. 1.2; Stations PS93/033 to /035). After having finished the oceanographic station work, we started the way back towards the west, towards the ice edge. During that transit we shortly stopped for one gravity corer run on Hovgaard Ridge, a location where we had failed last year (Fig. 1.2; Station PS93/037). This time we were successful and recovered a short but good core. During transit, we successfully used the "Underway CTD" to get continuous temperature and salinity profiles.

On July 12, two long cores with several metres of Holocene sediments were recovered that will allow a detailed study of short- and long-term climate-variability during the last about 12,000 years. With this successful coring event we finished our research programme in the western ice-covered East Greenland shelf area and steamed towards the SE, about 120 nm through the partly heavy ice. On July 14, early in the morning, we reached our next station, after a long time the first one again located out of the ice. Besides geological and biological sampling activities, two "sea gliders" were deployed (Fig. 1.2). These instruments are able to actively dive up and down and measure temperature, pressure and salinity. A final multidisciplinary station with all gears, i.e., CTD, multinet, giant box corer, multicorer, and gravity corer was carried out, followed by a 12-hours hydrosweep survey, the final end of the PS93.1 research!

On July 18 at 10:30 am, *Polarstern* arrived in Tromsø.

Finally, we would like to thank Captain Wunderlich and his crew for the excellent cooperation at all times. This cooperation had been the basis for the success of Expedition PS93.1!

2. WEATHER CONDITIONS DURING PS93.1 (ARK-XXIX/2.1)

Max Miller, Hartmut Sonnabend (DWD)

On Monday afternoon, June 29, 2:00 pm, *Polarstern* left Longyearbyen for the campaign PS93.1 (ARK-XXIX/2.1). Cloudy skies, 3° C and light south-easterly winds were observed.

Coming from Greenland a ridge crossed Fram Strait. Winds veered north and increased up to Bft 5 especially along the west coast of Svalbard. Steaming west we entered the centre of the ridge on Tuesday (June 30). Sunshine and only light and variable winds were present. Afterwards a trough followed. During the night to Wednesday winds veered southwest and freshened up to Bft 6 but abated quickly on Wednesday (July 01) while entering the trough's centre.

During the following days the pressure gradient over our operation area was weak but fog formed only for short times.

On Monday (July 06) a coastal effect could be observed at the north-eastern end of Greenland. South-easterly winds Bft 4 increased up to 6 while approaching the coast.

During the following week the high over Greenland did hardly move and lows over northern Russia and Scandinavia extended northwest a bit. This constellation caused northerly winds over Fram Strait but wind force 5 was observed only for short times.

From Saturday (July 11) until Monday (July 13) the high over Greenland built finally a ridge towards Svalbard and caused only light winds but lots of fog.

A low near Sewernaya Zemlya moved slowly southwest via Franz-Josef-Land and Bear Island. Therefore winds over Fram Strait veered north again from Tuesday (July 14) on, increased gradually and peaked at Bft 6 to 7 on Thursday (July 16). Already during the night winds abated and veered south at wind force 4 to 5 on Friday (July 17).

On Saturday morning, July 18, *Polarstern* reached Tromsø at light to moderate winds.

Further details and statistics are shown in Figures 2.1 – 2.4.

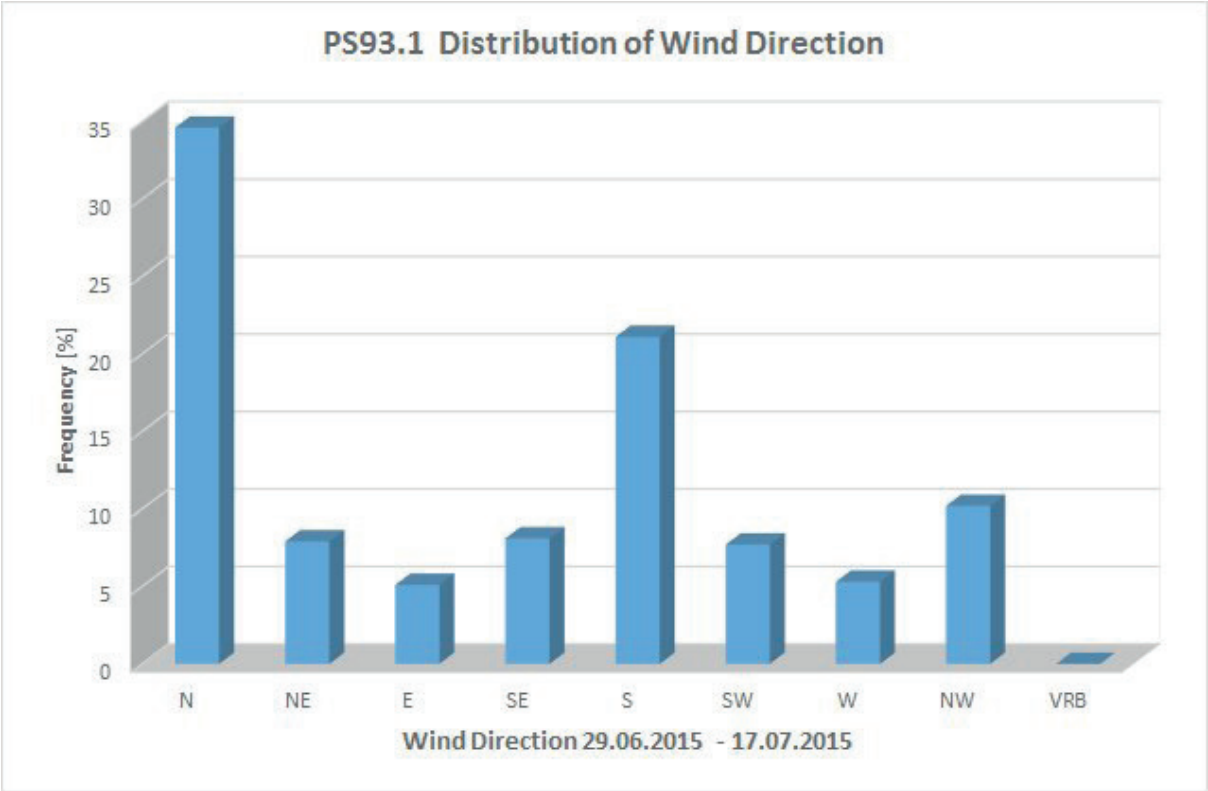

Fig. 2.1: PS93.1 Distribution of wind direction

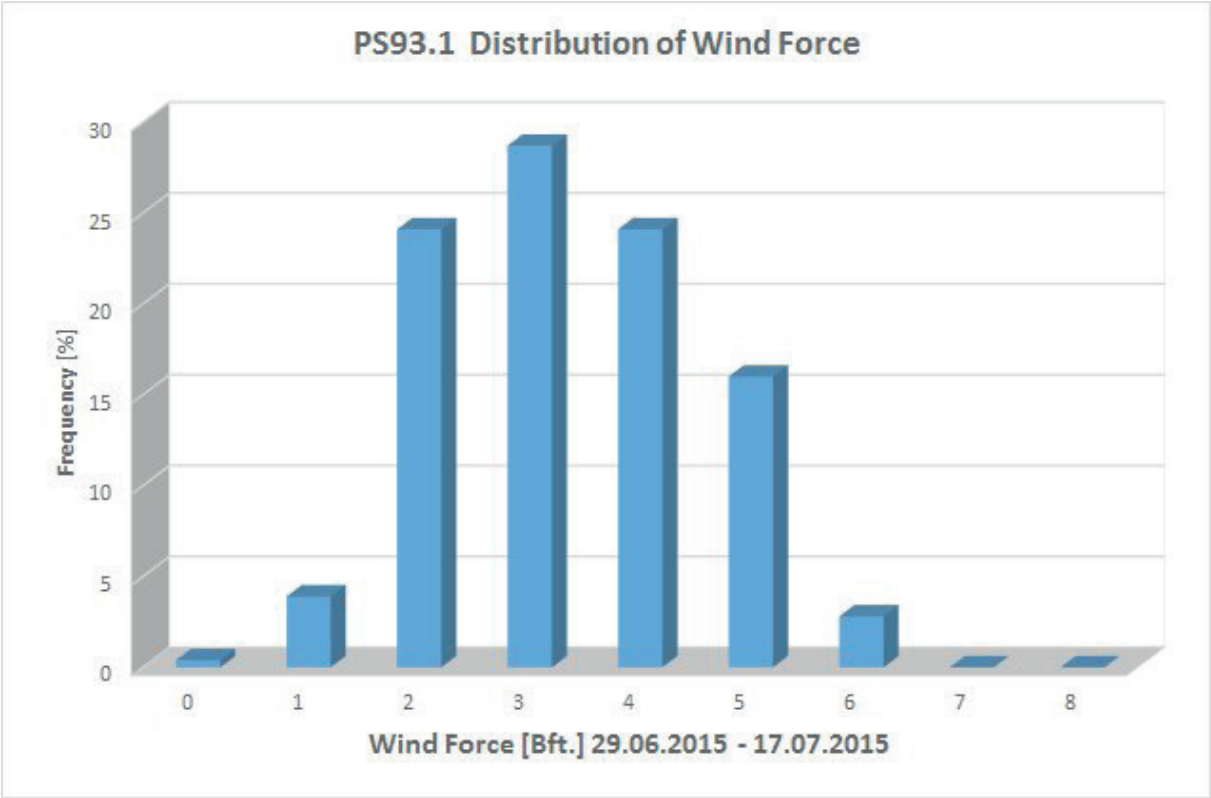

Fig. 2.2: PS93.1 Distribution of wind force

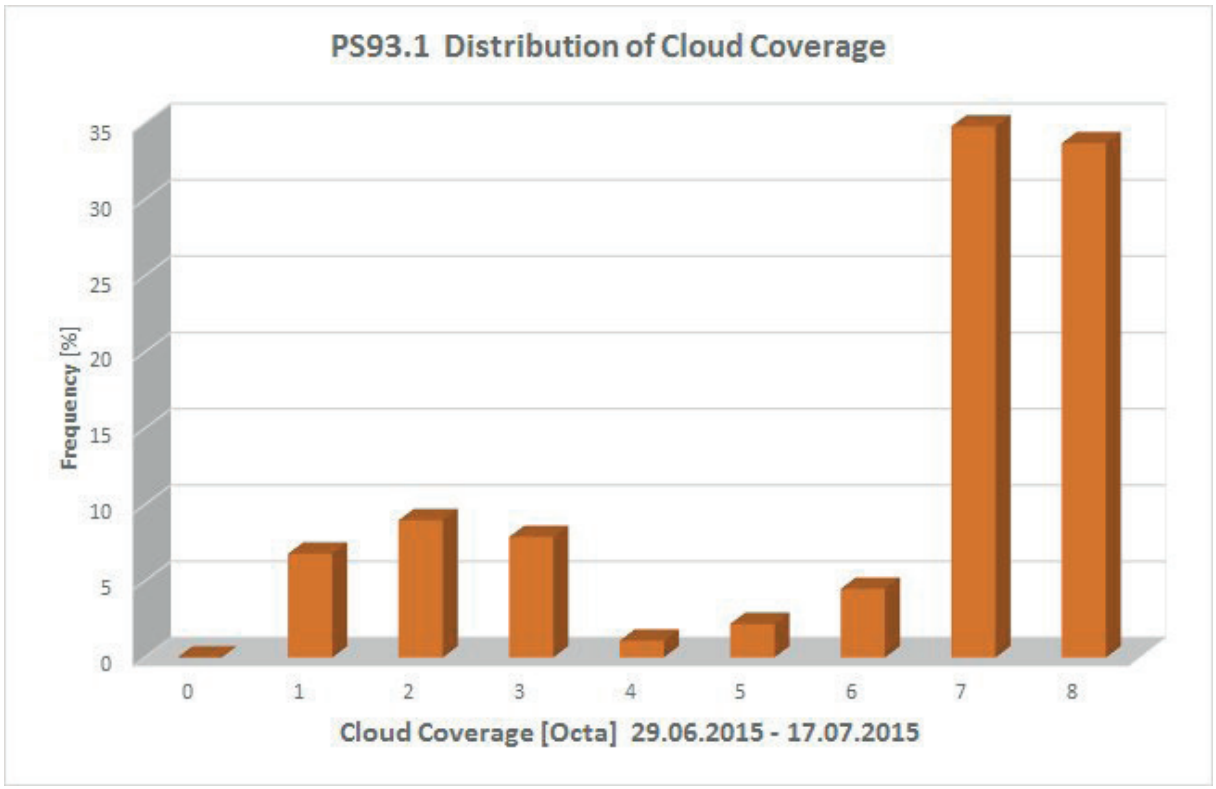

Fig. 2.3: PS93.1 Distribution of cloud coverage

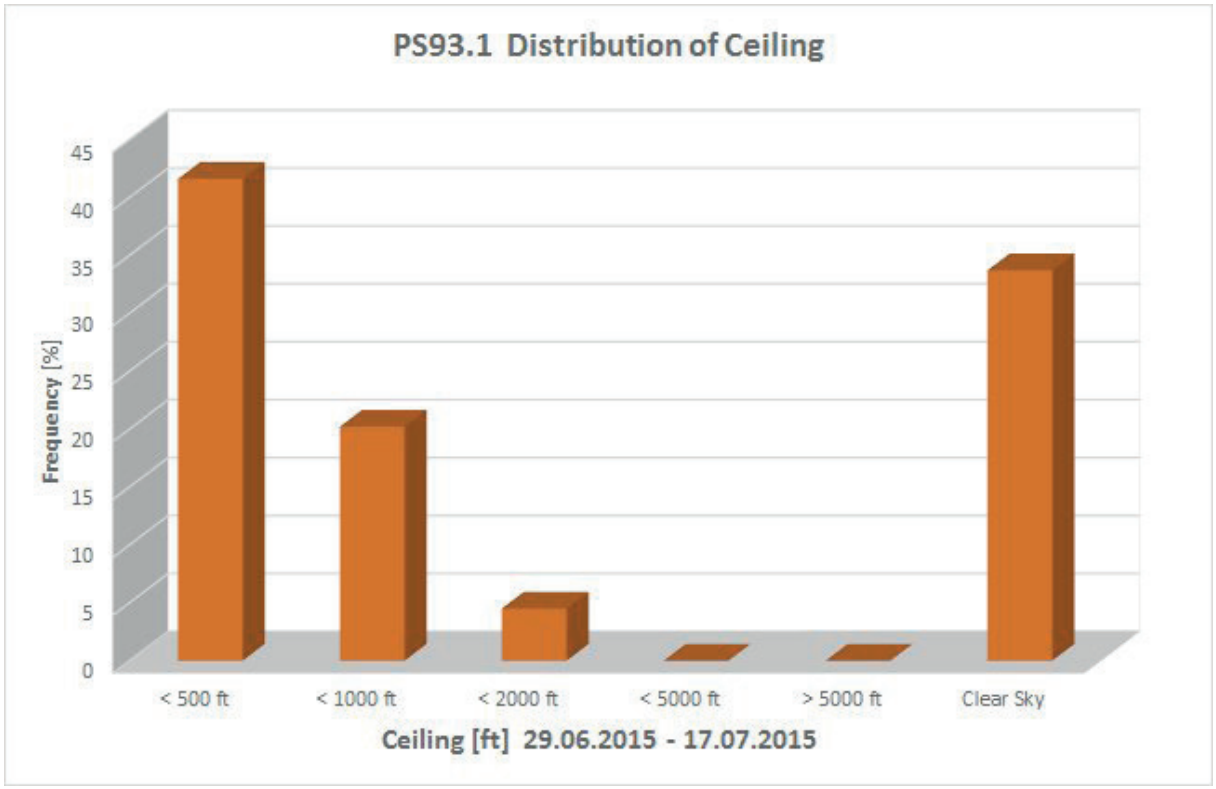

Fig. 2.4: PS93.1 Distribution of ceiling

3. ISOTOPE SIGNATURES OF WATER VAPOUR OVER THE ARCTIC OCEAN

Jean-Louis Bonne[1], [1]AWI
not on board: Sepp Kipfstuhl[1],
Hanno Meyer[1] , Benjamin Rabe[1] ,
Martin Werner[1], Melanie Behrens[1],
Lutz Schönicke[1]

Grant No: AWI-PS93.1_02

Objectives

For several decades, isotope research was focused on precipitation samples as end member products of the hydrological cycle, as vapour measurements in the field were most difficult to perform. Since very recently it has become possible to measure $H_2{}^{18}O$ and HDO in water vapour with necessary precision by commercially available light-weighted cavity-ring-down spectrometers (CRDS). For the first time in the history of water isotope research the CRDS technique allows to measure directly under *in-situ* conditions the isotopic content of the water vapour in the air on any place or platform almost autonomously, thus also on board of ships, planes or on remote stations in the Arctic or Antarctic (e. g. Dyroff et al. 2015; Bonne et al. 2014; Steen-Larsen et al. 2013).

From August to September 2014, a pilot study has successfully performed continuous isotopic measurements of specific humidity, $H_2{}^{18}O$ and HDO over 1 month with a Los Gatos Research (LGR) CRDS. This instrument was removed from the ship after the cruise. Within the project Iso-Arc, funded by AWI's strategy fond, the installation of a new CRDS instrument on board *Polarstern* in combination with surface water sampling will provide a unique simultaneous data set of $H_2{}^{18}O$ and HDO in both ocean surface and the atmosphere directly above the ocean surface. Thus, the imprint of marine boundary conditions (e.g. temperature variations, circulation changes, or meltwater input) to the isotopic composition of the atmospheric water cycle will be directly measured for the first time with a focus on North Atlantic and Arctic oceans. These records will be combined with simultaneous water isotope measurements at Iceland (Steen-Larsen et al. 2015), Svalbard (Masson-Delmotte et al. 2015), and Samoylov, North Siberia (by AWI; also part of this strategy fond proposal) and paired with complementing climate simulations enhanced by water isotope diagnostics. These data sets, covering an approx. 6,000 km transect of Northern Eurasia will allow for a quantitative assessment of the Arctic water cycle, with potential tracking of air masses at different stages of the atmospheric transport (similar to Bonne et al. 2015), its isotopic variations and imprint on various climate archives. The results of these analyses will also be of relevance for the interpretation of isotope signals found in ice cores and on terrestrial Arctic sites in terms of past climate change.

Work at sea

Before the PS93.1 expedition, a calibration system for the water vapour isotopic analyser had been designed and built at AWI, together with the definition of an analytical protocol. The analyser, a Picarro brand CRDS instrument, had been installed on board *Polarstern* in May 2015 in Bremerhaven. Fig. 3.1 presents the general view of the instrument.

Ambient air is continuously pumped through a heated tube, with an inlet located under platform B. The analyser either measures ambient air sampled from the inlet tube or air coming from the calibration unit. The calibration consists in regular measurements of 4 liquid water isotopic standards. 8 independent lines have been built for the standards injection: two lines are dedicated to each standard, thus providing back-up lines for a better instrumental robustness. The liquid water, stored in glass bottles, is pushed through fused silica capillaries by increasing the pressure in the bottles towards an oven heated at 170°C, where it is quantitatively vaporised and mixed with dry air originating from a high-pressure cylinder. The resulting water vapour has the same isotopic composition as the liquid water standard. After a test period of high frequency calibrations (one every 10 hours), the routine measurements procedure has been defined with one calibration every 25 hours during which the 4 isotopic standards are successively measured during 30 minutes each.

On the first day of the PS93.1 expedition, June 29 2015, the analyser was started in the Arctic field, in Longyearbyen fjord for the first time. Despite the procedure applied in May to dry the injection lines, 3 of the 4 lines revealed to have too much humidity at the instrument start-up. In order to be able to calibrate the system properly, these 3 lines were dried by injected dry air from the high-pressure cylinder during 1 to 2 hours for each line. The reasons of this humidity increase when lines are not used are still under investigation. This problem may happen later when the instrument is turned off, or when some lines are not used (for example the back-up lines) for a period of several weeks. For this reason, a simple automatic drying protocol was created.

During laboratory tests at AWI, the calibration system had shown sensitivity to clogging of the capillaries used to inject liquid water isotopic standards in the system. During the PS93.1 expedition, these clogging happened only twice, which is less frequent than during laboratory tests, probably due to a better filtering of the liquid water isotopic standards. Cutting a few millimetres of the capillaries in general easily resolves these clogging issues.

For the calibration, the sensitivity of isotopic measurements to humidity level needs to be corrected. Following previous recommendations from the literature (Aemisegger et al. 2012; Bastrikov et al. 2014), an experiment to evaluate the response function of isotopic measurements to humidity has been conducted during the PS93.1 expedition. A special version of the calibration unit controlling programme has been developed and tested to conduct this experiment. The 4 isotopic standards were measured at different humidity levels ranging from about 1,500 to 25,000 ppm, covering the range of humidity values that our analyser is expected to observe in ambient air. In future, this experiment will have to be performed about once per year when *Polarstern* is in Bremerhaven.

The instrument is dedicated to run autonomously during the next *Polarstern* expeditions. However, a daily monitoring by a scientist on board will be useful to ensure the best data coverage. Based on the experience of the PS93.1 expedition, a procedure has been defined for routinely checking a list of instrumental parameters and for potential troubleshooting. An automatic daily diagnostic script has been implemented on the analyser and tested. This script analyses the previous day calibration measurements and sends a report by e-mail to the AWI PIs, allowing for nearly real-time diagnostic of the instrumental performances and easy identification of potential troubles. A user manual was written to guide routine maintenance activities.

An automatic data treatment chain is under development to validate data, based on purge time criteria after switching from one sample to another and on instrumental parameters stability criteria, and to then calibrate the ambient air data based on the liquid water isotopic standards measurements.

Ocean water was sampled on a daily basis from an inlet situated at 6 m under the water surface. 19 samples were taken during the PS93.1 expedition and their water isotopic composition will be analysed using a mass spectrometer at AWI Potsdam. Material for the sampling during the future expeditions has been prepared.

The aims of this project were also presented on board during the ArcTrain seminars.

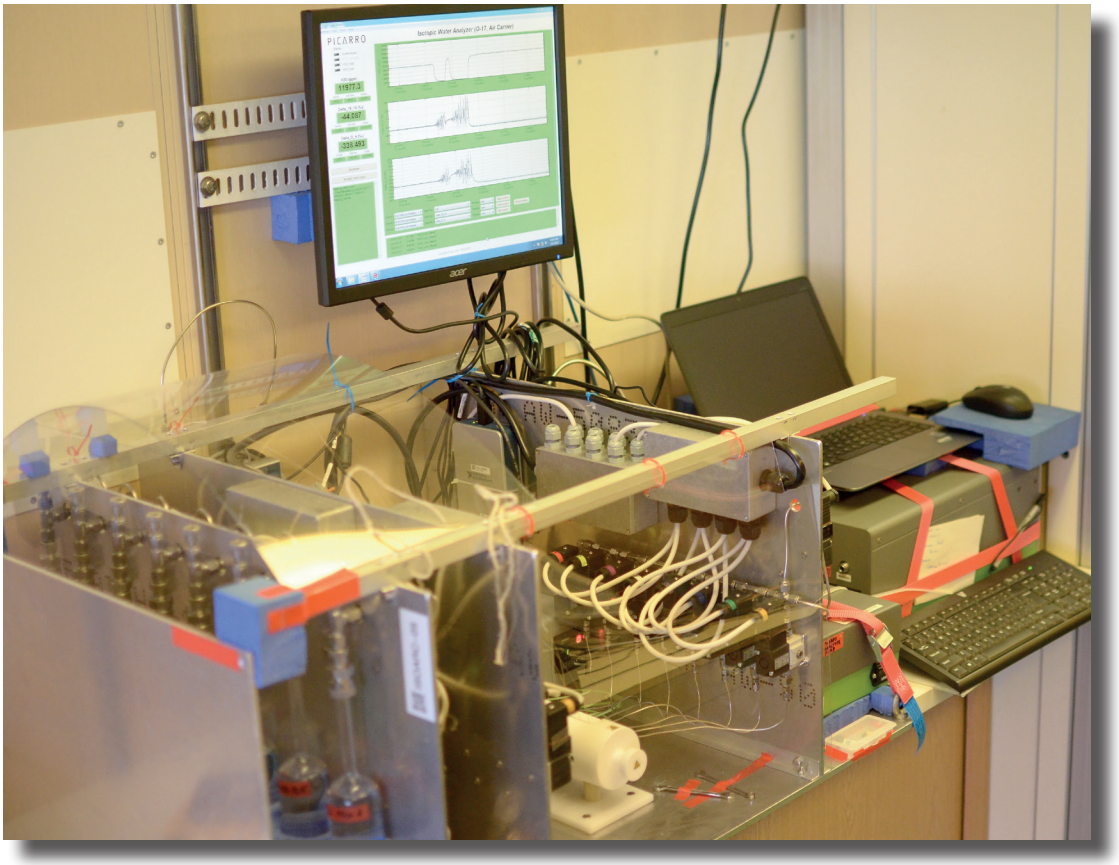

Fig. 3.1: Global view of the instrument installed in Polarstern

Preliminary (expected) results

During the PS93.1 expedition, the isotopic composition of water vapour had been recorded continuously from 29.06.2015 at 08:30 UTC to 17.07.2015 at 16:30 UTC. Over this period, gaps in the ambient air measurements are corresponding to the measurements of calibration standards, purge times after switching from calibration standards to ambient air measurements, and instrumental tests.

Fig. 3.2 presents time series of preliminary unselected and uncalibrated ambient air humidity, $\delta^{18}O$ and δD data during the expedition. The observed ranges of humidity and $\delta^{18}O$ in ambient air during this period are respectively from 7,000 to 14,000 ppm and -30 to -15 permil. After careful calibration, the combined measurements of $\delta^{18}O$ and δD will give access to the second order parameter deuterium excess (d-excess = $\delta D - 8 * \delta^{18}O$; Craig 1961).

During the first period of the cruise, from June 29 to July 9, 2015, the humidity values have been relatively stable, from about 7,000 to 9,000 ppm, with surprisingly similar isotopic composition in the western and eastern part of the Fram Strait, independently from the sea ice cover around the ship. This small variability can be associated with the relatively stable synoptic situation in the Frame Strait in this period.

Fig. 3.2: Preliminary unselected and uncalibrated ambient air data (humidity, $\delta^{18}O$ and δD) on the period June 29 to July 17, 2015.

On July 10, an important humidity spike has been observed from 8,000 to 13,000 ppm, associated with a significant increase in $\delta^{18}O$ values from -25 to -15 permil. This increase, the most important spike observed during the expedition, corresponds to a period of significant increase of wind activities, and the observed humidity and isotopic variations are typical from those previously observed during summer in Ny-Alesund, Svalbard (Masson-Delmotte et al. 2015). Between July 13 and 17, *Polarstern* transit towards lower latitudes is associated with an increase in both temperature and humidity. However, no significant isotopic variations have been observed during this transit, which is probably related with the compensating effect between the latitudinal and longitudinal gradients in the Fram Strait, as seen in averaged surface $\delta^{18}O$ values from isotopic models such as e.g. LMDZiso (Bonne et al. 2014, supplementary materials). In addition to the progressive humidity variations linked to the transit across Fram Strait, this period also presents humidity and isotopic variations at the synoptic scale, of smaller amplitude than the first event on July 10.

The combination of *Polarstern* records with observations around Fram Strait (Svalbard and Iceland), will help deciphering the influences of spatial and synoptic scale meteorological variations on our records. It will also be useful to study the atmospheric transport of water with potential analyses of similar air masses at different locations. The measurements obtained during the first days of the expedition, close to Ny-Alesund, are also an interesting opportunity for cross-comparison with the measurements performed in this location.

Data management

All humidity and isotope data of this project will be uploaded to the PANGAEA database after processing and post-operative calibration. Unrestricted access to the data will be granted within 2-3 years, pending analysis and publication.

References

Aemisegger F, Sturm P, Graf P, Sodemann H, Pfahl S, Knohl A, Wernli H (2012) Measuring variations of $\delta^{18}O$ and $\delta^{2}H$ in atmospheric water vapour using two commercial laser-based spectrometers: an instrument characterisation study. Atmospheric Measurement Techniques, 5:1491-1511.

Bastrikov V, Steen-Larsen HC, Masson-Delmotte V, Gribanov K, Cattani O, Jouzel J, Zakharov V (2014) Continuous measurements of atmospheric water vapour isotopes in Western Siberia (Kourovka). Atmospheric Measurement Techniques, 7(6):3-1776.

Bonne JL, Masson-Delmotte V, Cattani O, Delmotte M, Risi C, Sodemann H, Steen-Larsen HC (2014) The isotopic composition of water vapour and precipitation in Ivittuut, southern Greenland. Atmospheric Chemistry and Physics, 14(9):4419-4439.

Bonne JL, Steen-Larsen HC, Risi C, Werner M, Sodemann H, Lacour JL, Fettweis X, Cesana G, Delmotte M, Cattani O, Vallelonga P, Kjaer HA, Clerbaux C, Sveinbjörnsdottir AE, Masson-Delmotte V (2015) The summer 2012 Greenland heat wave: In situ and remote sensing observations of water vapor isotopic composition during an atmospheric river event. Journal of Geophysical Research: Atmospheres, 120(7):2970-2989.

Craig H (1961) Isotopic variations in meteoric waters. Science 133(3465):1702-1703, DOI: 10.1126/science.133.3465.1702.

Dyroff C, Sanati S, Christner E, Zahn A, Balzer M, Bouquet H, McManus JB, Gonzáles-Ramos Y, Schneider M (2015) Airborne in situ vertical profiling of HDO/H 2 16 O in the subtropical troposphere during the MUSICA remote sensing validation campaign. Atmospheric Measurement Techniques, 8(5):2037-2049.

Masson-Delmotte V, Steen-Larsen HC, Zanetti N, Cattani O, Maturilli M, Debatin S, Terzer S, Bonne JL, Schneider M (2015, April) Understanding climatic controls on Svalbard water vapour and precipitation isotopic composition. EGU General Assembly Conference Abstracts, 17:14482.

Steen-Larsen HC, Johnsen SJ, Masson-Delmotte V, Stenni B, Risi C, Sodemann H, Balslev-Clausen D, Blunier T, Dahl-Jensen D, Ellehoj MD, Falourd S, Grindsted A, Gkinis V, Jouzel J, Popp T, Sheldon S, Simonsen SB, Sjolte J, Steffesen JP, Sperlich P, Sveinbjörnsdottir AE, Vinther BM, White JWC (2013) Continuous monitoring of summer surface water vapor isotopic composition above the Greenland Ice Sheet. Atmospheric Chemistry and Physics, 13(9):4815-4828.

Steen-Larsen HC, Sveinbjörnsdottir AE, Jonsson T, Ritter F, Bonne JL, Masson-Delmotte V, Sodemann H, Blunier T, Dahl-Jensen D, Vinther BM (2015) Moisture sources and synoptic to seasonal variability of North Atlantic water vapor isotopic composition. Journal of Geophysical Research: Atmospheres, 120(12):5757–5774.

4. PHYSICAL OCEANOGRAPHY

Wilken-Jon von Appen[1], Olaf Strothmann[1] [1]AWI
and the ArcTrain team

Grant No: AWI-PS93.1_02

Background and objectives

The work of the Physical Oceanography group on this cruise supported a long-term effort to monitor and quantify the variability of oceanic fluxes through the Fram Strait.

The Arctic Ocean is a semi-enclosed marginal sea with the Bering Strait, the Canadian Arctic Archipelago, and the Barents Sea being three shallow connections to the world oceans. The Fram Strait is the only deep strait (2,700 m), thereby allowing for the exchange of intermediate and deep waters between the Arctic Ocean and the Nordic Seas, which are in turn a marginal sea of the North Atlantic. Atlantic origin water is cooled throughout the cyclonic boundary current circulation in the Nordic Seas and enters the Arctic through the Barents Sea and the eastern Fram Strait. The temperature and other properties of the inflowing warm and salty Atlantic Water change in response to interannual variability, to large scale-, multi-year climate patterns, such as the North Atlantic Oscillation, and to global climate change. The sum of these effects can be measured in the Fram Strait before it enters the Arctic Ocean, where it participates in the formation of the halocline north of Svalbard and forms a mid-depth cyclonic boundary current. Cooling, freezing, sea-ice melt, mixing with Pacific origin water, and the addition of large amounts of river runoff in the Arctic modifies the inflowing water before it exits through the western Fram Strait. Thus observations of the outflow from the Arctic make it possible to monitor the effects of many processes in the Arctic Ocean.

The complicated topography in the Fram Strait leads to a horizontal splitting of the inflowing branches of Atlantic Water. Additionally, some of the Atlantic Water participates in a westward flow called the recirculation that then turns southward to exit the Fram Strait back to the Nordic Seas. The southward flowing cold and very fresh East Greenland Current is responsible for a large part of the liquid freshwater export from the Arctic and most of the solid freshwater export in the form of sea-ice. This freshwater has the potential to impact convection in the Nordic Seas and the northern North Atlantic and in turn the meridional overturning circulation.

Since 1997 AWI and the Norwegian Polar Institute have maintained a mooring array across the Fram Strait to monitor the fluxes of volume and heat, and, in the western part of the strait, freshwater into and out of the Arctic Ocean through this gateway.

Next to the dramatic retreat of sea ice, the strongest climatic signal of the Arctic Ocean and the Nordic Seas in the past decade are changes in temperature and salinity. While additional heat and salt are advected northwards from the subpolar North Atlantic into the Nordic Seas, a strong accumulation of fresh water has been observed in the past decades in the Arctic Ocean. The aim of a glider programme, started in summer 2014 in the western Nordic Seas, is to observe whether the increasing amount of freshwater reaches the inner basins of the Nordic Seas and thus dampens vertical mixing and intermediate as well as deep water renewal during winter. This might lead to a slow-down of the northern branch of the AMOC.

Work at sea

The work of the Physical Oceanography group on-board entailed measuring vertical profiles of temperature and salinity both with a classical CTD rosette and with an underway CTD. To study variability and distribution of temperature and salinity in regions and times not covered by our expedition, we deployed and recovered instrumentation moored at the seafloor, and deployed gliders and floats for autonomous measurements.

CTD (conductivity-temperature-depth) profiles were measured with a Seabird 911+ system belonging to the AWI physical oceanography section. Two temperature sensors and two conductivity sensors as well as a transmissiometer and a fluorometer were attached to the system. The rosette contained 24 bottles (12 liter each) for the collection of water samples. Four water samples were collected by the physical oceanography group for calibration of the conductivity sensor of the CTD. The samples were analyzed on board with the Optimare Precision Salinometer. The locations of the 8 CTD profiles taken on PS93.1 are given in Table 4.1. These stations were chosen at the same locations as some of the geological sampling stations in order to allow for the comparison of geological proxies in the water column and in the upper most sedimentary layers. This means that the individual isolated CTD profiles are difficult to interpret from a physical oceanographic viewpoint, but it is expected that they will be valuable for regional studies when combined with CTD station data from other cruises to the area.

Tab. 4.1: CTD profiles measured during PS93.1

Station no	Date/time	Time [UTC]	Latitude	Longitude	Water depth [m]
PS93.1 011-01	2-Jul-2015	11:06	80° 22.49'N	6° 59.78'W	253
PS93.1 016-01	3-Jul-2015	11:57	81° 13.04'N	7° 20.73'W	1542
PS93.1 017-01	3-Jul-2015	23:26	81° 35.66'N	6° 34.98'W	3372
PS93.1 020-01	5-Jul-2015	8:35	82° 06.17'N	8° 57.15'W	2901
PS93.1 024-01	7-Jul-2015	13:36	80° 54.84'N	6° 22.15'W	1334
PS93.1 030-01	8-Jul-2015	22:38	79° 33.19'N	4° 51.09'W	1303
PS93.1 039-01	12-Jul-2015	12:24	78° 44.73'N	9° 38.44'W	401
PS93.1 046-01	15-Jul-2015	3:25	76° 05.10'N	6° 48.64'W	2496

In summer 2012, 12 moorings had been deployed across Fram Strait along 78°50’N. They were supposed to be recovered in 2014. However, due to technical problems of *Polarstern*, cruise PS85 was cut short such that only some of the moorings could be recovered. The upper most buoyancy floatation of the moorings usually contains an Argos transmitter. The Argos transmitter of mooring F2 had transmitted its location via satellite in 2014 indicating that the mooring had been damaged and it would not be possible to recover this mooring using conventional methods as the floating remaining on the mooring would not be sufficient for the mooring to come to the surface. Therefore, moorings F1-14, F3-15, F4-15, F5-15, F6-16, and F7-16 (Table 4.2) were supposed to be recovered on PS93.1.

Tab. 4.2: Mooring deployments and recoveries during PS93.1. The different instruments on the moorings are given and it is indicated what the instruments measured when. The abbreviations for the variables are “vel”=velocity, “T”=temperature, “S”=salinity, “P”=pressure and the abbreviations for the instruments are “ADCP QM”=Quarter Master (150kHz) acoustic Doppler current profiler, “SBE 37”=Seabird microcat, “RCM”=Aanderaa Rotor Current Meter.

Mooring	Latitude	Longitude	Water depth [m]	Top float at [m]	Station number	Working date	Status	Instrument type	Instrument SN	Instrument depth [m]	Variables measured	Data start	Data end	Data comment
F1-14	78° 50.01'N	8° 39.99'E	246	245	PS93.1 002-01	20-Jun-2015	recovery failed, possibly releaser too old	ADCP QM	14090	245		-		
								SBE 37	2384	245		-		
F1-15	78° 49.80'N	8° 40.14'E	246	245	PS93.1 002-02	20-Jun-2015	deployed, recovery planned summer 2016	ADCP QM	15500	245		-		
								SBE 37	1230	245		-		
F3-15	78° 49.91'N	8° 00.29'E	1005	49	PS93.1 003-01	20-Jun-2015	recovered	RCM 11	461	59	vel, T, P	22-Jun-2012	12-Oct-2014	
								SBE 37	1237	60	T, S, P	22-Jun-2012	30-Jun-2015	
								ADCP QM	14086	240	vel profiles, T,P	22-Jun-2012	30-Jun-2015	
								RCM8	9770	242	vel, T	22-Jun-2012	9-Oct-2014	
								SBE 37	9487	243	T, S, P	22-Jun-2012	30-Jun-2015	
								Holgiphone	33	493	passive acoustics	?		Data not yet recovered
								RCM 11	506	750	vel, T, P	22-Jun-2012	20-Nov-2013	
								SBE 37	230	991	T, S	22-Jun-2012	30-Jun-2015	
								RCM 11	504	997	vel, T, P	22-Jun-2012	30-Jun-2015	
F4-15	78° 50.01'N	6° 59.99'E	1420	64	PS93.1 004-01	20-Jun-2015	recovered	RCM 8	11887	74	vel, T, P	22-Jun-2012	9-Oct-2014	
								SBE 37	2392	75	T, S, P	22-Jun-2012	30-Jun-2015	
								ADCP QM	14087	235	vel profiles, T,P	22-Jun-2012	30-Jun-2015	
								RCM 8	9783	237	vel, T, P	22-Jun-2012	4-Jul-2014	
								SBE 37	2393	238	T, S, P	22-Jun-2012	24-Mar-2015	
								RCM 7	8048	692	vel,T	22-Jun-2012	30-Jun-2015	
								SonoVault	1026	743	passive acoustics	?		Data not yet recovered
								SonoVault	1024	1410	passive acoustics	?		Data not yet recovered
								RCM 8	10497	1412	vel	22-Jun-2012	30-Jun-2015	
F5-15	78° 50.01'N	6° 00.04'E	2418	63	PS93.1 005-01	20-Jun-2015	recovered	RCM 8	9194	74	vel, T	23-Jun-2012	9-Oct-2014	
								SBE 37	2396	75	T, S, P	23-Jun-2012	5-Jan-2015	
								ADCP QM	14088	225	vel profiles, T,P	23-Jun-2012	30-Jun-2015	
								RCM 8	10002	227	vel, T, P	23-Jun-2012	9-Oct-2014	
								SBE 37	2610	228	T, S, P	-		Instrument damaged, no data
								RCM 11	462	673	vel, T, P	23-Jun-2012	4-Oct-2014	
								RCM 11	486	1424	vel, T	23-Jun-2012	29-Jun-2015	vel only till 01-Mar-2015
								RCM 8	9390	2410	vel, T	23-Jun-2012	4-Oct-2014	
F7-12	78° 49.72'N	4° 00.51'E	2292	71	PS93.1 033-01	10-Jul-2015	recovered	SBE 37	9130	78	T, S, P	25-Jun-2012	12-Sep-2014	
								ADCP QM	14951	239	vel profiles, T,P	?		Data not yet recovered
								RCM 8	9997	241	vel	25-Jun-2012	30-Apr-2014	
								SBE 37	8131	242	T, S, P	25-Jun-2012	31-May-2014	
								RCM 7	8402	742	vel, T, P	25-Jun-2012	4-Oct-2014	
								RCM 8	3517	1498	vel, T	25-Jun-2012	4-Oct-2014	
								RCM 8	9782	2284	T	25-Jun-2012	4-Oct-2014	
F6-16	78°49.99'N	5° 00.00'E	2707	51	PS93.1 034-01	10-Jul-2015	recovery failed, possibly releaser too old	RCM 11	315	61		-		
								SBE 37	2237	62		-		
								ADCP QM	14089	252		-		
								RCM 11	491	254		-		
								SBE 37	244	255		-		
								Holgiphone	34	504		-		
								RCM 11	455	751		-		
								RCM 8	9186	1553		-		
								RCM 8	9188	2636		-		
F20-5	78° 44.99'N	5° 29.98'E	2410	88/0	PS93.1 035-01	10-Jul-2015	deployed, recovery planned summer 2016	NGK Profiler		88		12-Jul-2015		Profiler comes to the sea surface once every 48 hours
								NGK Winch		89		N/A		

Half of the locations were reached at the beginning of the cruise and the other half after the far northward excursion. Moorings F3-15, F4-15, F5-15, and F7-16 were successfully recovered while the recovery attempts of F1-14 and F6-16 failed. Since the moorings had been in the water for significantly longer than the planned two years, the batteries of many instruments and releasers were low or empty. Additionally, there was strong chemical corrosion to many mooring components (Fig. 4.1). Specifically, (supposedly) stainless steel used in the cages holding the ADCPs and the passive acoustic recorders had corroded. A hole in an ADCP cage (Fig. 4.1) was deeper than 1 cm and one of the 1 cm thick stainless steel rods holding the passive acoustic recorders had completely corroded. Therefore, it was broken and it was fortunate that the mooring could be recovered at all. Additionally, large deposits of a slimy substance, likely zinc oxide originating from the zinc anodes, were stuck on many of the releasers. This and/or the low battery levels probably contributed to the failure to recover moorings F1-14 and F6-16. F1-14 located on the shelf may also have sunk too deep into the muddy bottom for the release mechanism to function. The mooring recovery benefited from substantial help by the ArcTrain team.

The recovered instruments had generally performed well (Table 4.2) and most recorded good data for at least the two planned years before running out of battery or storage capacity.

Two moorings were also deployed on PS93.1. F1-15 is a trawl-resistant bottom mount containing an upward looking 150kHz Quarter Master ADCP designed to measure the

water velocity throughout the water column and a SBE 37 microcat designed to measured temperature, salinity, and pressure near the ocean bottom. F20-5 is a long mooring that only contains one system at its top. A winch at 150 m depth pays out line once every 24 hours. A profiler attached to that line floats up through the water column and measures temperature, salinity, and pressure along the way. The profiler is supposed to then acquire a GPS fix at the surface and establish an Iridium link to send its data to a server at the AWI.

Fig. 4.1: Hole corroded into the stainless steel cage of an ADCP. The whole is right next to the fingernail which gives the scale.

Recently, an Oceanscienc Inc underway CTD system had been purchased for *Polarstern*. Both this system and a similar system belonging to the physical oceanography group at the AWI were used on PS93.1. The UCTD sondes SN0186 and SN0240 were used. It was intended to obtain vertical profiles of temperature and salinity in the upper 150 m of the water column at the highest possible spatial resolution while *Polarstern* was transiting at normal speed (8 to 10 knots) between stations in ice-free waters. A tow-yo mode was used meaning that the CTD sonde was not brought back onto the ship's deck for about 2 hours at a time. The winch would be put into free-spooling mode and the CTD sonde would drop for about 70 seconds after which the winch would reel in the line for a little less than 4 minutes such that the CTD sonde was at the surface a few tens of meters behind the vessel. Then the winch would be put back to free-spooling mode such that on average a profile was obtained every 5 minutes. Depending on the ship speed this achieved a horizontal resolution between approximately 1,200 m and 1,800 m. Four long sections (Fig. 4.2) were achieved roughly across the center of Fram Strait and the East Greenland slope/shelf break. This operation was made possible through the support of the ArcTrain team.

Towards the end of the cruise during the second to last large geology station, two gliders of the Seaglider type were deployed (Table 4.3). First SG558 was deployed from a small boat. Then the boat returned to *Polarstern* and SG127 was loaded onto the boat and subsequently deployed. SG558 had been upgraded to a pumped Glider Payload CTD (GPCTD) during its refurbishment in early 2015. This system was new to the on board field team and to the pilots back at the AWI in Bremerhaven. As a result, the functionality initially was different from what had been expected. Therefore, SG558 had to be recovered from the small boat at the end of the SG127 deployment trip and some adjustments to settings and piloting routines were carried out. The problems were fixed over the subsequent 5 hours and SG558 could be redeployed later in the day. The gliders capture hydrographic sections between the inner Greenland Sea Basin and the East Greenland Current. Along the section dives of 500 to 1,000 m depth are carried out continuously to record temperature and salinity profiles. The data is transmitted

via Iridium satellites when the gliders return to the surface after each dive. The gliders are monitored and remotely steered by glider pilots at the AWI in Bremerhaven. Their mission will last approximately 3 months and it is planned to recover them from *Heincke* HE451.2 in the fall of 2015.

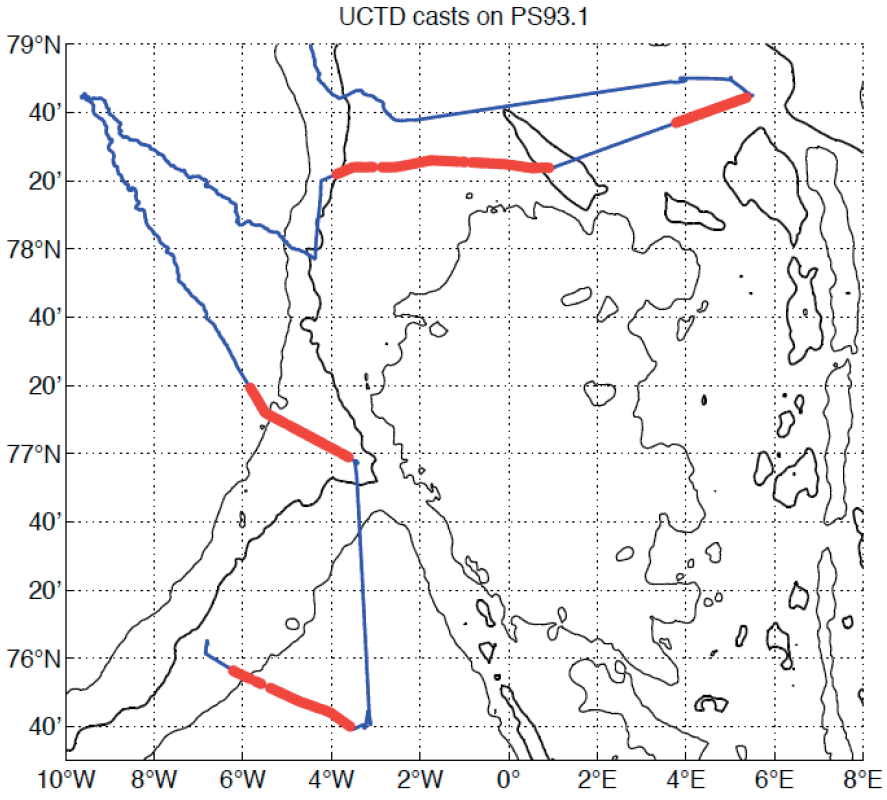

Fig. 4.2: Map of the cruise track (blue) and the UCTD casts (red dots) of PS93.1

Tab. 4.3: Deployments of autonomous gliders and floats during PS93.1

ID	Type	Station no	Date	Time	Latitude	Longitude	Action
SG558	Glider	PS93.1 042-04	14-Jul-2015	11:04	75° 44.39'N	3° 9.00'W	deployed
SG127	Glider	PS93.1 042-03	14-Jul-2015	12:27	75° 44.39'N	3° 9.05'W	deployed
SG558	Glider	PS93.1 042-03	14-Jul-2015	12:49	75° 44.39'N	3° 9.06'W	recovered due to technical problem
SG558	Glider	PS93.1 043-02	14-Jul-2015	18:00	75° 40.19'N	3° 16.30'W	deployed
ID22	Float	PS93.1 043-03	14-Jul-2015	18:49	75° 40.27'N	3° 16.11'W	deployed
ID23	Float	PS93.1 044-02	14-Jul-2015	21:24	75° 39.54'N	3° 32.07'W	deployed

Two Argo floats were deployed in the Greenland Sea near the glider deployment locations (Table 4.3). The floats drift at 1,000 m depth for 10 days. Then they will perform a CTD cast from 2,000 m to the surface and send their data home via Iridium satellites. It is expected that the floats will stay in the Greenland Sea Gyre for 1 to 2 years. The measurements contribute to the hydrographic monitoring of the Nordic Seas with Argo floats that has started in 2001.

Preliminary results

The data return of the instruments on the moorings was very successful (Table 4.2). Preliminary calibration of the data was possible and did not exhibit any major problems with the data. The seasonal cycle of temperature and salinity (Fig. 4.3) across the West Spitsbergen Current agreed with previous results. However, the moorings experienced major vertical mooring motions associated with very strong horizontal currents on the upper continental slope. Specifically, the microcat that was moored at a nominal depth of 75 m on mooring F3 at a water depth of 1,040 m was blown down to 500-650 m depth for short periods every deployment year between December and February (Fig. 4.3). The ADCP records indicated that the velocities at those times exceeded 0.5 m/s through a significant part of the water column. This information should be considered in the mooring design.

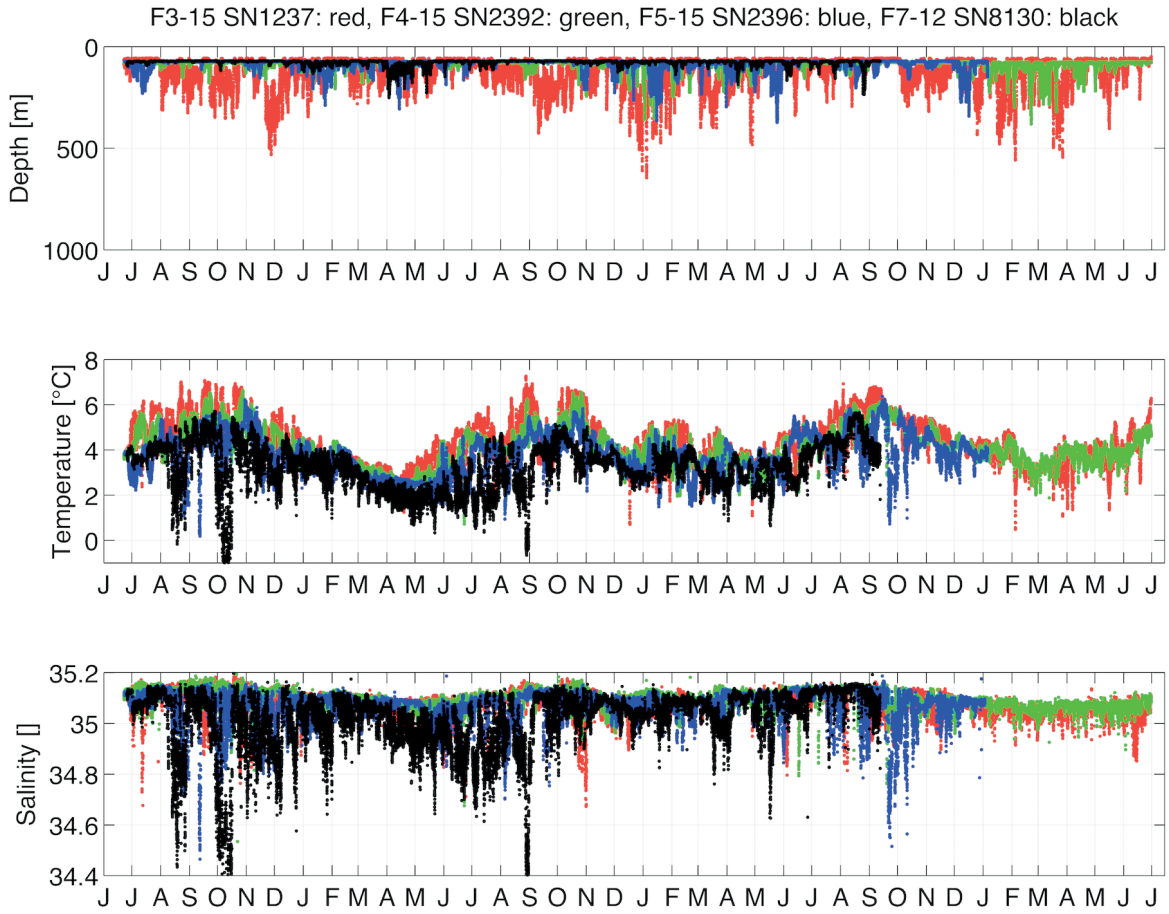

Fig. 4.3: Mooring records of instrument depth, temperature, and salinity at the nominal 75 m depth level of the four recovered moorings F3-15, F4-15, F5-15, and F7-12.

Atlantic Water in the eastern Fram Strait defined as water warmer than 2°C was found to have increased in temperature by ~1°C between 1997 and 2010 with a maximum in 2007 (Beszczynska-Möller et al. 2012). That analysis was based on a gridded field derived from data from all six moorings F1 to F6. Since F1 and F2 could not be recovered on PS93.1, we present a slightly different representation of the temperature evolution in the West Spitsbergen Current (Fig. 4.4). It again becomes clear that the temperature increased from 1997 until reaching a maximum in 2007. The temperatures after 2007, however, were lower than in 2007, but higher

than before such that 2007 appears to be an anomalous maximum. The temperature over the recent 8 years was relatively stable at elevated levels compared to the mid 1990s.

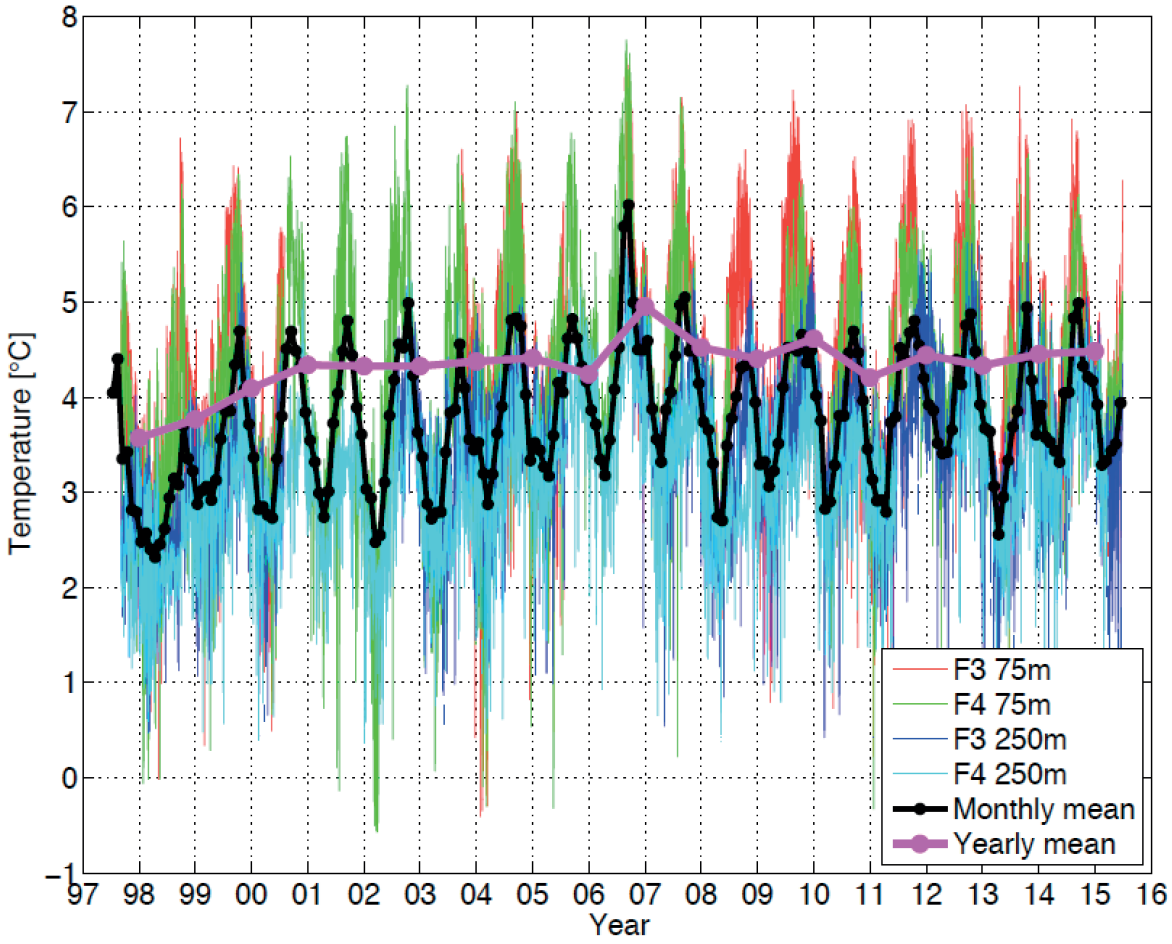

Fig. 4.4: Temperatures recorded at 75 m and 250 m depth on moorings F3 and F4 from 1997 to 2015. The monthly means of those four records are also shown as are the July to June yearly means. This figure shows similar information to Fig. 6a of Beszczynska-Möller et al. (2012).

Simplistic preliminary calibrations were applied to the UCTD downcast data. Nonetheless, the resulting temperature-salinity distribution (Fig. 4.5) seems reasonable. Offsets between the two sondes used (SN0186 and SN0240) are not discernible. However, it was found that the first downcast profile of a tow-yo section had significant offsets compared to the following profiles. This is likely due to the fact that the surface of the conductivity cell initially was dry adapted or due to the fact that the sonde initially was at room temperature rather than at water temperature. As expected the four sections (Fig. 4.2) showed the different water masses that they sampled. Section 1 was entirely in Atlantic Water. Section 2 was mostly in Atlantic Water, but also measured a mixture with meltwater. Section 3 sampled from the East Greenland shelf across the East Greenland Current and into Atlantic Water and therefore also detected proper Arctic halocline water. Finally, Section 4 was in the Greenland Sea Gyre and also detected some freshwater advected into the gyre at the surface by winds.

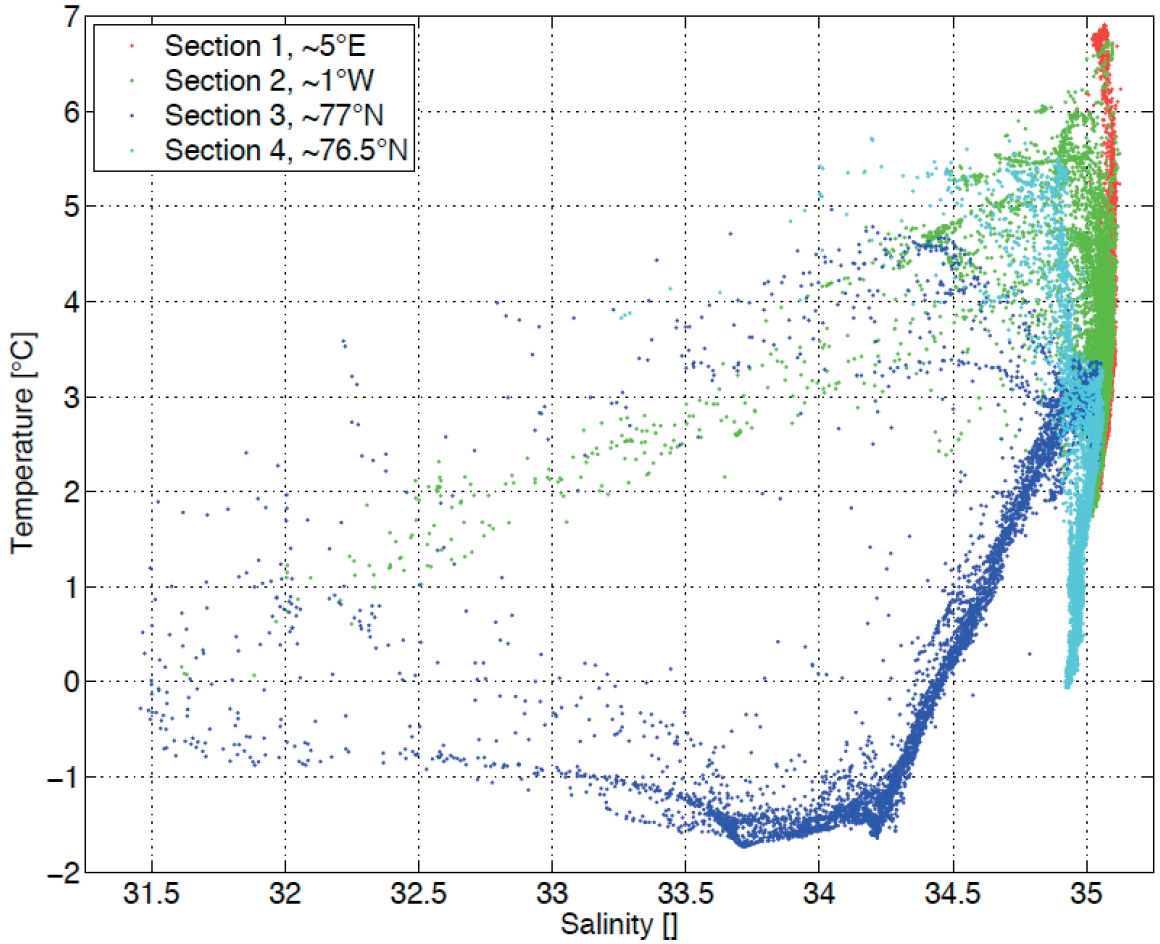

Fig. 4.5: TS diagram of the UCTD profiles on PS93.1. Section 1 near 5°E is marked in red, Section 2 near 1°W is marked in green, Section 3 near 77°N is marked in blue, and Section 4 near 76.5°N is marked in cyan.

The high horizontal resolution of the sections of between 1,200 m and 1,800 m properly resolves the hydrographic fronts. For example, section 3 (Fig. 4.6) shows that the primary front of the East Greenland Current is only about 10 km wide and the isopycnals slope by more than 50 m over this distance. This sustains the surface intensified East Greenland Current.

The gliders and floats have not returned any data yet that could be presented here.

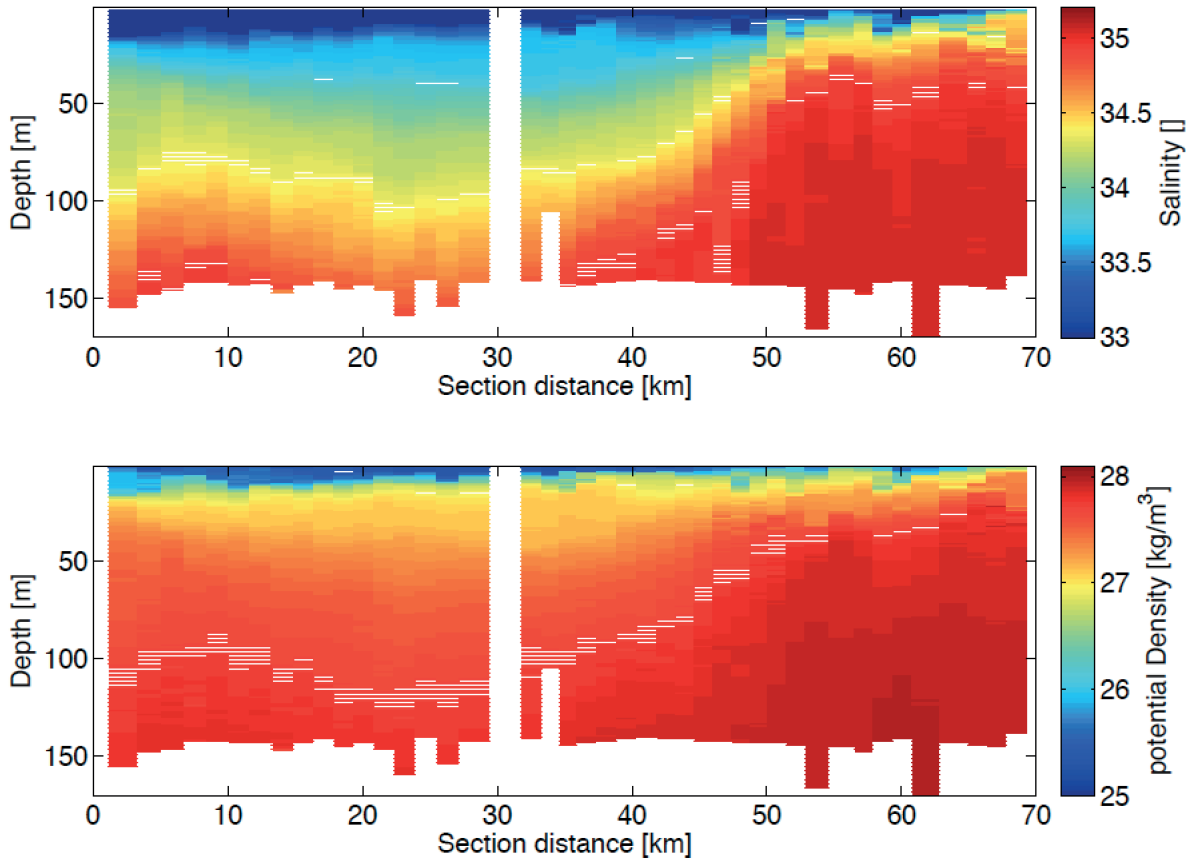

Fig. 4.6: Salinity and potential density section across the East Greenland Current (Section 3 near 77°N). The hole near 31 km section distance is due to the change from one sonde to the other and to the fact that the first cast of the new tow-yo section had to be discarded.

Data management

The CTD data collected during PS93.1 will be delivered after post-cruise calibration to the PANGAEA database and to the appropriate national data centers. The data recorded by the recovered moored instrumentation will be processed after the cruise at AWI and submitted to the PANGAEA database. The UCTD data will be calibrated after the cruise and submitted to the PANGAEA database. The gliders are piloted from AWI in real time. The calibration and final processing of the glider data will take place after completion of the mission, and the data will be delivered to the PANGAEA database. The ARGO float data will be provided in near-real time to the Coriolis data center and replaced by delayed mode quality controlled data afterwards.

References

Beszczynska-Möller A, Fahrbach E, Schauer U, Hansen E (2012) Variability in Atlantic water temperature and transport at the entrance to the Arctic Ocean, 1997–2010. ICES Journal of Marine Science: Journal du Conseil, 69(5):852–863, doi:10.1093/icesjms/fss056.

5. BIOLOGY/PLANKTON ECOLOGY

Grant No: AWI-PS93.1_02

5.1 Planktic proxy validation studies

Kirstin Werner[1], not on board: Dorothea Bauch[2] and the ArcTrain team

[1]BPCRC
[2]GEOMAR

Objectives

The Arctic Ocean is currently undergoing drastic changes due to sea ice loss. One reason for sea-ice loss in adjacent areas may be increases in seawater temperatures linked to the advection of warm and saline Atlantic Water deriving from the northern North Atlantic. The study area is not only influenced by the East Greenland Current that transports sea ice and polar waters from the Artic into the northern North Atlantic. It is also impacted by the Return Atlantic Current (RAC), a branch of Atlantic Water advected northwards by the West Spitsbergen Current which branches off towards the Western Fram Strait, hereby impacting those areas studied on this cruise.

Planktic foraminifers are widely used in paleoceanography to reconstruct past ocean variability. New insights on the modern characteristics of foraminiferal proxies under certain ambient water conditions can help enhancing modern-based proxy-to-ocean calibration. Improved calibration between foraminiferal characteristics and ambient water conditions allows for their a verified application of foraminiferal proxies to paleo records from the study area.

Work at sea

Multinet Studies

Multinet casts were carried out during the cruise collecting planktic foraminifers from different water masses in the area such as the Polar Surface Water, the Atlantic Layer, and the Upper Polar Deep Water. In total, eight multinet casts were deployed in order to complement micropaleontological investigation on planktic, nektonic microorganisms in the surface sediment records. Five nets each with a mesh size of 55 µm were applied to catch plankton samples at different water intervals. Water masses were identified according to preceding CTD casts from the same station. Plankton samples were sieved through 250 and 63 µm sieves and stained with Rose Bengal/ethanol mixture that allows for a differentiation between zooplankton that lived in a certain water column at the time of sampling from those of allochthonous origin. Further treatment of samples will be carried out in home laboratories.

Surface and Shallow Sediment Sampling

For comparison of planktic faunal assemblages as well as geochemical signatures of their calcareous shells used in paleoceanographic reconstructions, sediment surface samples were collected from multicore (MUC) tubes from the same station where multinet casts were deployed. The uppermost 1 cm of a MUC tube was sampled and stained with a Rose Bengal/

Ethanol mixture in order to ensure differentiation between individuals that relatively recently settled onto the sea floor and those being buried on the sediment surface for a longer time. In addition, every cm of the MUC tube was sampled for downcore studies of planktic foraminifera. Results of the comparison between multinet and surface sediment samples will later be applied to the foraminiferal abundance and respective geochemical conditions in downcore samples.

Water Sampling

In order to compare geochemical signatures of planktic foraminifers from multinet and sediment surface samples of MUC tubes to ambient modern water conditions, water samples were collected from each station at different depths (bottom to surface). Water samples were as well taken from bottom waters available in MUC tubes. K. Werner collected ca 120 water samples from different depths and stations for $\delta^{13}C$ and $\delta\ ^{18}O$ analyses, respectively.

Preliminary (expected) results

Surface and Shallow Sediment Sampling

K. Werner will be working on micropaleontological assemblages of planktic foraminifera and respective geochemical composition of abundant calcareous planktic foraminifer shells such as stable oxygen and carbon isotopes, trace metals, and if applicable, radiogenic isotopes. Results will be compared to geochemical signatures from both the surrounding water and the sediment surface.

Water Sampling

Analyses will be carried out in cooperation with Dorothea Bauch (GEOMAR). In addition, samples for nutrient analyses were taken for the same water depths.

Data management

Results will be uploaded to the public database PANGAEA after data having been published elsewhere in peer-reviewed journals.

5.2 Plankton Ecology and Biogeochemistry in the Changing ArcTic Ocean (PEBCAO group)

Steffi Gäbler-Schwarz and the ArcTrain team — AWI
not on board: Katja Metfies, Eva-Maria Nöthig, Ilka Peeken — (all AWI)

Objectives

The Arctic Ocean has gained increasing attention over the past years because of the drastic decrease in sea ice and increase in temperature, which is about twice as fast as the global mean rate. In addition, the chemical equilibrium and the elemental cycling in the surface ocean will alter due to ocean acidification. These environmental changes will have consequences for the biogeochemistry and ecology of the Arctic pelagic system.

Climate induced changes will also impact the biodiversity in pelagic ecosystems. A shift in species composition is expected to occur in all plankton size classes, however smallest algae may thrive the phytoplankton in the future Arctic Ocean. Diatoms, such as *Melosira arctica* as well as smaller planktonic algae will gain more importance in mediating elemental- and matter- as well as export fluxes. One of the latter, *Phaeocystis pouchetii*, having an intermediate position regarding size, can play a key role in the cycle of sulphur and carbon. Little is known about the diversity distribution, occurrence and physiology of these species in Arctic pelagic regions.

In order to examine changes, including the smallest fractions, molecular methods are well to complement traditional microscopy to assess composition and biogeography of marine protists here with the focus on the key species *Melosira arctica* and *Phaeocystis pouchetii*. The characterization of the communities with molecular methods is independent of cell-size and distinct morphological features.

Work at sea

In total 15 handnet hauls (20µm) were carried out along the cruise track to catch phytoplankton for isolation of clonal algal cultures. These handnet hauls were done at ship stations, by towing down to ~10m water up to 5 times, depending on the phytoplankton concentration in the water column and also on 4 Zodiak trips taking handnets near the ice.

Tab. 5.1: Biological stations

	Station	Date	Time	PositionLat	PositionLon	Depth [m]	Gear
1	PS93/007-1	01.07.2015	05:00	79° 22.90' N	2° 29.64' E	3062.0	Hand net
2	PS93/008-1	01.07.2015	18:22	79° 46.54' N	1° 37.66' W	2828.9	Hand net
3	PS93/010-1	02.07.2015	07:18	80° 17.11' N	6° 20.28' W	316.4	Hand net
4	PS93/011-2	02.07.2015	11:49	80° 22.75' N	6° 59.67' W	255.4	Hand net
5	PS93/016-2	03.07.2015	13:26	81° 13.03' N	7° 20.55' W	1549.2	Hand net
6	PS93/017-2	03.07.2015	23:46	81° 35.68' N	6° 35.20' W	3340	Hand net
7	PS93/018-1	04.07.2015	13:04	81° 44.15' N	8° 08.61' W	2508	Hand net
8	PS93/018-6	04.07.2015	13:15	81° 44.15' N	8° 08.48' W	2504.3	Rubber boat, Zodiak
9	PS93/019-1	04.07.2015	21:41	81° 45.10' N	9° 07.72' W	2055.7	Hand net
10	PS93/020-1	05.07.2015	07:48	82° 06.48' N	8° 58.95' W	2672.1	Hand net
11	PS93/020-7	05.07.2015	10:56	82° 05.85' N	8° 54.86' W	2803	Rubber boat, Zodiak
12	PS93/020-8	05.07.2015	11:09	82° 05.83' N	8° 54.64' W	2862.2	Hand net
13	PS93/023-1	07.07.2015	02:24	81° 15.81' N	7° 14.69' W	1501.4	Hand net
14	PS93/024-3	07.07.2015	14:59	80° 54.81' N	6° 21.84' W	1318.5	Hand net
15	PS93/024-7	07.07.2015	15:11	80° 54.82' N	6° 21.90' W	1317.7	Rubber boat, Zodiak
16	PS93/025-3	08.07.2015	01:18	80° 28.82' N	8° 29.38' W	292.1	Hand net
17	PS93/030-2	08.07.2015	22:49	79° 33.21' N	4° 50.70' W	1282.3	Hand net
18	PS93/039-2	12.07.2015	12:44	78° 44.76' N	9° 37.77' W	399.7	Hand net
19	PS93/039-9	12.07.2015	13:16	78° 44.88' N	9° 37.15' W	400.4	Rubber boat, Zodiak

All handnet samples taken were screened microscopically and the phytoplankton community composition was documented photographically with an AxioVert inverse microscope. The isolation was carried out in the cooling culture lab container with a temperature of 11°C. The isolates were stored in the back of the container at 4°C. Over the whole cruise leg the isolates where exposed to light for 24 h per day. During the cruise all samples were haltered in the cooling culture lab container on board and were brought back to the AWI directly after the cruise track. At the AWI the clonal culturing is continuing and soon molecular investigations and physiological experiments are planned with the established strains.

Preliminary results

In total 66x50 ml algal isolates have been established, and 63 field samples (in total 8.7 L) were taken for further isolation of phytoplankton species.

Data management

Cultures will be kept at AWI cool laboratories until genetic work and physiological experiments have been carried out. Data will be made available to the public via PANGAEA after publishing (depending on how many comparisons will be made, long-term study 2 to 5 years after the cruise or even later).

6. BATHYMETRIC INVESTIGATIONS

Lars Radig[1], Maria Winkler[1], Babajide Maiyegun[1] [1]AWI

Grant No: AWI-PS93.1_01

Objectives

Accurate knowledge of the seafloor topography is necessary to understand many marine processes. It is of particular importance for the interpretation of scientific data in spatial context. For barely surveyed areas like the North-East Greenland Continental Shelf (NEGCS) or other ice-covered high-latitude ocean areas, the bathymetry often provides the first view on the seafloor. Bathymetry, hence geomorphology, is furthermore a basic parameter for the understanding of the general geological setting of an area and many other geological processes such as sediment transport, sediment erosion and deposition. Also, information on tectonic processes can be inferred from the bathymetry.

During this cruise bathymetry was a key data set for the selection of target sites for sediment and rock sampling. In combination with sub-bottom profiler information, these data was used to optimise the on-site sampling strategy. For example, areas of outcropping older strata and areas of reduced or enhanced sediment accumulation were identified. In addition, the observed data directly supported other scientists on board in their work during the cruise by delivering accurate up to date depth information of the vessel's position and its proximity.

Work at sea

Bathymetric data was recorded with the hull-mounted *ATLAS Hydrosweep DS3* multibeam echosounding system. The system was controlled using *ATLAS Hydromap Control*. The *Hypack* program suite was used for on the fly visualization of the acquired data. Data storage was performed with *ATLAS Parastore* and additionally with *Hypack* raw data. Data processing and cleaning then was performed in *CARIS Hips and Sips* (see Fig. 6.1). For rapid and accurate knowledge of the seafloor topography the cleaned data was directly converted to *ArcGIS* compatible files. Otherwise the data was gridded and visualized in *QPS Fledermaus* software.

Sound velocity corrections from CTD stations were applied to the bathymetric data. Icebreaking activities disturbed the sounding signal and necessitated increased effort in cleaning the data. Due to heavy sound disturbances in the water column while icebreaking, occasionally the system lost the correct depth horizon. In such cases the system was manually steered back to the seafloor by adjusting its depth window.

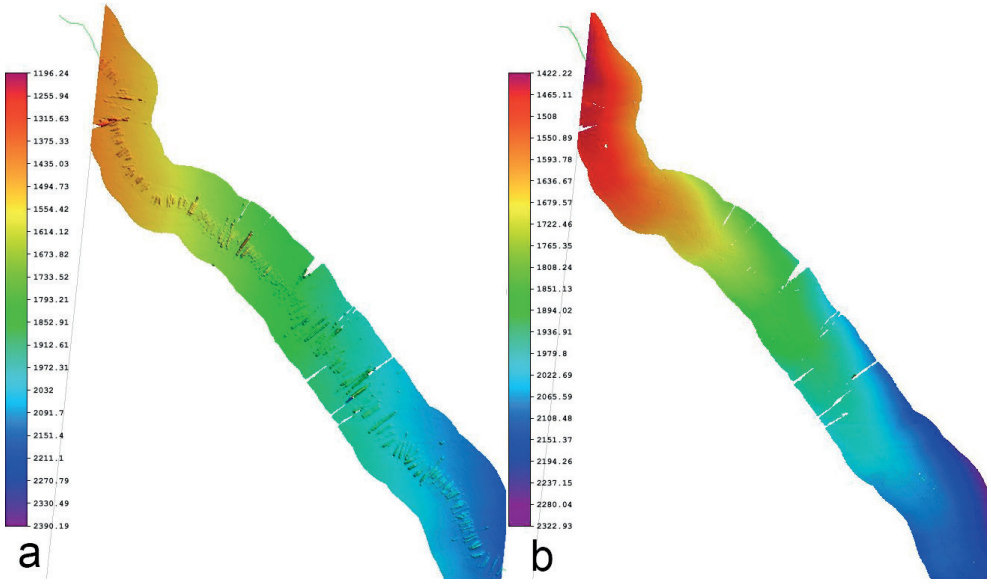

Fig. 6.1: Bathymetric data before (a) and after (b) data cleaning using CARIS Hips and Sips

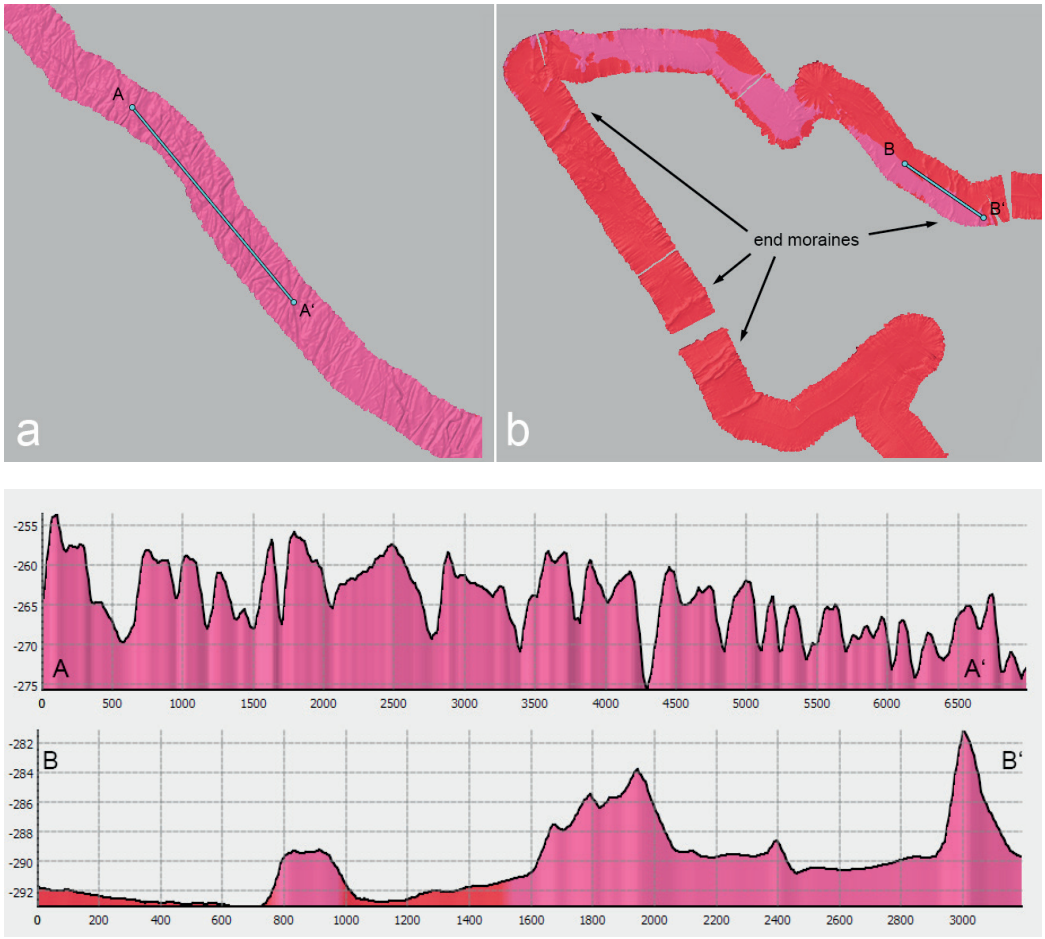

Fig. 6.2: Bathymetry showing iceberg plowmarks (a), end moraines (b) and corresponding profiles (scales in meters)

Preliminary results

The bathymetric data acquired in this expedition was used for high-resolution seabed maps along the cruise track and from the target research areas. Together with the sediment acoustic data it was analysed in detail to provide geomorphological information and the local topographic setting of the seabed in the Fram Strait. The data was made available for target site selection. In addition during transit between the research stations, survey cruises were made to increase the high-resolution swath bathymetry coverage in these areas.

Furthermore, the recorded data on the NEGCS (North-East Greenland Continental Shelf) shows again that nearly the entire shelf is covered by seafloor morphology related to recent and older glacial activity. Shoals are widely eroded by icebergs (see Fig. 6.2), most probably exported from the Arctic Ocean with the East-Greenland Current. On the other site, end moraines are showing that the Ice Sheet advanced at least until the mid-shelf in the northern Westwind Trough (Evans et al. 2008, Winkelmann et al. 2010).

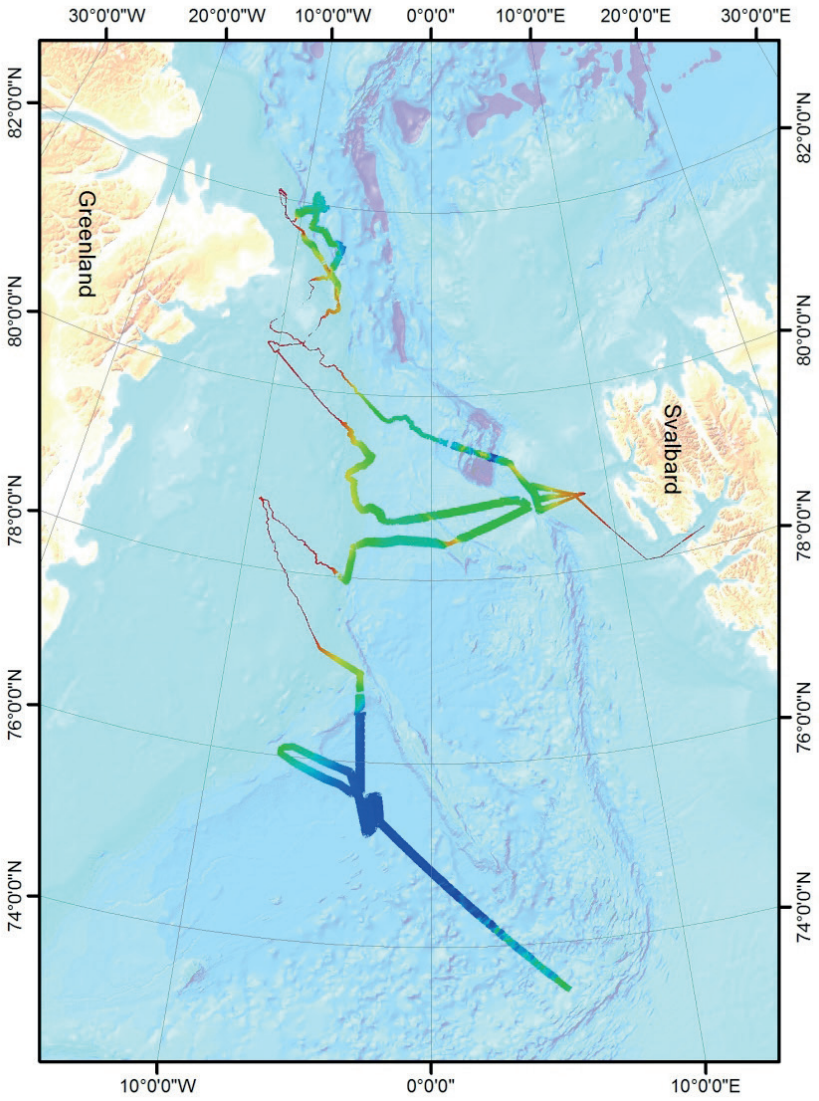

Fig. 6.3: Overview of swath bathymetry coverage of PS93.1

Data management

All acquired bathymetric data (see Fig. 6.3) will be stored at the scientific data warehouse PANGAEA at the AWI. Furthermore, the data will be provided to mapping projects and included in regional data compilations such as *IBCAO* and *GEBCO*.

References

Evans J, Cofaigh CO, Dowdeswell JA, Wadhams P (2008) Marine geophysical evidence for former expansion and flow of the Greenland Ice Sheet across the north-east Greenland continental shelf, Journal of Quaternary Science, doi: 10.1002/jqs.1231.

Winkelmann D, Jokat W, Jensen L, Schenke H-W (2010) Submarine end moraines on the continental shelf off NE Greenland e Implications for Lateglacial dynamics, Quaternary Science Reviews, 29: 1069-1077, doi: 10.1016/j.quascirev.2010.02.002.

7. MARINE GEOLOGY

Grant-No. AWI-PS93.1_01

7.1 The PS97 Marine Geology Programme: Background and summary of shipboard activities

Robert Spielhagen[1], Ruediger Stein[2], Frank Niessen[2], Michael Schreck[3], Henning Bauch[1], Matthias Forwick[4], Sigrun Hegstad[4], Tanja Hörner[2], Anne Kremer[2], Ingrid Olsen[4], Florian Petersen[5], Anna Quatmann-Hense[6], Maciej Telesinski[1], Kristin Werner[7], Antje Wildau[5] and the ArcTrain Team

[1]GEOMAR
[2]AWI
[3]KOPRI
[4]UoT
[5]UoK
[6]UoB
[7]BPRC

Objectives and background

On multimillennial and longer timescales the history of sea ice coverage and water mass distributions in the Fram Strait, as well as the linkages to terrestrial environmental variability (e.g., ice sheet growth and decay) seem quite well understood (see Stein 2008 for review). The rapid changes observed in the Arctic in the last 100 years, however, have opened questions about past natural Arctic climate variabilty within warm periods on much shorter timescales (centennials to decades). Almost all the sedimentary sequences obtained in the Fram Strait since the early 1980s had sedimentation rates in the range of 1-5 cm/1000 yr in interglacials and are thus not suitable for high-resolution paleoclimatic studies. For the Holocene history of the eastern Fram Strait (western Svalbard margin), high-resolution records have been established in the last few years by our working groups (see below). So far, no high-resolution sedimentary sequences have ever been obtained from the western Fram Strait (NE Greenland margin and shelf). Therefore, details on short-term variabilities in sea ice coverage and water mass distributions in this area remain unexplored. The same accounts for the history of last interglacial (Eemian) variability in the entire Fram Strait and Arctic Ocean.

Thus, main objectives of Expedition PS93.1 include

- to survey potential areas along the NE Greenland continental margin, on the NE Greenland shelf, and in the central Fram Strait for sites with high sediment accumulation;
- to identify the most suitable sites with unusually high sediment accumulation and obtain undisturbed long and short large-volume sediment cores from these sites;
- to obtain a set of young (recent) sediment surface samples as a reference for the reflection of modern environmental oceanic parameters (ice coverage, temperature, salinity, stratification) in shelf, slope, and deep-sea sediments.

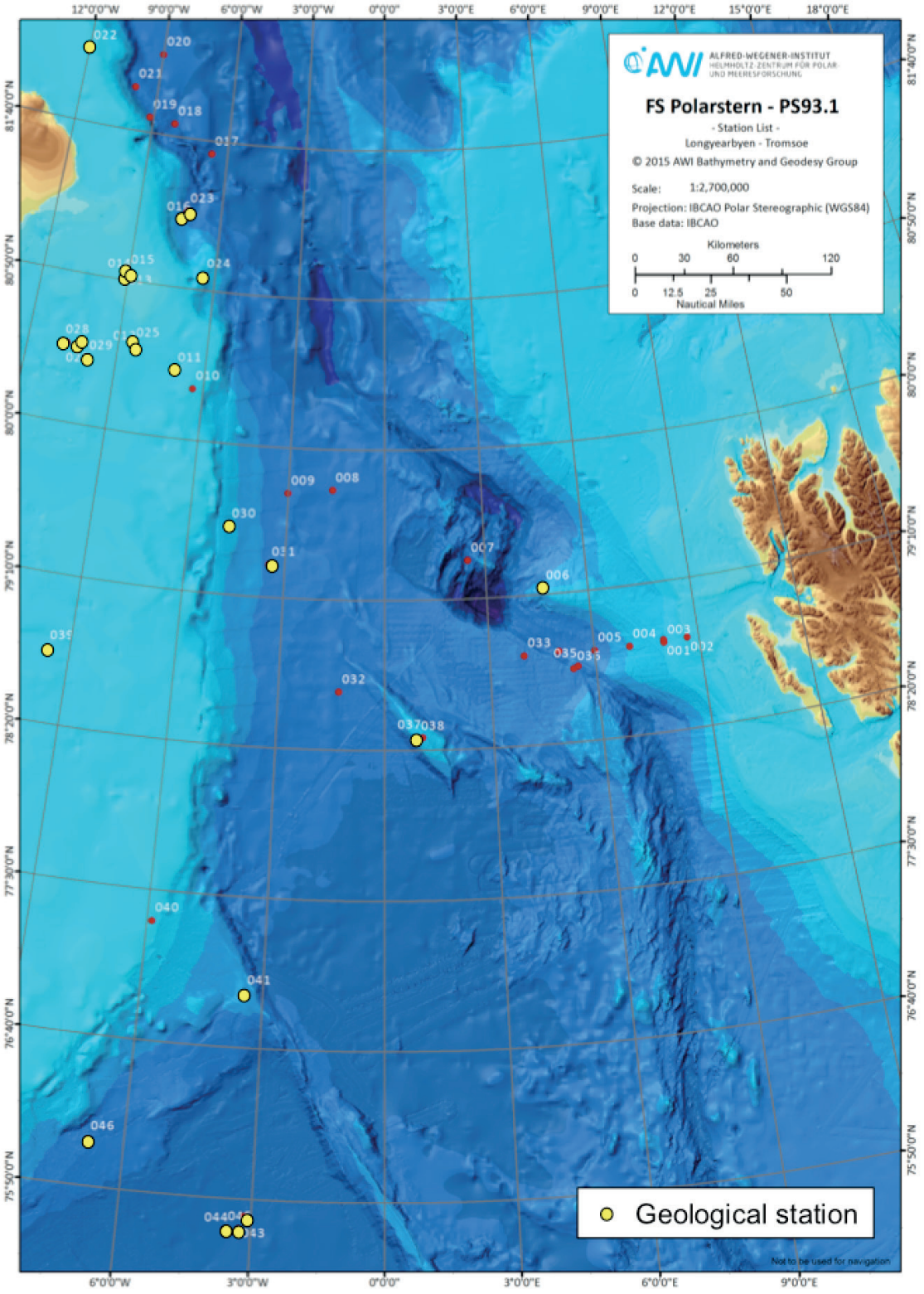

Fig. 7.1: Geological stations of Expedition PS93.1 (yellow circles)

Tab. 7.1: Geological stations of Expedition PS93.1

Station	PositionLat	PositionLon	Depth [m]	Gear Abbreviation	Recovery [cm]
PS93/006-1	79° 12.22' N	4° 40.13' E	1593.3	KAL-12m	786 cm
PS93/006-2	79° 12.20' N	4° 40.08' E	1605.2	GKG	
PS93/011-4	80° 23.13' N	6° 56.49' W	258.4	MUC	
PS93/012-1	80° 27.88' N	8° 26.33' W	295.4	GKG	
PS93/012-2	80° 27.37' N	8° 25.83' W	296.9	GC-5m	223 cm
PS93/013-1	80° 50.81' N	9° 6.17' W	58.8	GC-5m	empty
PS93/014-1	80° 51.27' N	9° 11.44' W	56.7	GC-3m	empty
PS93/015-1	80° 52.83' N	9° 2.95' W	74.9	GC-3m	empty
PS93/016-4	81° 13.02' N	7° 20.44' W	1549.8	GKG	
PS93/016-5	81□13.04' N	7°20.48' W	1568.9	MUC	
PS93/016-6	81□13.01' N	7° 20.46' W	1548.3	KAL-12m	746 cm
PS93/022-1	82° 4.12' N	11° 57.72' W	217.6	GKG	empty
PS93/022-2	82° 4.02' N	11° 57.15' W	216.5	GKG	empty
PS93/023-2	81° 15.79' N	7° 14.68' W	1500.9	GKG	empty
PS93/023-3	81° 15.43' N	7° 11.37' W	1505	GKG	
PS93/023-4	81° 15.96' N	7° 12.60' W	1509	MUC	
PS93/023-5	81° 15.11' N	7° 14.79' W	1508.2	GC-10m	624
PS93/024-4	80° 54.62' N	6° 23.43' W	1307.3	GKG	
PS93/024-5	80° 54.49' N	6° 25.09' W	1295.8	GKG	
PS93/024-6	80° 54.58' N	6° 22.90' W	1308.3	MUC	
PS93/025-1	80° 28.84' N	8° 29.24' W	291.3	GKG	
PS93/025-2	80° 28.90' N	8° 29.40' W	290.2	KAL-6m	260
PS93/026-1	80° 26.42' N	10° 13.36' W	292.5	GC-5m	168
PS93/027-1	80° 25.64' N	10° 16.64' W	284.7	GC-5m	120
PS93/028-1	80° 26.27' N	10° 40.64' W	289.3	GC-5m	229
PS93/029-1	80° 22.19' N	9° 58.50' W	307.6	GC-5m	124
PS93/029-2	80° 22.19' N	9° 58.54' W	318.2	GKG	
PS93/029-3	80° 22.18' N	9° 58.62' W	318.2	GKG	
PS93/030-4	79° 33.66' N	4° 48.84' W	1305.7	MUC	
PS93/030-5	79° 33.83' N	4° 49.36' W	1294.9	GKG	
PS93/030-6	79° 33.99' N	4° 50.54' W	1277.5	GC-10	535
PS93/031-1	79° 21.10' N	3° 28.39' W	2145.7	GKG	empty
PS93/031-2	79° 20.63' N	3° 32.03' W	2123.8	MUC	
PS93/031-3	79° 21.09' N	3° 28.36' W	2144.0	GKG	empty
PS93/031-4	79° 21.08' N	3° 28.24' W	2147.3	KAL-12	825
PS93/031-5	79° 20.97' N	3° 31.43' W	2134.5	GKG	
PS93/037-1	78° 24.09' N	1° 2.78' E	1168.9	GC-10m	413
PS93/039-4	78° 44.91' N	9° 35.73' W	400.3	GKG	empty
PS93/039-5	78° 44.92' N	9° 35.53' W	401	GKG	
PS93/039-6	78° 44.94' N	9° 35.35' W	402.4	GKG	
PS93/039-7	78° 44.97' N	9° 35.30' W	403.3	MUC	
PS93/039-8	78° 44.97' N	9° 35.12' W	402.8	GC-10m	502
PS93/039-10	78° 45.08' N	9° 35.23' W	403.4	GC-10m	681
PS93/039-11	78° 45.31' N	9° 34.95' W	400.9	GC-10m	556
PS93/041-1	76° 57.79' N	3° 26.85' W	1768.3	GKG	
PS93/041-2	76° 57.81' N	3° 26.94' W	1746.8	MUC	
PS93/041-3	76° 57.81' N	3° 26.92' W	1718.3	GC-5m	493
PS93/042-1	75° 44.39' N	3° 9.05' W	3625.8	GKG	
PS93/042-2	75° 44.39' N	3° 9.03' W	3622.3	GC-10m	empty
PS93/043-1	75° 40.20' N	3° 16.32' W	3614.3	GC-10m	352
PS93/044-1	75° 39.48' N	3° 31.52' W	3605.8	GC-10m	535
PS93/046-3	76° 5.08' N	6° 48.72' W	2457.2	GKG	
PS93/046-4	76°5.10' N	6° 48.76' W	2457.9	MUC	
PS93/046-5	76° 4.33' N	6° 49.07' W	2461.7	GC-10m	829

Work at sea

A preselection of potential survey areas has been made on the basis of experience with previous work in the Arctic and especially on the western Svalbard continental margin (see Expedition's Programme, http://expedition.awi.de/object/oai:epic.awi.de:37881). Most earlier expeditions (including RV *Polarstern* cruises to the western Fram Strait and Greenland Sea) had concentrated on the recovery of sediment cores from morphologic highs (e.g., ridges) in the deep-sea or plateaus on continental margins. However, we are now aware that boundary currents and deep-sea currents in the relatively narrow Fram Strait lead to a non-uniform deposition. Because of these current activities, fine-grained sediment material (e.g., much of the sediment made available by (sub)glacial erosion) often does not settle uniformly (i.e., as a blanket). This results in relatively low average Holocene sedimentation rates of 3-5 cm/ky on the western Svalbard margin and on morphologic highs in the central Fram Strait and in relatively coarse (5-20% >63 µm) interglacial deposits (e.g., Köhler and Spielhagen 1990; Hebbeln and Wefer 1997). In contrast, deposition of fines is found preferentially in lee positions of morphologic protrusions along the continental margins, often only at very specific water depths. Sites selected on the basis of above described considerations yielded cores with 20-30 cm/ky and very fine-grained sediments (<2% >63 µm), sufficient for paleoceanographic records with multidecadal resolution (Spielhagen et al. 2011; Müller et al. 2012).

During Expedition PS93.1, a detailed Hydrosweep and Parasound sediment echosounder surveys was conducted in the areas identified as described above. Based on this survey, sediment coring stations were selected. In total, 24 geological stations were carried-out (Fig. 7.1), and 23 sediment cores were taken by means of gravity corer and kastenlot corer, with a recovery ranging between 0 and 829 cm (Table 7.1). In addition, surface sediment samples were taken by the giant box corer (Großkastengreifer – GKG) and the multicorer (MUC) (Table 7.1).

The kastenlot cores were described and photographed on board. For a continuous sampling of these cores large-volume archive boxes were taken. Samples/subcores were stored cool or frozen for further analyses in the home laboratories. This work will comprise a huge set of analyses and proxy investigations like, e.g., XRF-scanning, grain sizes, biomarkers, stable carbon and oxygen isotopes of foraminifers, microfossil associations, Mg/Ca ratios of carbonate microfossils, clay and bulk mineralogy, etc.

Expected results and objectives of post-cruise research

Post-cruise research will concentrate on:

- Stratigraphic analyses of the sediment sequences, using a multi-proxy-approach (AMS^{14}C, oxygen and carbon stable isotopes, biostratigraphy, natural radionuclides, physical properties, XRF scanning, cyclostratigraphy, and correlation to other existing Arctic Ocean records).
- Quantification and characterization of terrigenous sediment fraction in order to reconstruct transport processes, oceanic currents, and circum-Arctic ice-sheet history (Proxies/approach: grain size, clay minerals, heavy minerals, major, minor, trace and rare earth elements, organic carbon fractions, and physical properties; analytical techniques: X-ray diffraction (XRD), X-ray fluorescence (XRF), inductivity-coupled plasma mass spectrometry (ICP-MS), and microscopy of coarse fraction as well as MSCL-logging and XRF-scanning.
-

- Reconstruction of surface-water sub-surface and deep-water characteristics: paleo-sea-ice distribution, surface-water productivity, sea-surface and deep-water temperature, deep-water ventilation, etc., using specific biomarkers (e.g., n-alkanes, sterols, alkenones; U^{k}_{37} Index, IP_{25} Index), micropaleontological proxies (dinoflagellates, foraminifers, etc.), and inorganic-geochemical proxies (stable isotopes, radiogenic isotopes, etc.). Analytical techniques to be used include LECO ($CaCO_3$, TOC, C/N), Rock-Eval pyrolysis, gas chromatography (GC), gas chromatography/ mass spectrometry (GC/MS), and high-performance liquid chromatography/mass spectrometry (HPLC/MS), XRF, ICP-MS, and microscopy as well as XRF scanning.
- Studies of sea ice and sea-ice sediments (biomarkers, mineralogy, geochemistry, biology, etc.).

Data management

All data will be uploaded to the PANGAEA database. Unrestricted access to the data will be granted after about three years, pending analysis and publication.

References

Hebbeln D and Wefer G (1997) Late Quaternary paleoceanography in the Fram Strait. Paleoceanography 12(1):65–78.

Köhler S E I and Spielhagen R F (1990) The Enigma of Oxygen Isotope Stage 5 in the Central Fram Strait. In: Geological History of the Polar Oceans: Arctic versus Antarctic (Bleil, U. and Thiede, J., eds.), NATO ASI Series C, Kluwer Academic Publishers, Dordrecht, 308:489-497.

Müller J, Werner K, Stein R, Fahl K, Moros M and Jansen E (2012) Holocene cooling culminates in sea ice oscillations in Fram Strait. Quat. Sci. Rev. 47:1-14.

Spielhagen RF, Werner K, Sørensen SA, Zamelczyk K, Kandiano E, Budeus G, Husum K, Marchitto TM, Hald M (2011) Enhanced modern heat transfer to the Arctic by warm Atlantic Water. Science 331:450-453. doi: 10.1126/science.1197397.

Stein R (2008) Arctic Ocean Sediments: Processes, Proxies, and Palaeoenvironment. Developments in Marine Geology, Vol. 2, Elsevier, Amsterdam, 587 pp.

7.2 Marine sediment echosounding using Parasound

Frank Niessen[1], Florian Petersen[2] and the ArcTrain Shipboard Team

[1]AWI
[2]UoK

Objectives

In marine sedimentary environments, bottom and sub-bottom reflection patterns obtained by Parasound characterize the uppermost sediments in terms of their acoustic behaviour down to about 100 m below the sea floor. This can be used to study depositional conditions on larger scales in terms of space and time, of which the uppermost sediments may also be sampled. The general objectives of sediment echosounding during PS93-1 were:

- to select coring stations based on acoustic pattern and reflection amplitude,
- to obtain different pattern of high-resolution acoustic stratigraphy useful for lateral correlation over shorter and longer distances thereby aiding correlation of sediment cores retrieved during the cruise, and
- to provide a high-resolution sub-botton counterpart for the sea-floor swath bathymetry recorded during the cruise.

Cruise and area specific objectives of the sediment echosounding include:

- to search for areas where interglacial deposits of the Holocene and Eemian can be cored in sufficient quantities for good time resolution,
- to localize areas with undisturbed sedimentation suitable for recording the glacial history of East Greenland on shorter and longer time scales, and
- to identify and interpret current-induced stratigraphic pattern such as sediment drift structures.

Work at sea

Since 2007 RV *Polarstern* has been equipped with the upgraded Deep Sea Sediment Echo Sounder Parasound DS III-P70 (Atlas-Teledyne Rason, formerly ATLAS HYDROGRAPHIC, Bremen, Germany). A summary of the development and technical specification of the DS III-P70 is provided by Niessen & Petersen (2015) and references therin. For more technical details the reader is referred to the system manuals provided by the manufacturer (ATLAS Hydrographic 2007a,b).

The hull-mounted Parasound system generates two primary frequencies, of which the lower frequency is selectable between 18 and 23.5 kHz transmitting in a narrow beam of 4° at high acoustic power (245 dB). As a result of the non-linear acoustic behavior of water, the so-called “Parametric Effect”, two secondary frequencies are generated of which one is the difference (e.g. 4 kHz) and the other the sum (harmonic, e.g. 40 kHz) of the two primary frequencies, respectively. As a result of the longer wavelength, the difference parametric frequency allows sub-bottom penetration up to 100 m in the Arctic marine environments (depending on sediment conditions) with a vertical resolution of about 30 cm. The primary advantage of parametric echosounders is based on the fact that the sediment-penetrating pulse is generated within the narrow beam of the primary frequencies, thereby providing a very high lateral resolution compared to conventional 4 kHz-systems. This capability, however, limits good survey results on sea-floor slopes, which are inclined by more than 4° relative to horizontal. The reason is that the energy reflected from the small inclined footprint on the seafloor is out of the lateral range of the receiving transducers in the hull of the vessel. As a consequence, the survey results are poor along some distances of the continental slopes of Svalbard and East Greenland.

Tab. 7.2: Settings of ATLAS HYDROMAP CONTROL for operating Parasound during cruise PS93-1

Used Settings	**Selected Options**	**Selected Ranges**
Mode of Operation	P-SBP/SBES	PHF, (SHF), SLF
Frequency	PHF SHF SLF	20 kHz (19.935 kHz) (44 kHz) 4 kHz (3.987 kHz)
Pulselength	No. of Periods Length	2 0.5 ms
Transmission Source Level	Transmission Power Transmission Voltage	100% 159 V
Beam Steering	none	
Mode of Transmisson	Single Pulse Quasi-Equidistant Pulse Train	Auto according to water depth Interval 400-1200 ms none
Pulse Type	Continuous Wave	
Pulse Shape	Rectangular	
Receiver Band Width	Output Sample Rate (OSR) Band Width (% of OSR)	6.1 kHz 66%
Reception Shading	none	
System Depth Source	Fix Min/Max Depth Limit or Variable Min/Max Depth	Manual Other (Atlas Hydrosweep) Atlas Parastore
Water Velocity	C-Mean C-Keel	Manual 1500 m/s System C-keel
Data Recording	PHF SLF	Full Profile Full Profile

Parasound DS III-P70 is controlled by two different operator software packages plus server software running in the background. These processes are running simultaneously on a PC under Windows-7. (i) ATLAS HYDROMAP CONTROL is used to run the system by an operator. The selected modes of operation, sounding options and ranges used during the cruise are summarized in Table 7.2. A list of abbreviations is given at the end of this chapter. (ii) ATLAS PARASTORE-3 is used by the operator for on-line visualization (processing) of received data on PC screen, for data storage and printing. It can also be used for replaying of recorded data, post-processing and further data storage in different output formats (PS3 and/or SEG-Y).

During PS93-1 Parasound digital data acquisition and storage were switched on while crossing the western Svalbard continental shelf towards the first station on 29.06.15 at 11:47 UTC (78° 11.05' N; 14° 22' E). The system was switched off in the Greenland Abyssal Plain heading back to Tromsø on 16.07.15 at 10:29 UTC (74°31.8' N; 1°10.4' E). During the entire period of acquisition the system was operator controlled (watch keeping). Book keeping was carried out including basic Parasound system settings, some navigation information and various kinds of remarks.

Time windows with data of specific interest (e.g. geological situations at or near stations) were selected and replayed during the cruise using optimal settings of ATLAS PARASTORE-3

and Software SeNT (courtesy of Hanno Keil, MARUM, University of Bremen). In addition, Parasound data from previous *Polarstern* cruises (PS62, PS64, PS66, PS72, PS74, PS86, PS87) were used during the cruise in order to preselect suitable coring locations in the area of the Fram Strait and mainly the East Greenland continental margin. This turned out to be useful, because the short time available during Leg PS93-1 did not allow any new intensive site surveys.

Preliminary results

Some Parasound records from coring stations are selected as data examples from the different areas under investigation. These areas include the eastern flank of the Fram Strait at 79°12 N, the East Greenland continental slope between 82°06' N and 76°04' N, and the East Greenland continental shelf between 80°25' and 80°29' N. If not included in the text below the Parasound records near all other stations with gravity cores are presented in Appendix 6 of this report. The lateral scales of these figures are distance (one black or white bar is one kilometre), the numbers on this scale are recording time (UTC). The dates of the stations are given in the Station List of this report. Geo-reference allocation of Parasound data (including the examples presented in this report) are handled via recording time (formate yyyymmddhhmm) for which GPS position data can be found in the *Polarstern* data acquisition system "DShip" (https://dship.awi.de/*Polarstern*-from-28-10-11.html).

In the Fram Strait west of Spitsbergen several cores with very good time resolution (e.g. of the Holocene) were retrieved during previous cruises. During PS93-1 we were searching for condensed deposits indicative of lower sedimentation rates in order to recover stratigraphic units containing the last interglacial (Eemian). Along a drift deposit the point of most condensed but still notably undisturbed sedimentation was selected to retrieve Kastenlot core PS93-1/006 (Fig. 7.2).

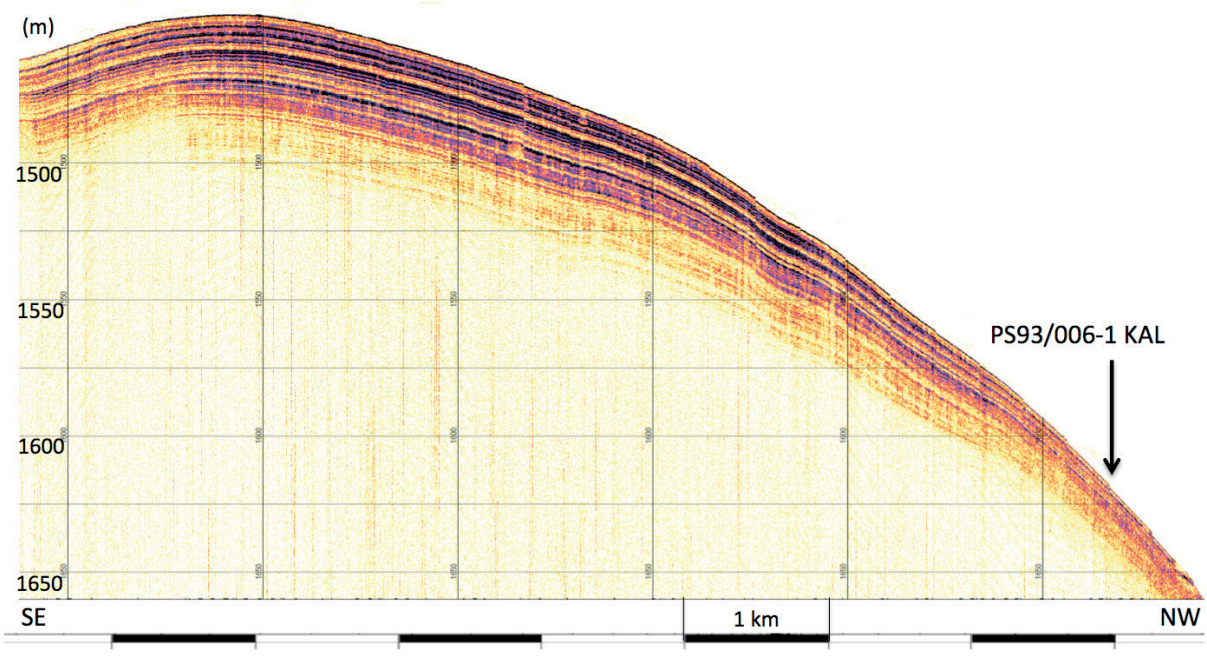

Fig. 7.2: Parasound example from the Fram Strait. End points of the profile, NE and SW are 20:21 and 20:55 UTC, respectively. The position selected to recover KAL PS93/006-1 is marked. The black and white bars at the bottom give lateral distance in km. The depth has been determined by the Parasound system.

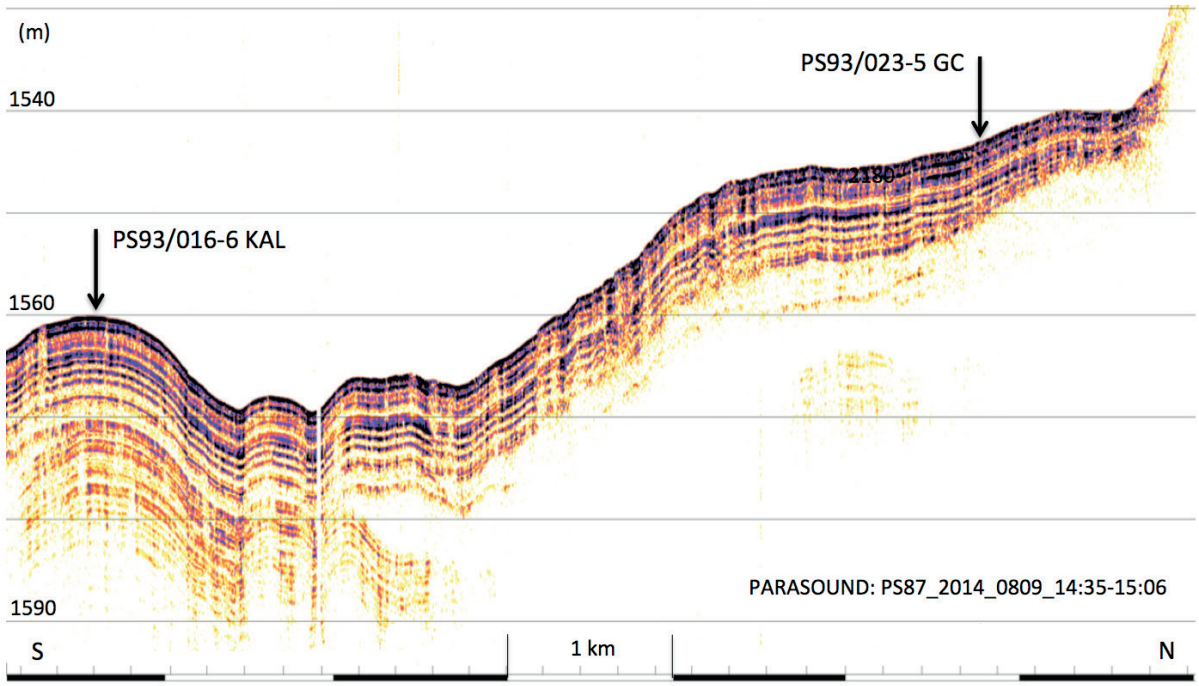

Fig. 7.3: Parasound example from the East Greenland continental slope recorded during expedition PS93.1. Position of coring locations PS93/026-6 and /023-5 are marked. The white and black bars at the bottom give lateral distance. The depth had been determined by the Parasound system. The presented time window (UTC) is 14:35 (S) - 15:06 (N).

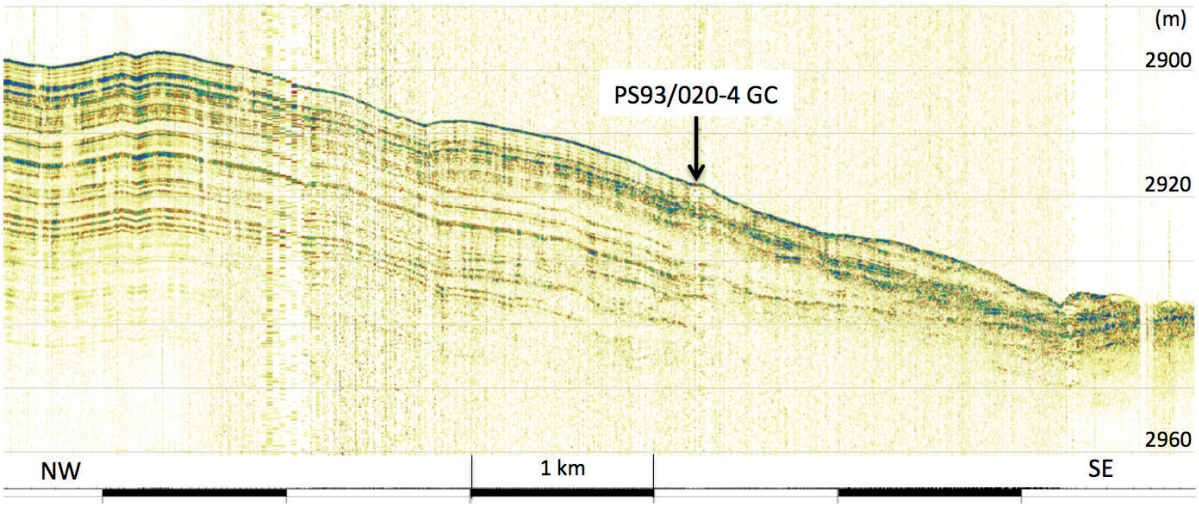

Fig. 7.4: Parasound example from the East Greenland continental slope recorded during expedition PS93.1. The black and white bars at the bottom give lateral distance. The depth had been determined by the Parasound system. The presented time window (UTC) is 07:32 (NW) - 20:42 (SE) on 05 July 2015.

The East Greenland continental slope north of 81° N is characterized by irregular topography of deeply incised canyon-like structures alternating with ridges. In places small-scale plateaux or gently inclined slopes are found, which are covered by undisturbed sediments. Bathymetrically the area is not well surveyed. Most slopes are too steep to show a sedimentary cover in Parasound profiles or are characterizes by slumps and debris flow deposits. In this area, a largely undisturbed sedimentary cover was found between 81°13' and 81°15' N during *Polarstern* cruise PS87, from which the coring sites PS93/016 and /023 were selected (Fig. 7.3). The section exhibits well-stratified sediments of up to 25 m thickness intercalating with debris flow deposits (acoustically transparent). Sediment thinning towards the northern end of the section indicates that the sedimentation is somehow influenced by currents and more condensed towards shallower water, where core PS93/023-5 was retrieved (Fig. 7.3). Another indication for current activity can be identified in the Parasound data recorded around station PS93/020 (Fig. 7.4) near 82°06' N, where well-layered undisturbed strata condense and/or are removed by erosion towards the deepest point of the section. Also, in deeper water reflectors are stronger within otherwise more diffuse backscatter pattern, which suggests an increase in sediment grain size towards this end of the profile (SE, Fig. 7.4). The overall situation may be described as a channel-levee complex. Core PS93/020-4 is retrieved from the transition between undisturbed sediments in the northwest and channel facies in the southeast of the profile (Fig. 7.4).

On the East Greenland Shelf near 80°30' N, an infill of up to 4 m of acoustically transparent undisturbed sediments of probably largely Holocene age can be found in a depression below 280 m water depth (Fig. 7.5). Core PS93/025-2 was recovered from the nearly deepest spot of what was likely a glacial trough during the LGM and/or its retreat phase. This is also the area in which submarine moraine ridges were discovered and mapped during *Polarstern* cruise PS72 (Jokat 2010; Winkelmann et al. 2010). During PS93-1 we revisited the area to recover cores outside (east), between, and inside (west) these ridges in order to possibly date the moraines (cores PS93/026-1 to PS93/029-1, see Appendix A6). An example of the glacial facies covered by a thin veneer of postglacial sediments and the sampling location of PS93/028-1 is given in Fig. 7.6.

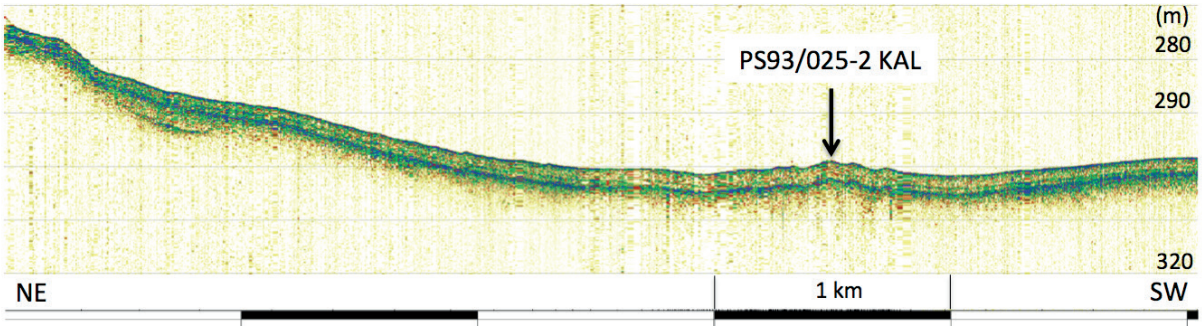

Fig. 7.5: Parasound example from the East Greenland shelf. The black and white bars at the bottom give lateral distance in km. The depth has been determined by the Parasound system. The presented time window (UTC) is 00:45 (NE) - 04:00 (SW) on 08 July 2015.

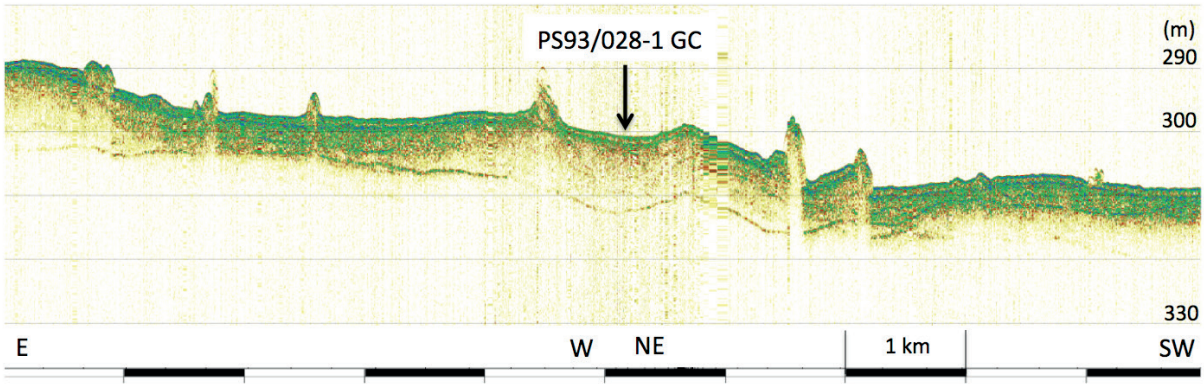

Fig. 7.6: Parasound example from the East Greenland shelf. The black and white bars at the bottom give lateral distance in km. The depth had been determined by the Parasound system. The presented time window (UTC) is 08:10 (NE) - 09:10 (SW) on 08 July 2015.

On the East Greenland continental slope near 79°30' N, the sediments are characterized by very young-appearing debris-flow deposits from the shelf break down to water depth of about 1,000 m where they interfinger with undisturbed pelagic sediments. Near this transition, core PS93/030-6 was recovered from undisturbed sediments (see Appendix A6). Further down along the Parasound line, at about 2,200 m water depth, core PS93/031-4 was retrieved from a section of well-stratified sediments (Fig. 7.7). This location was selected from Parasound data recorded during PS87 (Fig. 7.7), where the sediment cover is slightly thicker than in shallower and deeper water indicating characteristics of a sediment drift. The small differences in local sedimentation rates suggest that the influence of currents is rather weak.

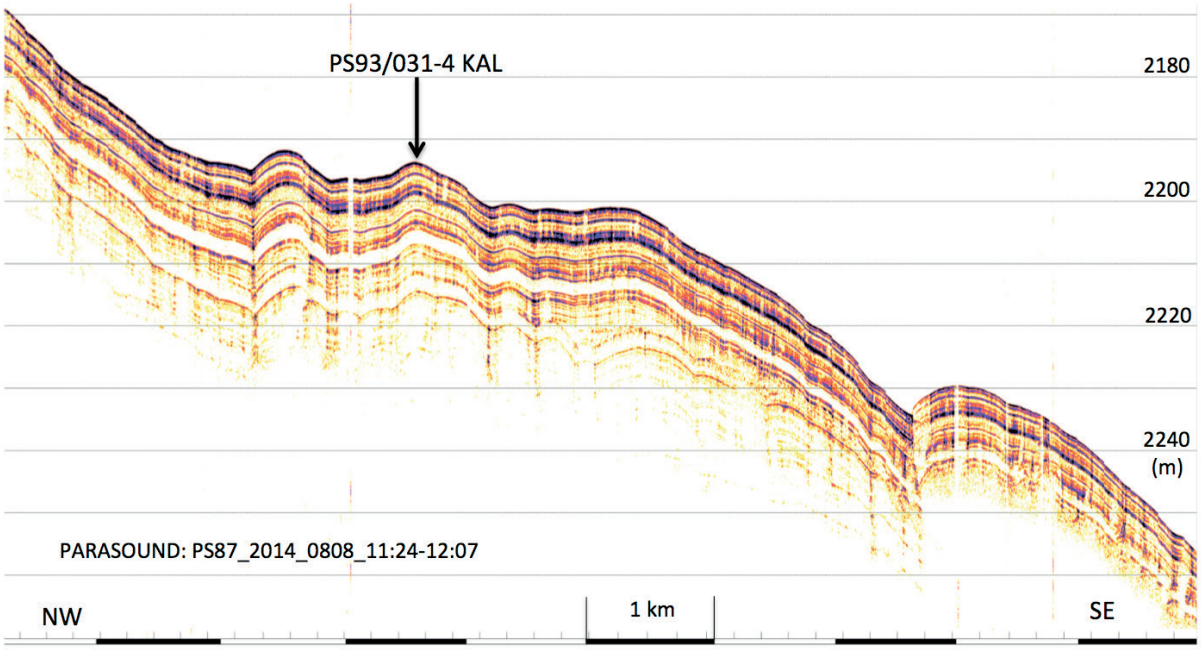

Fig. 7.7: Parasound example from the East Greenland continental slope recorded during expedition PS87 including coring position of PS93/031-4. The black and white bars at the bottom give lateral distance. The depth had been determined by the Parasound system. The presented time window (UTC) is 11:2 (SE) - 12:07 (NW) on 08 August 2014.

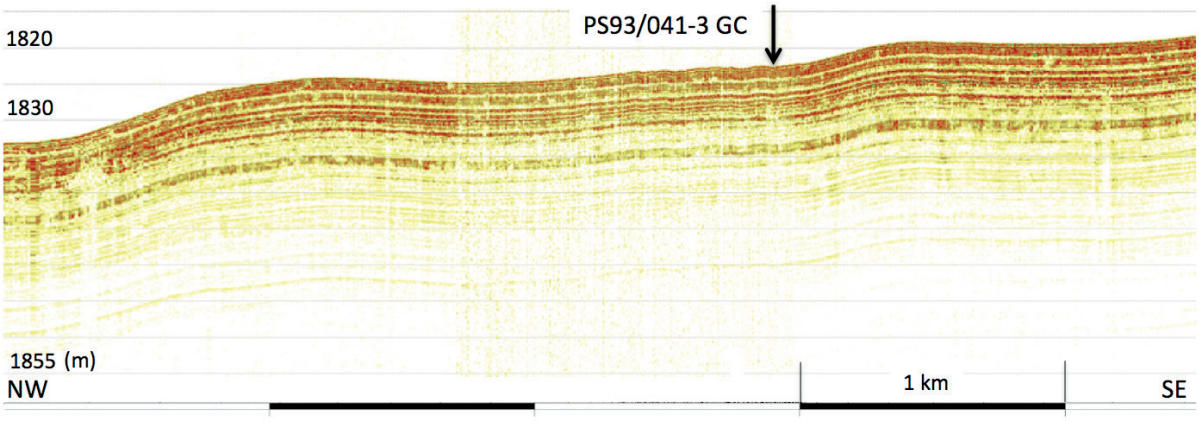

Fig. 7.8: Parasound example from the East Greenland continental slope recorded during expedition PS93-1 including coring position of PS93/041-3. The black and white bars at the bottom give lateral distance. The depth had been determined by the Parasound system. The presented time window (UTC) is 21:25 (NW) - 02:08 (SE) on 13/14 July 2015.

Core PS93/37-1 was recovered from the top of the Hovgaard Ridge (see Appendix A6). Here we re-visited a sampling location of PS87 (Stein 2015) and tried to gain more core recovery in order to date ice-grounding events on the ridge described in a recent paper by Arndt et al. (2014). On the East Greenland shelf at 87°45' N an area was sampled in a former glacial trough now filled with 5 to 6 m of Holocene mud (see Appendix A6, cores PS93/039) very similar to the situation described above for core PS93/025-2 (Fig. 7.5).

On the East Greenland continental slope south of 77° N (southern area of exploration of PS93-1) below the shelf break and at least down to 1,900 m water depth, the sediments consists of stacked debris-flow deposits typical for glacial trough-mouth fans. In a situation near 77°N, where the Greenland Fracture Zone intersects with the East Greenland continental slope, a small plateau and slope section is covered by undisturbed well-stratified pelagic sediments from 1,830 m to 1,960 m water depth, where core PS93/041-3 was recovered (Fig. 7.8). Further south, at the northern end of the Greenland Abyssal Plain we crossed over a feature, which may be a deep-sea channel-levee complex probably fed by glacial mud released from the grounding line of the LGM (and/or older) Greenland ice sheet(s). Here, in facies that belongs to the levee part of the complex, cores PS93/43-1 and /44-1 were retrieved (see Appendix A6). Large areas east of the deep-sea channel-levee complex of the northern Greenland Abyssal Plain appear like a deep-sea "sandy" fan apron with an irregular surface and very limited acoustic penetration. The last core of the expedition (PS93/046-5) was recovered from a small area on the East Greenland continental slope near 76° N, where well-stratified sediments are found in water depth of 2,500 m (see Appendix A6). These deposits may have been protected from glacial drifts and re-deposition during glacial times by a large morphological feature upslope of the coring site. Otherwise, the slope is characterized by debris-flow deposits like in most places of the East Greenland continental slope.

Data Management

Parasound data acquisition included PHF and SLF data during the entire time the system was in operation. Both PHF and SLF traces were visualized as online profiles on screen. SLF profiles (200-m depth window) and online status (60-s intervals) were saved as PNG files and printed on A4 pages. The PHF profiles (200-m depth window) were saved only as PNG

files. One system crash has occurred for no obvious reasons on 07 July at 23:06 UTC, which affected the entire system. A complete switch off and restart became necessary. Some data were lost for a time period of about two hours.

For the entire period of operation and simultaneously with sounding five different types of Parasound data files were stored on hard disc:

- PHF data in ASD format
- PHF data in PS3 format
- SLF data in ASD format
- SLF data in PS3 format
- Navigation and Auxiliary data (60s intervals) in ASCI format
- ATLAS PARASTORE 3 settings in XML files

All ASD data are automatically packed into “cabinet files” by Atlas software. The files are named according to date and time of recording (containing 10 minutes of acquired data per file). The data have been sorted by the operator into folders according to data type and recording dates (0 to 24 hours UTC), copied to the storage PC via LAN and checked for completeness and readability (ATLAS PARASTORE-3 in replay mode, selectively only). Once checked, the data folders were copied to the RV *Polarstern* mass storage for daily back ups and final transfer into the AWI database after the end of cruise. In total data with volume of 151 GB were transferred. The total time of acquisition was 17 days, 22 hours and 42 minutes.

As a result of several problems with online-printing in the past, a PNG-creator was re-installed on the operator-PC at the beginning of the cruise as it has been done during the previous cruises PS86 and 87 (Niessen and Petersen 2015). This module created files instead of hard-copy prints. An additional PNG-creator has been re-installed for auxiliary data files. The PNG files of PHF, SLF and AUX data can later be used for printing and storage and will be archived together with the actual data files.

List of Abbreviations

ASD	Atlas Sounding Data
AUX	Auxiliary
GC	Gravity Core
KAL	Kastenlot Core
LGM	Last Glacial Maximum (Marine Isotope Stage 2)
PNG	Portable Network Graphic
PHF	Primary High Frequency
P-SBP	Parametric Sub-bottom Profiling
PS3	Export format of Parasound data

SBES Single-Beam Echo-Sounder

SHF Secondary High Frequency

SLF Secondary Low Frequency

UTC Coordinated Universal Time

References

Arndt J E, Niessen F, Jokat W, Dorschel B (2014) Deep water paleo-iceberg scouring on top of Hovgaard Ridge–Arctic Ocean, Geophysical Research Letters, 41(14):5068-5074.

ATLAS Hydrographic (2007a) ATLAS HYDROMAP CONTROL Operator Manual. Doc.-Id.: ED 1060 G 312, File: ED-1060-G-312_ V5-0. Edition: 04.2007. ATLAS HYDROGRAPHIC, Bremen, Germany.

ATLAS Hydrographic (2007b) ATLAS PARASTORE-3 Operator Manual. Doc. Id.: ED 6006 G 212:/ Version: 4.0 / Edition: 05/2007. ATLAS HYDROGRAPHIC, Bremen, Germany.

Jokat W (2010) The expedition of the research vessel *Polarstern* to the Arctic in 2009 (ARK-XXIIV/3) / Ed. by Wilfried Jokat with contributions of the participants. Reports on Polar and Marine Research, 615, 181 pp.

Niessen F, Petersen F (2015) Sediment Echosounding using Parasound. In: Stein, R (Ed.) with contributions of the participants. The expedition PS87 of the Research Vessel *Polarstern* to the Arctic Ocean in 2014. Reports on Polar and Marine Research, 688, pp 87-96.

Stein R (2015) The expedition PS87 of the Research Vessel *Polarstern* to the Arctic Ocean in 2014 / Ed. by Rüdiger Stein with contributions of the participants. Reports on Polar and Marine Research, 688, 274 pp.

Winkelmann D, Jokat W, Jensen L, Schenke H-W (2010) Submarine end moraines on the continental shelf off NE Greenland - Implications for Lateglacial dynamics. Quaternary Science Reviews 29:1069-1077.

7.3. Physical properties and core logging

Frank Niessen[1], Sigrun Hegstad[2], Ingrid Olsen[2], Wei Leng[3]

[1]AWI
[2]UoT
[3]UoB

Objectives

Physical properties of sediments provide data for initial core characterization with a very high vertical resolution. Commonly physical properties are measured with automated multi-sensor tracks such as the Multi Sensor Core Logger (MSCL) manufactured by GEOTEK Ltd. (UK). In addition, MSCL data can be compared to physical properties of single samples of discrete volumes and weights in order to validate specific MSCL calibrations such as Wet Bulk Density (WBD) or volume-specific Magnetic Susceptibility (MS). Physical properties can be used to define and interpret stratigraphical patterns, including a comparison with lithology. In combination with other data, down-core pattern of physical properties provide a powerful tool for lateral core correlation. MSCL data are also useful to link the cores to high-resolution echosounding profiles obtained by systems such as the Parasound DSIII-P70 on RV *Polarstern* thereby aiding the projection of core data from a single spot of a coring station into larger spatial and temporal scales. During cruise PS93-1 a major goal of MSCL core logging is to provide high-resolution records of density, sonic velocity, and loop as well as discrete sample magnetic susceptibility.

In the following paragraphs we briefly describe the acquisition of the data and provide a few examples based on preliminary results. For a more detailed description of the physical properties data acquisition the reader is referred to the cruise report of the RV *Polarstern* expedition PS87 (Stein 2015). Descriptions of detailed analysis and core-to-core correlation are beyond the scope of this report and will be carried out after the cruise.

Work at sea

The physical properties have been measured on whole cores (gravity cores, GC), subsampling cores trumped from box cores (GKG) using GC liner, and subsampling boxes used to cut off sediments from Kastenlot cores (KAL). The logged cores including the state of data acquisition and processing are summarized in Table 7.3. Discrete samples were directly taken out of Kastenlot cores using plastic containers.

A) Whole core logging

Whole-core measurements in the ship laboratory included non-destructive, continuous determinations of core geometry (diameter), WBD, P-wave velocity (Vp), and loop sensor MS at 10 mm intervals on all cores obtained during the cruise. A standard MSCL track (GEOTEK Ltd., UK, Ser. No. 14) was used to measure temperature, core diameter, P-wave travel time, gamma-ray attenuation, and MS. The technical specifications of the MSCL system are summarized in Table 7.4. The principle of logging cores is described in more detail in the GEOTEK manual “Multi-Sensor Core Logging”, which can be downloaded from the web (http://www.geotek.co.uk). The orientation of the P-wave and gamma sensors was horizontal. GC were measured in coring liners including end caps, whereas KAL cores were measured in sub-cores retrieved from the original core using length-wise open transparent plastic boxes of 1,000 mm nominal length. In the following we summarize the data acquisition of the different sensors, data conversion to standard parameters and the calculation of secondary physical properties.

Tab. 7.3: Summary of cores logged for physical properties during Leg PS93-1 and state of processing at the end of the cruise. (x) = 2nd processing is not complete for MS (see details in text).

Station	Date	Depth [m]	Gear	Recovery [cm]	MSCL log	Process 1	Process 2
PS93/006-1	30.06.15	1593.3	KAL-12m	786	x	x	(x)
PS93/006-2	01.07.15	1605.2	GKG		x		
PS93/012-1	02.07.15	295.4	GKG		x		
PS93/012-2	02.07.15	296.9	GC-5m	223	x	x	
PS93/016-4	03.07.15	1549.8	GKG		x		
PS93/016-6	03.07.15	1548.3	KAL-12m	746	x	x	(x)
PS93/017-4	04.07.15	3351.1	GKG		x		
PS93/017-6	04.07.15	3333.7	GC-10m	563	x	x	
PS93/018-3	04.07.15	2475	GKG		x		
PS93/018-5	04.07.15	2561.4	GC-10m	612	x	x	
PS93/019-2	04.07.15	2033.9	GC-10m	678	x	x	
PS93/020-4	05.07.15	2844.7	GC-10m	510	x	x	
PS93/023-3	07.07.15	1505	GKG		x		
PS93/023-5	07.07.15	1508.2	GC-10m	624	x	x	
PS93/024-4	07.07.15	1307.3	GKG		x		
PS93/025-1	08.07.15	291.3	GKG		x		
PS93/025-2	08.07.15	290.2	KAL-6m	260	x	x	(x)
PS93/026-1	08.07.15	292.5	GC-5m	168	x	x	
PS93/027-1	08.07.15	284.7	GC-5m	120	x	x	
PS93/028-1	08.07.15	289.3	GC-5m	229	x	x	
PS93/029-1	08.07.15	307.6	GC-5m	124	x	x	
PS93/029-2	08.07.15	318.2	GKG		x		
PS93/030-5	09.07.15	1294.9	GKG		x		
PS93/030-6	09.07.15	1277.5	GC-10m	535	x	x	
PS93/031-4	09.07.15	2147.3	KAL-12m	825	x	x	(x)
PS93/031-5	09.07.15	2134.5	GKG		x		
PS93/037-1	11.07.15	1168.9	GC-10m	413	x		
PS93/039-5	12.07.15	401	GKG		x		
PS93/039-8	12.07.15	402.8	GC-10m	502	x		
PS93/039-10	12.07.15	403.4	GC-10m	681	x		
PS93/039-11	12.07.15	400.9	GC-10m	556	x		
PS93/041-1	13.07.15	1768.3	GKG		x		

Station	Date	Depth [m]	Gear	Recovery [cm]	MSCL log	Process 1	Process 2
PS93/041-3	14.07.15	1718.3	GC-5m	493	x		
PS93/042-1	14.07.15	3625.8	GKG		x		
PS93/043-1	14.07.15	3614.3	GC-10m	352	x		
PS93/044-1	14.07.15	3605.8	GC-10m	535	x		
PS93/046-3	15.07.15	2457.2	GKG		x		
PS93/046-5	15.07.15	2461.7	GC-10m	829	x		

Tab. 7.4: Technical specifications of the GEOTEK MSCL-14 used during Leg PS93-1

1. P-wave velocity and core diameter Displacement tranducer orientation: horizontal Plate-transducer diameter: 40 mm Transmitter pulse frequency: 500 kHz Pulse repetition rate: 1 kHz Received pulse resolution: 50 ns Gate: 900 Delay: 100 s
Density Radiation beam orientation: horizontal Gamma ray source: Cs-137, Ser. No. 0874/13 Activity: 356 Mbq (year 2013) Energy: 0.662 MeV Collimator diameter: 5.0 mm Gamma detector: Gammasearch2, Model SD302D, Ser. Nr. 3043 , John Count Scientific Ltd., 10 s counting time
Temperature Sensor: PT-100
Magnetic susceptibility Loop sensor: BARTINGTON MS-2C Loop sensor diameter: 14 cm Alternating field frequency: 565 Hz, counting time 10 s, precision 0.1 * 10-5 (SI) Magnetic field intensity: ca. 80 A/m RMS Counting time: 10 s

- Geometry

The core diameter (GC including liner) and core width (KAL including sub-sample box) is measured as the distance between the faces of the Vp-transducers by using rectilinear displacement transducers coupled to the Vp transducers. Three to five plastic cylinders were used lengthwise to calibrate the core-diameter logging (Table 7.5). The cylinder, of which the length is closest to the average diameter of liners (GC) or boxes (KAL) logged during the cruise, is defined as the Reference Core Thickness (RCT). Using the Geotek Utility Software A/D readings were obtained from the test panel for each of these cylinders and plotted as a function of the deviation from the reference. The resulting linear regression is put into the logger settings (http://www.geotek.co.uk) in order to log core-thickness deviation from the RCT in mm as saved in the raw-data. The sediment thickness is calculated using the following equation of the Geotek processing software module:

X = RCT - W + CTD/10;
with RCT = Reference Core Thickness;
W = total wall thickness of liner (GC) or box (KAL);
CTD = core thickness deviation (raw data in mm, see above).

In case the cores are measured including the section caps, the thickness deviation caused by caps is added to the sediment thickness, because W is assumed to be constant. The software does not allow an extra input for wall thickness of the caps (plus tape). This induces an error to both WBD and Vp calculations using Geotek processing software (see below). The Geotek processing software adds the thickness of the caps to the sediment thickness although the actual sediment core diameter will hardly vary at the caps compared to the rest of the core. A correction for this error is described in the MSCL cruise report of PS87 (Stein 2015). This correction is not applied here due to lack of time during the short cruise.

Tab. 7.5: Core-thickness calibration parameter used during PS93-1 (RCT = reference core thickness, W = wall thickness of liner or box, CYL = calibration cylinder).

	GC/GKG [mm]	**KAL transparent [mm]**
RCT	125.25	83.4
W	2 x 2.5	2 x 3
CYL 1	120.2	65.8
CYL 2	125.25	77.95
CYL 3	130.2	83.4
CYL 4		88.35
CYL 5		93.35

- Density

Wet Bulk Density (WBD) was determined from attenuation of a gamma-ray beam transmitted from a radioactive source (137Cs). A collimator was used to focus the radiation through the core-centre into a gamma detector (Table 7.4). To calculate density from gamma counts, Geotek-MSCL processing software module was used (www.geotek.co.uk), which applies the following function:

$\ln (GA) = A (GD * X)^2 + B (GD * X) + C;$

with GA = Gamma Attenuation (raw data, cps);

X = Sediment thickness (see above);

A, B, C = constants.

For calibration, A, B and C are determined empirically for each day by logging a standard core consisting of different proportions of aluminum and water as described in Best and Gunn (1999). The data of the standard stair-shaped blocks of aluminum logged in a liner (GC) or in transparent boxes (KAL) filled with water are given in Tables 7.6 and 7.7.

Tab. 7.6: Thickness and density of gamma-attenuation calibration box (KAL, transparent) filled with stair-shaped block of aluminum in water. Density of aluminum: 2.71 g/cm3, density of water: 0.998 g/cm3, internal box width along gamma ray: 7.3 mm.

Aluminium Thickness [cm]	**Average Density [g/cm³]**	**Av. Den. * Thickness [g/cm²]**
7.02	2.644	19.3
6.58	2.54	18.54
5.76	2.348	17.14
4.93	2.153	15.72
4.12	1.963	14.33
3.29	1.768	12.91
2.48	1.58	11.53
1.65	1.385	10.11
0.93	1.216	8.88
0.00	0.998	7.29

Tab. 7.7: Thickness and density of gamma-attenuation calibration liner (GC/GKG) filled with stair-shaped block of aluminum in water. Density of aluminum: 2.71 g/cm3, density of water: 0.998 g/cm3, internal liner diameter along gamma ray: 12.25 mm.

Aluminium Thickness [cm]	**Average Density [g/cm³]**	**Av. Den. * Thickness [g/cm²]**
10.00	2.40	29.35
9.01	2.26	27.65
8.01	2.12	25.94
7.01	1.98	24.22
6.00	1.84	22.49
5.01	1.70	20.80
4.00	1.56	19.08
3.01	1.42	17.37
2.00	1.28	15.64
1.01	1.14	13.96
0.00	0.998	12.23

- Porosity

Fractional Porosity (FP) is the ratio of the total volume over the volume of the pores filled with water. FP determined by MSCL-logging is not an independent data-acquisition parameter but can be calculated from the WBD using the Geotek processing software module as follows:

FP = (dg - WBD) / (dg - dw);
with dg = grain density (2.7gcm-3);
dw = pore-water density (1.03gcm-3).

This approach makes the assumption that grain density and pore-water density are constant.

- Temperature

Temperature (T) was measured as room temperature in air on top of the logging bench in the laboratory. The cores were stored for 24 hours in the laboratory before logging in order to allow equilibration with room temperature. The sensor was calibrated using water samples of known temperatures ranging from 15°C to 35°C in a similar way than described for displacement transducers above. Temperature is measured to monitor core-temperature, which is needed by the Geotek software to normalized Vp to 20°C.

- Velocity

For determination of sonic velocity across the core the travel time (TT) of ultrasonic pulses (Table 7.4) are measured which are transmitted and received via plate transducers (see geometry above). Vp was then calculated using the following equation from the Geotek processing software module:

Vp = X / (TT-PTO);
with: X = Sediment Thickness (see above);
TT = total travel time measured between the transducers (raw data in µs);
PTO = P-Wave Travel-time Offset.

The PTO is the travel time through the core liner walls (see geometry above), transducer, electronic delay, and detection offset between the first arrival and second zero-crossing of the received waveform (see GEOTEK Manual for details), where the travel time can be best detected. This travel-time offset was determined using a GC/KAL-liner filled with freshwater (Vp = 1481 m/s) logged together with the density standard (see above) and together with all logged cores (Initial Calibration Piece, see GEOTEK Manual for details). In order to find the correct PTO we used the Geotek processing software approaching the correct Vp in water (table-output function) by inputs of different PTO values into the processing panel and repetitive processing. During Leg PS93-1 we determined PTO values of 7.5 µs and 8.34 µs for GC/GKG and KAL cores, respectively.

- Magnetic Susceptibility (MS)

The specifications of the Bartington MS-2 loop sensor used on board are summarized in Table 7.4. The MS-2 meter was set to zero 200 mm before the core reached the MS sensor. Sensor was checked for possible drift above the top and below the bottom of the core by logging a

200 mm long liner (GC) and a 500 mm long box (KAL), respectively, filled with water as initial and final calibration piece. Any drift observed, which was larger than 1 or -1, was corrected assuming a linear drift over the entire core length.

MS_{dc} = MS - CD*(Drift/Core Length);
with MS_{dc} = the drift corrected MS;
MS = the MS raw data;
CD = depth in core (raw data, mbsf).

All MS data shown in this report are raw data or drift-corrected raw data (10^{-5} SI). There was not enough time to calculate volume-specific MS according to the Geotek manual.

B) Discrete samples

KAL cores PS93/016-6, PS93/025-2 and PS93/031-4 were subsampled for discrete determination of physical properties in intervals of 200 mm (Table 7.8). Plastic containers with an internal diameter and height of 25.5 mm and 26.8 mm, respectively, were filled with sediments. The sediment volume of each sample is 13.687 cm^3. During the cruise all sediment samples were measured for MS using a Bartington MS2B single sample dual-frequency sensor combined with a MS2 meter. The MS2B sensor is normalized for output values as volume susceptibility for sampling volumes of 10 cm^3. In both modes of high frequency (4.65 kHz) and low frequency (0.465 kHz) each sample was measured three times combined with three measurements in air after zeroing the meter in order to detect the system noise. The data is displaced as raw data (10^{-5} SI). The determination of WBD and volume as well as mass specific susceptibility will be carried out after the cruise.

Preliminary results

Minor gaps of data are at or near the end of individual liner sections. No meaningful Vp data are recorded along the end caps of core sections, because the arrival times of the acoustic pulse were not detectable through end caps. In addition, a fault in the thumbwheel unit to adjust Vp detection Gate and Delay (Table 7.4) on the MSCL-14 processor led to failure of Vp pulse detection. As a result, sections of cores or some entire cores have no Vp-data. On the other hand, MS and WBD logs provide nearly complete records in all cores. Thus, these parameters offer a good database for core correlation. In particular combined plots of MS and WBD versus depth (Fig. 7.9) are very useful to document numerical response to changes in the sedimentary environments, which also correlate with lithological changes. At the present level of investigation, there is no obvious lateral correlation possible between the four KAL cores PS93/006-1, PS93/016-6, PS93/025-2 and PS93/031-4. There is no example of physical properties from GC cores, because it has not been possible to carry out any secondary processing on GC cores during the cruise (Tab. 7.3).

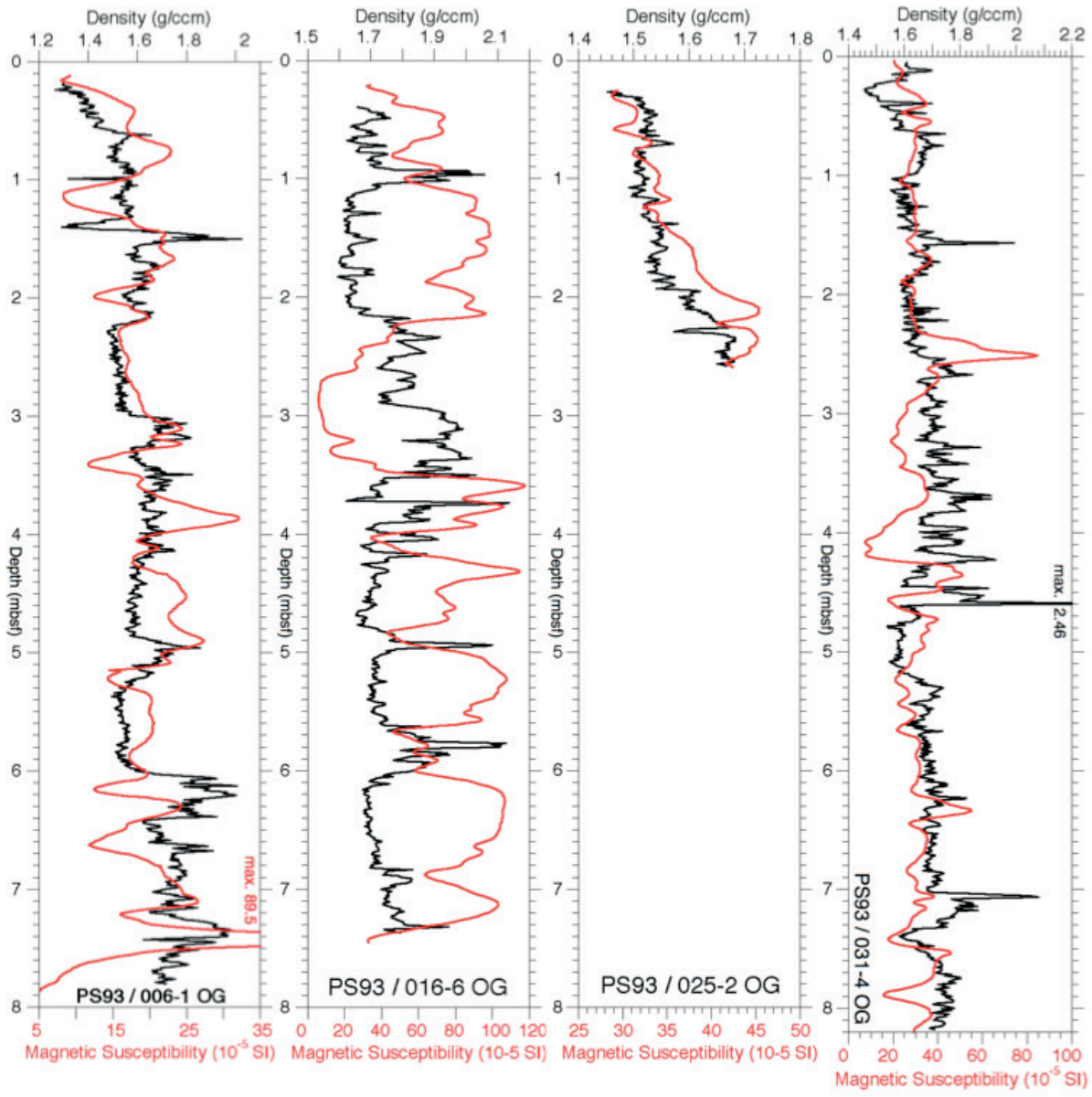

Fig. 7.9: Examples of MS and WBD logs of four KAL cores obtained during Leg 93-1

For plots of the available Vp versus corrected WBD data, a relatively good fit of a second order polynomial function with the plotted data is obvious (Fig. 7.10, core PS93/006-1). Since the data of the other two cores also show similar trends, it is suggested to use this polynomial function in order to calculate Vp data from WBD in case no Vp signals were recorded. The larger scatter in the data of core PS93/016-6 above 1.9 g cm^{-3} (Fig. 7.10) is probably the result of worse data quality rather than an invalidity of the displayed polynomial function. However, more data from the other cores are needed to test this statement.

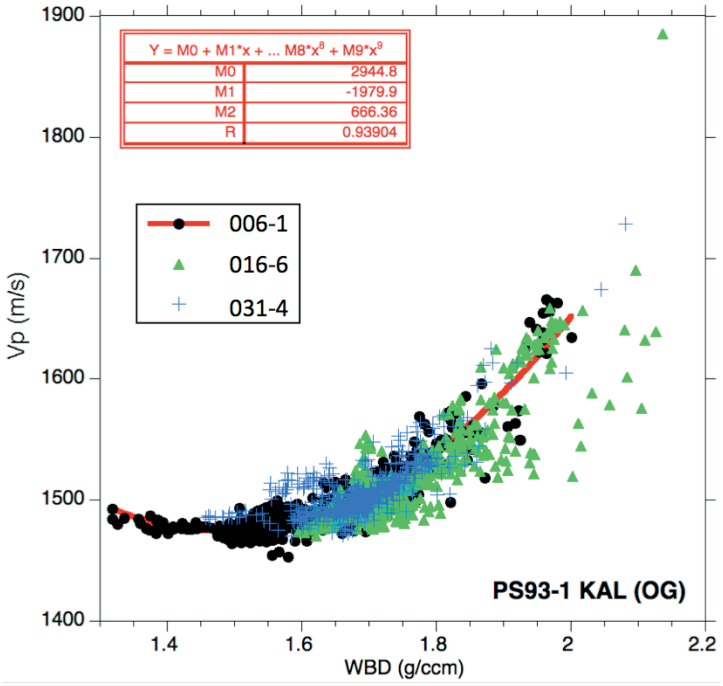

Fig. 7.10: Left: Core velocity (Vp) as a function of density (WBD). The polynomial function defined in the red box refers to data of core PS93/00:-1

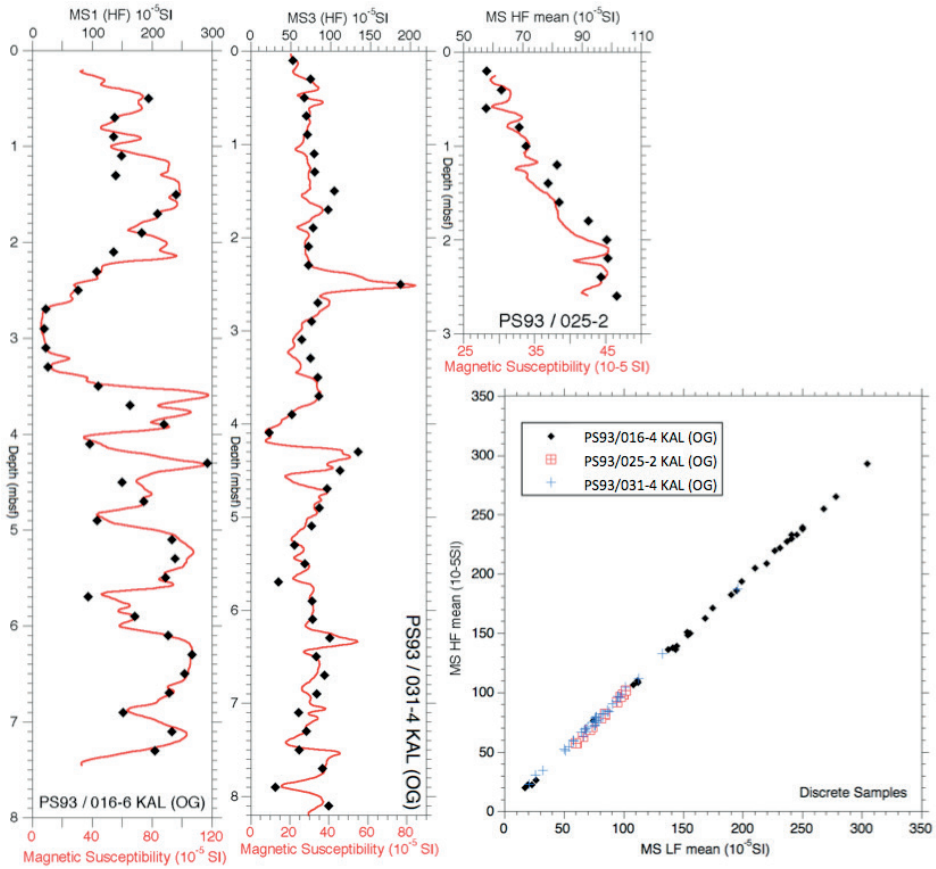

Fig. 7.11:Comparison of whole-core and discrete sample MS data (both in raw-data formate) and comparison of high frequency (HF) and low frequency (LF) MS data of discrete samples (right bottom corner).

Tab. 7.8: Dual-frequency magnetic susceptibility of discrete samples (10^{-5} SI; HF=high frequency, LF=low frequency)

	Depth	HF/SI							LF/SI						
Core	(cm)	Air	Sample	Air	Sample	Air	Sample	Air	Air	Sample	Air	Sample	Air	Sample	Air
PS93/016-6	50	3.4	193.7	3.3	193.4	3.2	193.7	3.4	-0.1	198.6	0.1	198.7	0.2	198.6	0.1
PS93/016-6	70	1.6	137.4	1.4	137.7	1.5	137.9	1.4	0.1	140	0.1	144.4	0.2	143.5	0.1
PS93/016-6	90	1.4	135.8	1.8	136.2	1.8	136.6	2	0.1	143.4	0.2	143.2	0.1	143.3	0.3
PS93/016-6	110	2	148.7	2.1	148.6	2.2	148.8	2.6	0.3	153.6	0.2	153.9	0.2	153.6	0.2
PS93/016-6	130	2.6	138.9	2.7	139.4	2.7	139.2	2.9	0.2	144	0.3	144.1	0	144.6	0.3
PS93/016-6	150	3.4	239.8	3.5	238.8	3.7	239.8	3.7	0.3	249.4	0.3	251.5	0.2	250.3	0.3
PS93/016-6	170	3.7	209	4.2	208.7	4.2	208.5	4.2	0.3	219.8	0.4	219.9	0.4	219.6	0.3
PS93/016-6	190	4.2	182.7	4.5	182.4	4.4	182.1	4.6	0.3	190.2	0.4	189.7	0.4	189.8	0.3
PS93/016-6	210	4.6	135.7	4.8	136.3	5	136.4	5.2	0.3	137.1	0.3	137.4	0.4	137.2	0.3
PS93/016-6	230	5.2	107.1	5.3	106.9	5.4	106.7	5.6	0.3	107.8	0.4	107.6	0.4	107.8	0.4
PS93/016-6	250	5.6	76.3	5.7	76.8	5.8	76.8	6.1	0.4	74.3	0.4	74.2	0.4	74.8	0.4
PS93/016-6	270	3.7	22.3	3.6	22.2	3.6	22.4	3.7	0.4	19.3	0.4	19.4	0.5	19.4	0.5
PS93/016-6	290	3.7	19.7	3.9	20	3.9	20	3.9	0.5	16.9	0.5	16.9	0.5	16.7	0.4
PS93/016-6	310	0.6	22.5	0.6	22.3	0.5	22.3	0.7	0.4	22.8	0.5	22.8	0.5	22.7	0.5
PS93/016-6	330	0.7	26.1	0.8	26.3	0.8	26.2	1	0.5	26.4	0.5	26.3	0.4	26.4	0.4
PS93/016-6	350	1	110.3	1.1	110.4	1.2	110.2	1.3	0.4	111.1	0.4	111	0.4	111.1	0.4
PS93/016-6	370	1.3	163	1.4	162.4	1.6	162.6	1.8	0.4	168	0.4	168	0.4	168.2	0.4
PS93/016-6	390	1.8	219.3	1.6	219.7	1.7	219.4	1.8	0.4	227.4	0.4	223.5	0.3	225.4	0.4
PS93/016-6	410	1.8	96.2	2.1	96.6	2.2	96.6	2.3	0.4	98.3	0.3	98.3	0.4	98.3	0.4
PS93/016-6	430	2.3	292.4	2.3	293.8	2.2	292.6	2.4	0.4	304.7	0.4	302.7	0.3	303.6	0.3
PS93/016-6	450	2.6	149.5	2.6	149.8	2.6	150.2	2.7	0.3	155.7	0.3	155.8	0.3	155.9	0.2
PS93/016-6	470	2.7	186	2.7	185	2.7	186.7	3	0.2	194	0.2	192.9	0.3	195.4	0.2
PS93/016-6	490	3	107.9	3	108.2	3.2	109	3.2	0.2	111.5	0.1	112.4	0.2	112.2	0.2
PS93/016-6	510	3.2	232.8	3.2	233.7	3.2	233	3.4	0.2	245.2	0.2	243.9	0.2	244.7	0.1
PS93/016-6	530	3.4	238.5	3.4	238.4	3.5	237.9	3.5	0.1	250.1	0.2	250.6	0.2	249.6	0.2
PS93/016-6	550	3.5	222.4	3.6	222	3.7	221.1	3.8	0.2	231.2	0.2	231.4	0.4	230.8	0.1
PS93/016-6	570	3.8	93.1	3.8	94.1	3.8	93.7	4	0.1	93	0.2	92.9	0.1	93.4	0.2
PS93/016-6	590	4	171.3	3.9	171.7	4	171.6	4.2	0.2	174.8	0.2	175.3	0.2	174.8	0.1
PS93/016-6	610	4.2	226.6	3.9	227.1	4	228.2	4	0.1	236.9	0.2	236.8	0.3	236.8	0.3
PS93/016-6	630	4.1	266.3	3.8	264.5	3.8	264.6	3.7	0.3	278.2	0.2	278.2	0.2	278.1	0.2
PS93/016-6	650	3.7	254.1	3.7	254.9	4.1	256.1	4.2	0.2	267.8	0.2	267	0.4	267.7	0.1
PS93/016-6	670	4.2	228.8	3.8	230.3	3.8	229.6	3.8	0.1	240.2	0.1	240.6	0.1	241.4	0.1
PS93/016-6	690	3.8	151.1	3.6	151.1	3.6	151.2	3.6	0.1	153.5	0	152.1	0	153	0.1
PS93/016-6	710	3.6	232.9	3.6	232.6	3.5	233.4	3.4	0.1	240.3	0.1	240.4	0	242	0
PS93/016-6	730	3.4	204.3	3.4	205.1	3.3	205.1	3.4	0	210.2	-0.1	209	0	209.6	-0.2
PS93/025-2	20	-0.2	57.5	-0.1	57.8	0	58.1	0.3	-0.2	60.4	-0.2	60.7	-0.1	60.2	-0.1
PS93/025-2	40	0	62.8	0.1	62.8	0.3	63	0.5	-0.1	65.4	-0.2	65.4	-0.2	65.7	-0.3
PS93/025-2	60	0.5	58	0.6	57.6	0.6	57.6	0.7	-0.3	59.6	-0.2	59.7	-0.3	59.8	-0.3
PS93/025-2	80	0.7	68.8	0.8	68.7	0.9	69.1	1.2	-0.3	71.5	-0.3	71.5	-0.4	71.4	-0.4
PS93/025-2	100	1.2	70.9	1.2	71.3	1.4	70.9	1.5	-0.4	73.3	-0.3	73.7	-0.4	73.3	-0.5
PS93/025-2	120	1.5	81.2	1.5	81.8	1.7	81.7	1.8	-0.5	83.9	-0.3	84	-0.2	83.9	-0.3
PS93/025-2	140	1.8	78.6	1.6	78.5	1.7	78.4	1.8	-0.3	80.9	-0.3	80.8	-0.3	80.7	-0.5
PS93/025-2	160	1.8	82	2	82.4	2.3	82.3	2.4	-0.5	84.5	-0.5	84.2	-0.5	84.3	-0.4
PS93/025-2	180	2.4	92.2	2.7	91.8	2.6	92.5	3	-0.4	94.4	-0.4	94.5	-0.3	94.3	-0.4
PS93/025-2	200	3	98.1	3.2	98.5	3.2	98.8	3.5	-0.4	99.6	-0.5	99.6	-0.4	99.6	-0.4
PS93/025-2	220	3.5	99.1	3.6	98.2	3.7	98.6	3.9	-0.4	99	-0.4	99	-0.2	99.1	-0.4
PS93/025-2	240	3.9	96.3	3.8	96.2	3.8	96.7	3.9	-0.4	97.3	-0.3	97	-0.1	96.9	-0.4
PS93/025-2	260	3.9	101.8	4.1	101.3	4.1	102	4.2	-0.4	101.9	-0.3	101.8	-0.3	101.4	-0.3
PS93/031-4	10	4.2	52.7	4.2	52.8	4.3	52.8	4.4	-0.3	50.2	-0.3	50.3	-0.3	50.1	-0.4
PS93/031-4	30	4.4	75	4.7	75	4.8	75	4.9	-0.4	73.9	-0.4	73.7	-0.4	73.7	-0.4
PS93/031-4	50	4.9	66.9	4.9	66.9	5	67.1	5	-0.4	64.1	-0.3	64.1	-0.3	64.2	-0.4
PS93/031-4	70	5	69.3	5.1	69.9	5.3	69.6	5.4	-0.4	67.9	-0.3	68	-0.3	68.1	-0.4
PS93/031-4	90	5.4	70.9	5.5	70.8	5.5	71	5.6	-0.4	69.6	-0.2	69.3	-0.3	69.3	-0.3

Tab. 7.8: cont.

PS93/031-4	110	5.6	79.3	5.3	79.1	5.6	79.5	5.7	-0.3	76.7	-0.2	76.3	0	76.3	-0.2
PS93/031-4	130	5.7	79.7	5.9	79.8	5.8	80	6.1	-0.2	76.9	-0.2	77.1	-0.2	77.1	-0.3
PS93/031-4	150	6.1	105.2	6	104.7	6.1	104.6	6.1	-0.3	101.3	-0.2	100.5	0	101.2	-0.1
PS93/031-4	170	6.1	96.8	6	96.7	6.1	96.8	6.5	-0.1	95.2	-0.2	95.7	-0.1	95	-0.2
PS93/031-4	190	6.5	78.6	6.4	78.6	6.5	78.3	6.5	-0.2	75.8	-0.2	75.9	-0.2	75.6	-0.2
PS93/031-4	210	0	72.7	0.1	72.4	0.1	72.3	0.5	-0.2	76	-0.2	76.3	-0.2	75.6	-0.2
PS93/031-4	230	0.5	72.2	0.5	72.7	0.6	72.2	0.5	-0.2	75.7	-0.2	75.4	-0.1	75.8	-0.3
PS93/031-4	250	0.5	186.8	0.5	187.3	0.6	187.8	0.6	-0.3	195.5	-0.1	195.5	-0.2	195.5	-0.1
PS93/031-4	270	0.6	83.9	0.7	83.8	0.7	83.9	1	-0.1	86.2	-0.1	86.3	0	86.1	-0.2
PS93/031-4	290	1	76.2	1.1	75.9	1.1	75.8	1	-0.2	78.8	-0.2	78.5	-0.2	79	-0.1
PS93/031-4	310	1	63.1	1.1	63.3	1	63.6	1	-0.1	65.9	-0.1	65.9	-0.1	66.1	-0.1
PS93/031-4	330	1	74.4	1.1	74.2	1.2	74.8	1.4	-0.1	77.5	-0.1	76.4	-0.1	77	-0.3
PS93/031-4	350	1.4	84.4	1.5	84.7	1.7	84.2	1.7	-0.3	87.7	-0.1	87.1	0	87.7	-0.1
PS93/031-4	370	1.7	84.8	1.8	85.8	1.8	85.3	1.9	-0.1	85.9	-0.2	85.7	-0.1	86.1	-0.2
PS93/031-4	390	1.9	51.1	1.8	51.2	1.9	51.5	2.2	-0.2	51.3	-0.2	51.4	0	51.3	-0.3
PS93/031-4	410	2.2	22.7	2.4	22.8	2.1	22.7	2.3	-0.3	20.5	-0.2	20.4	-0.1	20.5	-0.2
PS93/031-4	430	2.3	132.2	2.3	132.7	2.4	134.3	2.5	-0.2	131.9	-0.3	132.8	-0.2	131.7	-0.3
PS93/031-4	450	2.5	112	2.5	111.6	2.6	112	2.6	-0.3	111.9	-0.3	112.4	-0.3	113.1	-0.2
PS93/031-4	470	2.6	95.7	2.5	95.8	2.6	95.9	2.6	-0.2	96.6	-0.3	97	-0.2	96.7	-0.3
PS93/031-4	490	2.6	85.2	2.6	85.4	2.8	85.6	2.5	-0.3	85.6	-0.4	86.3	-0.2	86.3	-0.4
PS93/031-4	510	2.5	76.7	2.9	76.3	2.7	76.2	2.6	-0.4	76.9	-0.3	76.9	-0.1	77.2	-0.4
PS93/031-4	530	2.6	54.5	2.8	54.7	2.9	54.7	2.8	-0.4	53.8	-0.3	53.8	-0.3	54	-0.4
PS93/031-4	550	2.8	67.9	3.1	66.8	2.9	67.6	2.7	-0.4	68.7	-0.3	68.6	0	68.7	-0.5
PS93/031-4	570	2.7	35	2.8	34.7	2.7	34.6	2.8	-0.5	32.2	-0.4	31.9	-0.4	32.1	-0.5
PS93/031-4	590	2.8	75.1	2.7	76	2.9	76.6	3.1	-0.5	76.4	-0.4	76.5	-0.5	77.1	-0.5
PS93/031-4	610	3.1	78	3.2	77.4	3	77.2	3	-0.5	78.4	-0.5	78.5	-0.3	78.9	-0.5
PS93/031-4	630	3	98.7	2.8	98.8	3	98.9	3.3	-0.5	97.5	-0.5	98.6	-0.4	98.7	-0.4
PS93/031-4	650	3.3	81.8	2.8	81.6	2.9	81.9	3	-0.4	82.4	-0.3	82.6	-0.5	82.4	-0.4
PS93/031-4	670	3	93.6	2.9	92	2.9	92.3	3.1	-0.4	93.9	-0.4	93.8	-0.4	93.3	-0.4
PS93/031-4	690	3.1	82.3	3	81.9	2.9	82.4	3.5	-0.4	80.9	-0.5	81.2	-0.5	81.8	-0.4
PS93/031-4	710	3.5	59.2	3.1	59.4	3.3	60	3.6	-0.4	57.2	-0.5	57.7	-0.6	58.1	-0.6
PS93/031-4	730	3.6	69.3	3.5	69.4	3.6	69.6	3.9	-0.6	67.2	-0.4	67	-0.5	67	-0.5
PS93/031-4	750	3.9	60.1	3.7	59.5	3.9	60.2	4.2	-0.5	57.5	-0.5	57	-0.7	57.2	-0.5
PS93/031-4	770	4.2	90.5	4.1	90.5	4.4	90	4.4	-0.5	90.2	-0.7	90.1	-0.5	91.6	-0.6
PS93/031-4	790	4.4	30.6	4.5	30.5	4.7	30.7	4.8	-0.6	26.1	-0.5	25.9	-0.6	26	-0.6
PS93/031-4	810	4.8	96.9	4.9	97.1	5.1	97.3	5.3	-0.6	95.2	-0.7	94.9	-0.7	95.2	-0.6

Visual comparisons of single-sample sensor MS data with those obtained by the MSCL loop sensor generally show good correlations (Fig. 7.11). However, a perfect correlation cannot be expected, because the loop data are obtained from a larger core volume as the single sample data so that data from different material is compared. Also, the effect of clasts in the core is more pronounced in loop data than in single sample data, because larger clasts do not fit into the single sample containers. In addition, some differences between loop and single-sample data seem to be caused by the limited resolution of the loop sensor (Fig. 7.11) integrating over nearly 20 cm depth range of the cores in a similar way like a Gaussian Filter would smooth high-resolution point data sampled in 10 mm intervals.

A first comparison low-frequency and high-frequency MS data (Fig. 7.11, Table 7.8) exhibits a nearly linear relationship with a gradient of close to 1. This demonstrates only minor differences in response of the samples to magnetic induction by different frequencies. This result indicates that there is no significant content of very fine-grained ferrimagnetic minerals, described as superparamagnetic, in the samples. Superparamagnetic minerals are mostly secondary in origin such as bacterial magnetite or authigenic/biogenic greigeite and react very sensitively to dual-frequency magnetic induction. Thus, the lack of superparamagnetic minerals suggests that the origin of magnetic minerals is detrital and most likely entirely terrestrial.

Data management

Data acquisition and processing of whole cores are summarized in Table 7.3 and went through several steps:

MSCL Raw-data acquisition of whole cores using GEOTEK software.

First processing of whole-core data using GEOTEK software. This includes the calculation of core thickness, Vp, and WBD. WBD data have errors along liner caps. MS sensor response remained in raw-data state (10^{-5} SI).

Second processing of whole-core data using software Kaleidagraph ™. This includes a data quality control on calibration sections logged on top and below the bottom of the core (200 mm liner filled with water) and a removal of these data from the core. It also includes a correction of core-section length according to the obtained recovery (e.g. elimination of errors induced by core caps for GC or box walls for KAL adding to the recovery during logging), and cleaning for odd data points. In addition, MS is corrected for sensor drift. A full second processing was not carried out as the MS was not yet converted to volume-specific susceptibility. For this reason second processing is marked (x) in Table 7.3.

All data will be available to the shipboard science party for joint publication. In addition the data is stored as a function of core depth in the databank PANGAEA (www.pangaea.de) once fully processed and corrected on land.

References

Best A I, Gunn DE (1999) Calibration of marine sediment core loggers for quantitative acoustic impedance studies. Marine Geology, 160:137-146.

Stein R (2015) The Expedition PS87 of the Research Vessel POLARSTERN to the Arctic Ocean in 2014 with contributions of the participants. Reports on Polar and Marine Research, 688, 273pp. doi:10.2312/BzPM_0688_2015 or http://doi.org/10.2312/BzPM_0688_2015.

7.4 Surface and near-surface sediment sampling during PS93.1

Robert Spielhagen[1], Anna Quatmann-Hense[2], Antje Wildau[3], Anastasia Zhuravleva[1], and the ArcTrain Team

[1]GEOMAR
[2]UoB
[3]UoK

Objectives

Sampling and analysis of surface sediments are important because (provided there is no erosion) these sediments and their physical and chemical properties are thought to reflect the modern environment at the core site. Therefore a detailed assessment of the sediment composition with regard to sediment transport (e.g., by icebergs or sea ice) and of organism occurrences, abundances, diversity and potential for preservation is necessary. It gives important information needed for the interpretation of downcore sediment variability as a reflection of paleoenvironmental change. In addition, recovery of sea floor deposits by a box corer provides undisturbed samples of the uppermost sediment column which is, because of the high water content, often disturbed in long sediment cores .

Sediment sampling with a giant box corer (GKG) was performed during expedition PS93.1 as a standard procedure at the majority of the marine geological stations (Table 7.1). The box corer (manufactured by Fa. Wuttke, Henstedt-Ulzburg, Germany) has a total weight of ca. 500 kg and a maximum sample volume of 0.15 m^3 (box measures: 50*50*60 cm). It was successfully deployed at 16 stations, but failed several times due to problems probably caused by the large swivel used at the first stations. The use of a smaller swivel strongly improved the success rate of giant box corer deployments. At station PS93/022 (Greenland shelf) sampling failed because a large rock fragment (diameter ca. 30 cm) was captured and damaged the metal box. All box cores were photographed (surface and vertical profile) and visually described.

From each successful box corer a set of surface sediments was obtained:
- 100 ml NUNC container (palynology: de Vernal/GEOTOP Montreal)
- 100 ml NUNC container (sediment chemistry: Stein et al.)
- 100 ml NUNC container (sedimentology/mineralogy: Stein et al.)
- 100 ml NUNC container (planktic foraminifera, stable isotopes: Spielhagen)
- 50 ml glass vial (org. geochemistry: Stein/Hörner)

After openening of the box cores, downcore sampling was performed as follows:

- 2 archive tubes of diameter 12 cm (AWI archive)
- 1 archive box (50 x 15 x 8 cm cm; AWI archive)
- 2 archive boxes (50 x 15 x 8 cm cm; planktic foraminifera, stable isotopes: Spielhagen)
- 1 archive box (50 x 7.5 x 8 cm; org. geochemistry: Stein/Hörner)
- 20 ml syringes for dry bulk density at 1, 5, 10, 15, 20, 30, 40, 50 cm (Spielhagen)
- 2 X-ray slabs

Apart from the archive tubes, which were pressed into the sediment from the top, all other downcore sampling was performed parallel to the stratification. Usually the narrow archive box was logged (MSCL, see Chapter 7.3).

Table 7.9. Giant Box Corer (GKG) stations and characteristics of the near-surface sediments

Station no.	Depth (m)	Location	Recovery (cm)	Color	Lithology	Remarks
PS93/006-2	1605	Western Svalbard margin	46	Dark grayish brown (2.5Y4/2)	Sandy silty clay	Even surface, abundant arenaceous benthic foraminifers, rare small IRD
PS93/012-1	295	Northeast Greenland shelf	37	Dark grayish brown (2.5Y4/2)	Sandy silty clay	Even surface, channel-like structures, common sm. mudballs
PS93/016-4	1550	Northeast Greenland continental margin	41	Dark grayish brown (10YR4/2)	Sandy clayey silt	Uneven surface, 3 crater-like struktures, abundant arenaceous benthic foraminifers, abundant IRD, common small mudballs
PS93/017-4	3351	Northeast Greenland continental margin	41	Brown (10YR4/3)	Sandy silty clay	Even surface, Abundant small mudballs
PS93/018-3	2475	Northeast Greenland continental margin	33	Dark grayish brown (10YR4/2)	Sandy silty clay	Even surface, one crater-like structure, common arenaceous benthic foraminifers, abundant calc. be. foram., common small IRD and mudballs
PS93/019-3	2033	Northeast Greenland continental margin	20		Gravelly sandy silty clay	Surface tilted (45°), even surface, very abundant gravel (mostly black), common large be. foram.
PS93/023-3	1505	Northeast Greenland continental margin	41	Dark grayish brown (10YR4/2)	Sandy silty clay	Even surface, abundant sponges (4-8 cm), common bivalves and arenaceous benthic foraminifers, common IRD, mudballs, gastropods
PS93/024-4	1307	Northeast Greenland continental margin	33	Dark grayish brown (10YR4/2)	Sandy silt	Uneven surface, common sponges (3-8 cm), abundant small mudballs, common bivalves, arenaceous benthic foraminifers, IRD
PS93/025-1	291	Northeast Greenland shelf	45	Dark grayish brown (2.5Y4/2)	Sandy silty clay	Soft even surface, common large calc. be. foram., rare small mudballs and worm tubes
PS93/029-2	318	Northeast Greenland shelf	40	Dark grayish brown (2.5Y4/2)	Sandy silty clay	Soft even surface, common large calc. be. foram., rare sm. mudballs and worm tubes
PS93/030-5	1294	Northeast Greenland continental margin	45	Dark grayish brown (10YR4/2)	Sandy silty clay	Even surface, abundant arenaceous benthic foraminifers, common small IRD and mudballs
PS93/031-5	2135	Northeast Greenland continental margin	38	Dark grayish brown (10YR4/2)	Sandy silty clay	Even surface, 4 crater-like structures, abundant arenaceous benthic foraminifers, abundant Pyrgo and small mudballs
PS93/039-5	401	Northeast Greenland shelf	43	Very dark grayish brown (10YR3/2)	Silty clay	Soft even surface, abundant planktic foraminifers, common calcareous benthic foraminifers and mudballs
PS93/041-1	1768	Northern Greenland Fracture Zone	40	Dark brown (10YR3/3)	Sandy silty clay	Even surface, 4 crater-like structures, abundant arenaceous benthic foraminifers and small mudballs, common Pyrgo
PS93/042-1	3625	Northern Greenland Sea	44	Dark brown (10YR3/3)	Sandy silty clay	Even surface, 4 crater-like structures, abundant arenaceous benthic foraminifers and small mudballs, common Pyrgo
PS93/046-3	2457	East Greenland continental margin	36	Dark grayish brown (2.5Y4/2)	Sandy silty clay	Even surface, abundant arenaceous benthic foraminifers, planktic foraminifers, calc. benthic foraminifers, common IRD and mudballs

Preliminary results

Characteristics of surface sediments

The sediment surfaces recovered by the box corer consisted of soft, silty and clayey sediments of dark grayish brown color, with a variable content of coarser grains and biogenic organisms (Table 7.9). An exception was the northernmost box core station PS93/19 (81°45'N) where the sea floor was largely covered with gravel, interpreted as ice-rafted debris. In most cases the surfaces were even, but at five sites, burrowing organisms had formed crater-like structures with diameters of several centimeters. At sites from the continental margin and deep-sea, elongated arenaceous benthic foraminifers up to several centimeters in length were abundant at the sediment surface, often together with smaller calcareous benthic foraminifers. Small mudballs (<2 cm) were a common feature at almost all sites and reflect the melting of sea ice and deposition of sediment accumulations (cryoconites) which had formed in the ice surface. Dropstones were found as single occurrences at only a few sites, with exception of Stn. PS93/022 (where the box corer was damaged by a large stone of 30 cm) and of Stn. PS93/019.

Uppermost sediment sequences

The composition of the uppermost sediment sequence varied with region and water depth. The one box core from the Svalbard margin (Stn. PS93/006) consisted of homogeneous dark gray sandy silty clay with brownish deposits at the top (4 cm) which likely represents the oxidized layer.

Three box cores were obtained from the NE Greenland shelf at ca. 80.5°N (Stns. PS93/012, /025 and /029) from water depths of ca. 300 m. They were very similar in color and lithology, consisting of homogeneous sandy silty clay which was dark grayish brown in the uppermost 3-5 cm (oxidized layer) and dark gray below. Coarse ice-rafted debris was absent or very rare which suggests that deposition of rock fragments from icebergs played only a very minor role on this part of the Greenland shelf during the last 1-2 millennia that may be represented by the sequences contained in the box cores. The one box core obtained from the shelf at 78.45°N (Stn. PS93/039, 401 m water depth) was very similar, but the uppermost brownish layer was somewhat thicker (ca. 7 cm) and the sediment appeared more fine-grained (silty clay).

The box cores from the NE Greenland continental margin obtained between 79°20' and 81°45'N at water depths of ca. 1,300-3,350 m contained sedimentary sequences which were more variable in color and grain size than the cores from the shelf. The colors ranged from brown to dark grayish brown and at most sites several layers could be distinguished in the uppermost 30-40 cm of the sediment column. Some of these layers appeared almost perfectly homogenized, while in others horizontal and vertical burrows and streaky features reflect a strong mixing by burrowing organisms. Sandy silty clay is the dominating lithology in the cores, but single layers appeared more fine-grained and consist of silty clays with very few or no sandy components. At stations PS93/016, /024, /030 and /031 (79°20'-81°13'N), the lowermost layer of the box cores contained common or even abundant dropstones up to several centimeters in size. The core depth of the top of this layer varied between 13 and 35 cm. Tentatively, this layer is correlated to the deglaciation of the Greenland shelf which occurred at ca. 17-12 ka, according to a compilation by Funder et al. (2011). Since little is known about the timing in NE Greenland, the cores obtained during expedition PS93.1 may help to elucidate the deglaciation history of this part of the Greenland shelf.

The box cores from the southern part of the working area (Stns. PS93/041, /042, /046; northern Greenland Fracture Zone and northernmost Greenland Sea) mostly consisted of sandy silty clay layers of colors varying from brown to dark grayish brown. At sites PS93/042 and /046 more sandy layers were intercalated in the lower part of the cores. The deposits were strongly burrowed or even perfectly homogenized. In the core from site PS93/046 the uppermost layer

of ca. 17.5 cm thickness contained abundant calcareous benthic and planktic foraminifers and is tentatively assigned to the Holocene. Dropstones were rare in the cores from this area and may indicate that deposition from icebergs was not a a dominating factor during the time represented by the uppermost 30-40 cm of the sediment column.

Data management

Raw data and processed data (shipboard and shorebased), as well as core photos, core descriptions and X-ray photos will be made available in PANGAEA

References

Funder S, Kjellerup Kjeldsen K, Kjær KH, Ó Cofaigh C (2011) The Greenland Ice Sheet During the Past 300,000 Years: A Review. In Ehlers J, Gibbard PL, Hughes PD, editors: Developments in Quaternary Science, Vol. 15, Amsterdam, The Netherlands, 699-713.

7.5 Main lithologies and lithostratigraphy of PS93.1 kastenlot cores

Ruediger Stein[1], Frank Niessen[1], [1]AWI
Maciej Telesinski[2] [2]GEOMAR

Objectives

One important objective of the shipboard studies of the opened PS93.1 sediment cores was the establishment of a preliminary lithostratigraphy and age model of these cores, based on visual core description, MSCL records and correlation with dated sediment cores recovered in the study area in 1997 during Expedition ARK-XIII/2 (Stein and Fahl 1997) and Expedition ARK-XIII/3 (Krause 1998) (Fig. 7.12).

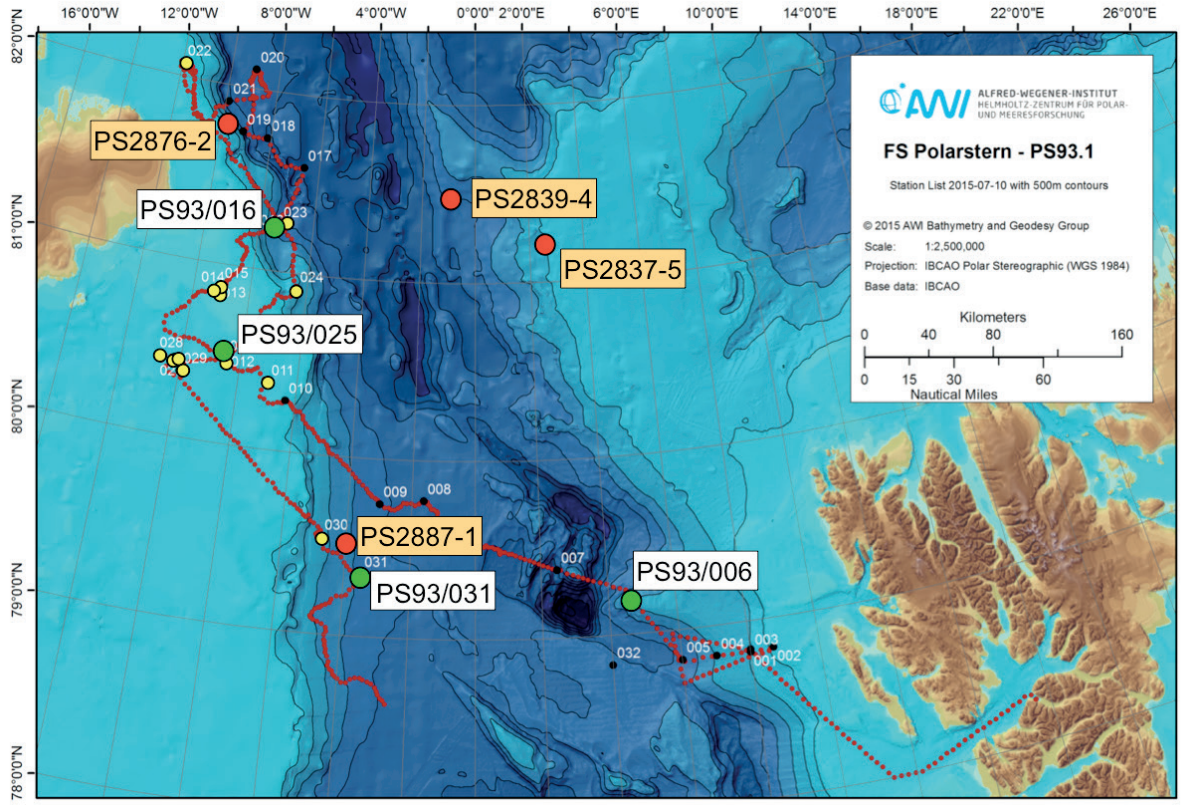

Fig. 7.12: Locations of sediment cores (small yellow circles) recovered in the northern part of the working area during Expedition PS 93.1. The four kastenlot cores PS93/006-1, PS93/016-6, PS93/025-2, and PS93/031-4 are highlighted as large green circles. In addition, locations of cores PS2837-5 and PS2839-4 recovered during Polarstern Expedition ARK-XIII/2 (Stein and Fahl 1997) and cores PS2876-2 and PS2887-1 recovered during Polarstern Expedition ARK-XIII/3 (Krause 1998) are shown.

Work at sea

During the *Polarstern* Expedition PS93.1, 23 long sediment cores were taken in the area between NE Greenland and Svalbard (Fig. 7.1; Table 7.1). Four of them are kastenlot cores that have been described and sampled onboard *Polarstern* (Fig. 7.12). In the following, main lithologies of these cores are shortly described, and a lithostratigraphic concept and preliminary age model as well as some preliminary interpretations are presented.

Preliminary results

Core PS93/006-1

Core PS93/006-1 (see Fig. 7.12 for location) is mainly composed of dark grayish brown (2.5Y 4/2) and very dark grayish brown (2.5Y 3/2) silty clays. Gray (10YR 6/1), dark gray (2.5Y 4/0) and very dark gray (2.5Y 3/0) sandy silty clay intervals with partly common dropstones occur at 145-180, 305-320, 350-370, 460-500, 610 640, 660-690, and 725-685 cm core depth (Fig. 7.13). Below 600 cm, coal fragments were found. These coal fragments are a very potential indicator for MIS 6 deposits as shown in numerous dated sediment cores from the North Atlantic/Arctic (Bischof et al. 1990; Köhler and Spielhagen 1990). The coarsed-grained intervals are mostly characterized by increased WBD values. Based on the physical properties and the major lithologies, Core PS93/006-1 can be correlated very well with Core PS2839-4 (Fig. 7.13). Based on this correlation, Core PS93/006-1 probably represents MIS 6 to MIS1. Especially during the glacial MIS 6, coarser-grained sediments with dropstones are dominant, suggesting increased iceberg discharge.

Core PS93/016-6

The sedimentary sequence of Core PS93/016-6 (see Fig. 7.12 for location) is dominated by reddish brown (5YR 5/4) silty clays characterized by increased magnetic susceptibility values (Fig. 7.14). In these more fine-grained lithologies, grayish brown, more coarse-grained horizons with high WBD values and low magnetic susceptibility values are intercalated. Between 290 and 350 cm core depth, a prominent interval of very dark gray (N3) (sandy) silty clay occurs. Based on MSCL and lithology data, the core can be correlated with nearby Core PS2876-2, suggesting that the thick very dark gray interval is probably of MIS 4 age (Fig. 7.14). Taking mean sedimentation rates of about 4 cm/ky, the interval of coarse-grained sediments between 560 and 610 cm core depth might represent MIS 6.

The dominance of the fine-grained reddish lithologies and a site location close to NE Greenland suggest that sediment supply from local sources, i.e., the Proterozoic and Phanerozoic Red Beds (Fig. 7.15; Bond and Lotti 1995; Bond et al. 2001), was probably most important. These red sedimentary rocks are characterized by increased Fe-oxid (i.e., hematite and magnetite) that may have caused the maxima in magnetic susceptibility (Fig. 7.14). Occasionally, especially during MIS 4 (?) and MIS 6 (?) coarser sediments from different (Arctic Ocean?) sources were supplied by iceberg transport. Here, of course, more sedimentological, mineralogical and geochemical investigations as well as a much better age control are needed for a detailed reconstruction of the origin and pathways of the terrigenous sediment fractions and its relationship to the Greenland ice sheet and climate history.

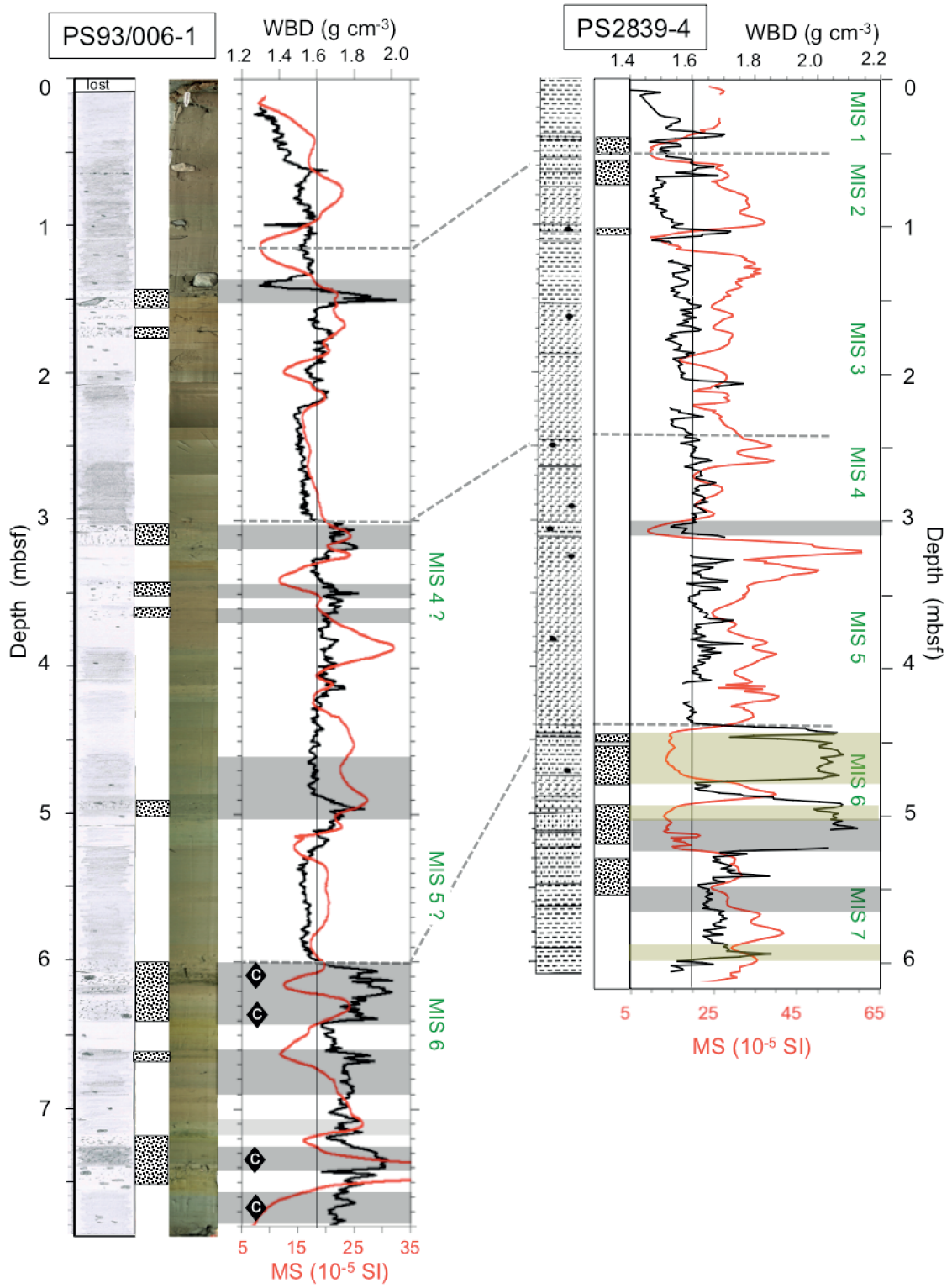

Fig. 7.13: Preliminary (litho-) stratigraphic framework of Core PS93/006-1. Correlation of Core PS93/006-1 and Core PS2839-4 based on main lithologies and MSCL (WBD = wet bulk density and MS = magnetic susceptibility) data. Lithologies, MSCL data and proposed Marine Isotope Stages (MIS - in green) of Core PS2839-4 from Niessen et al. (1997) and Schubert et al. (1997), respectively. Gray and olive bars mark lithologies characterized by (dark) gray and (dark) olive (gray) colors, respectively. The occurrence of coal fragments (indicative for MIS 6; cf., Bischof et al. 1990) is indicated by black rhombs.

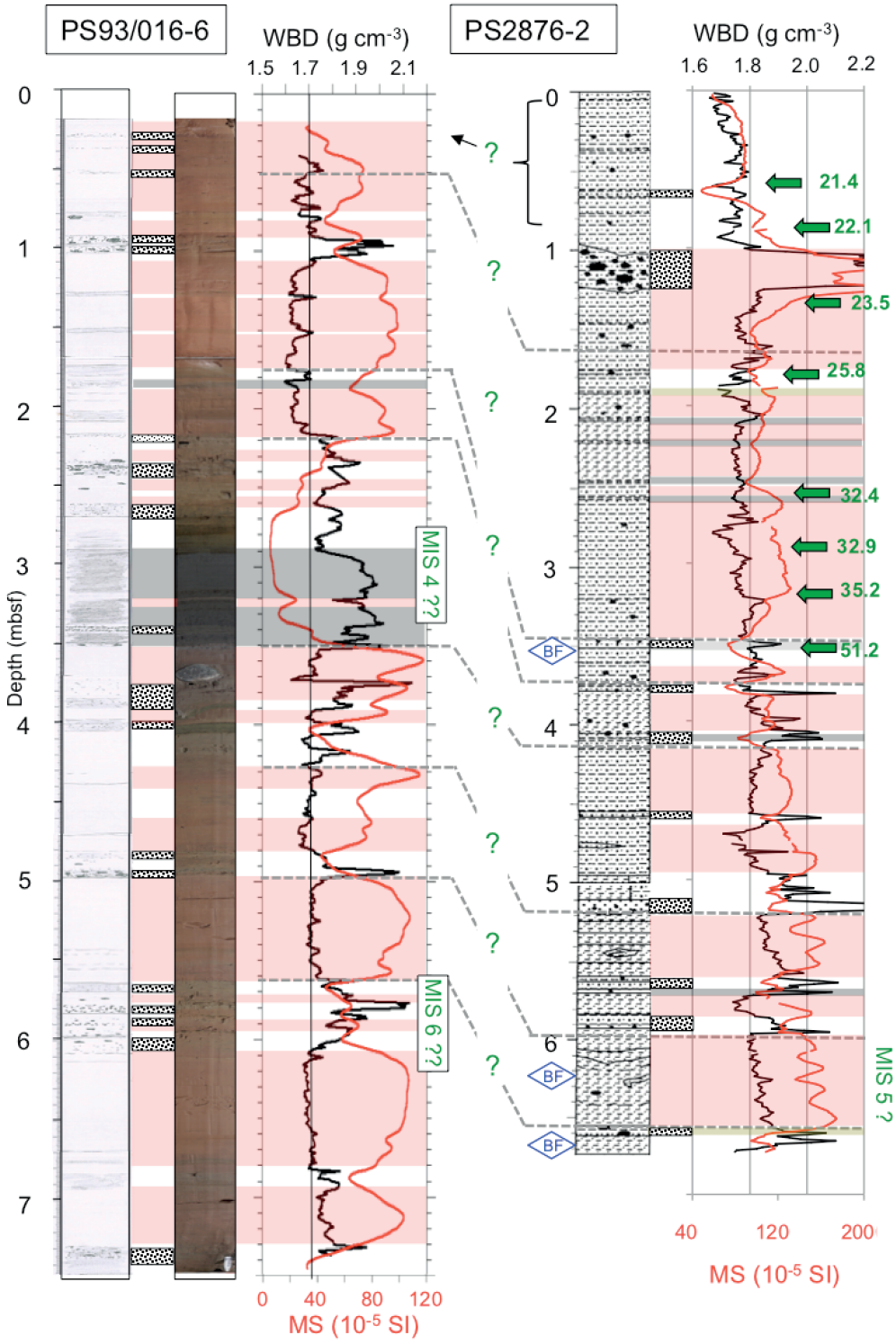

Fig. 7.14:. Preliminary (litho-) stratigraphic framework of Core PS93/016-6. Correlation of Core PS93/016-6 and Core PS2876-2 based on main lithologies and MSCL (WBD = wet bulk density and MS = magnetic susceptibility) data. Lithologies and MSCL data of Core PS2876-2 from Kleiber and Swientek (1998) and Nørgaard-Pedersen (1998), respectively. BF indicates occurrence of benthic foraminifers. Green arrows with green numbers show AMS ^{14}C ages in calendar kiloyears BP (Nørgaard-Pedersen et al. 2003). Gray and light red bars mark lithologies characterized by (dark) gray and reddish colors, respectively.

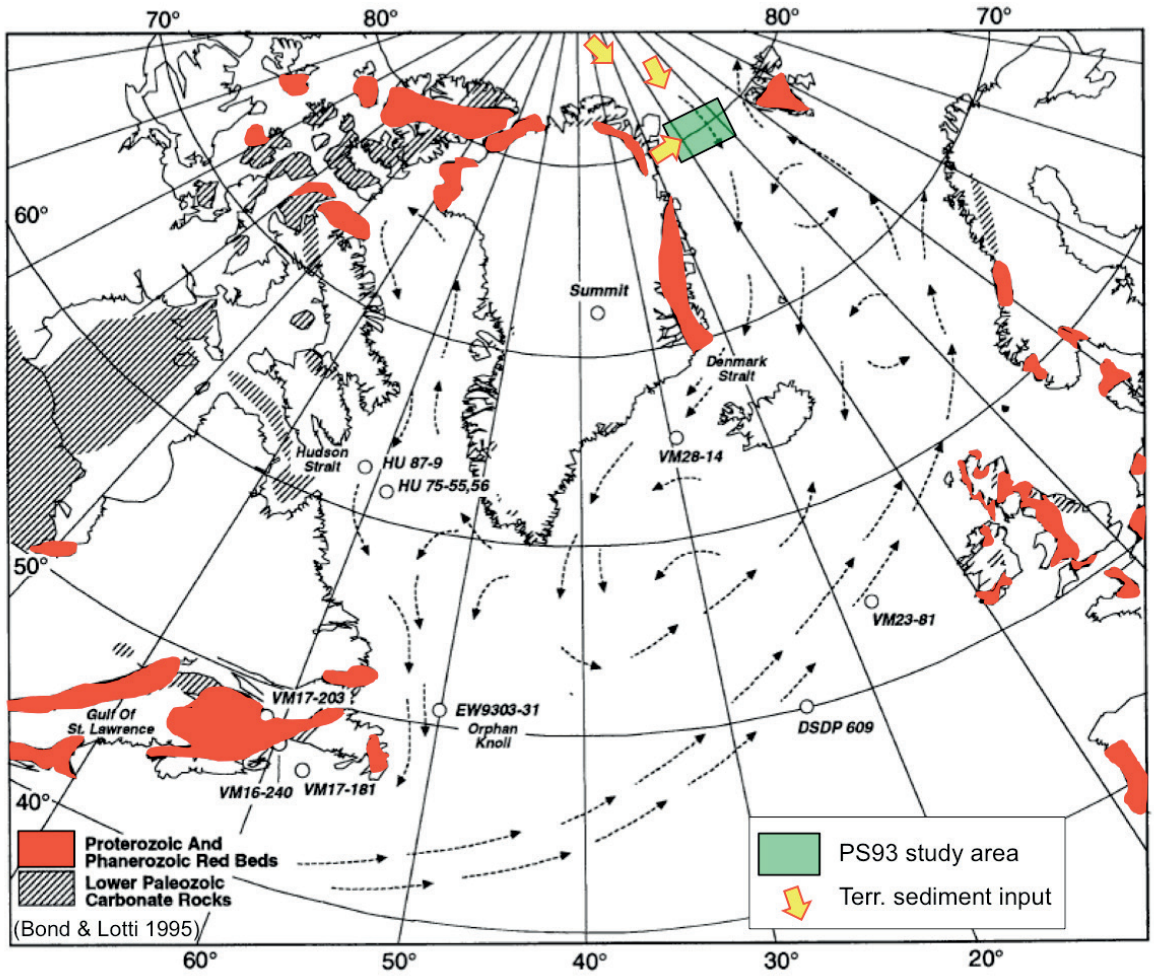

Fig. 7.15: Map showing potential source areas of the reddish lithologies found in marine sediment cores from the Atlantic and Arctic oceans (from Bond and Lotti 1995, supplemented), including the PS93.1 sediment cores. The PS93.1 study area is indicated.

Core PS93/025-2

Core PS93/025-2 (see Fig. 7.12 for location) is mainly composed of dark grayish brown (2.5Y 4/2) homogenous silty clay. Magnetic susceptibility and WBD values are relatively low (30-45 $x10^{-5}$ SI and 1.5-1.7 g cm^{-3}, respectively), decreasing from bottom to top (Fig. 7.16). Based on the pyhsical property data, the sedimentary sequence of Core PS93/025-2 can be correlated to the very well dated Core PS2837-5 (Fig. 7.16; Nørgaard-Pedersen et al. 2003). Based on this correlation the 260 cm thick sedimentary section of Core Core PS93/025-2 probably represents the last about 10 ky. Thus, this core is very well suitable for a high-resolution reconstruction of the short-term Holocene climate variability.

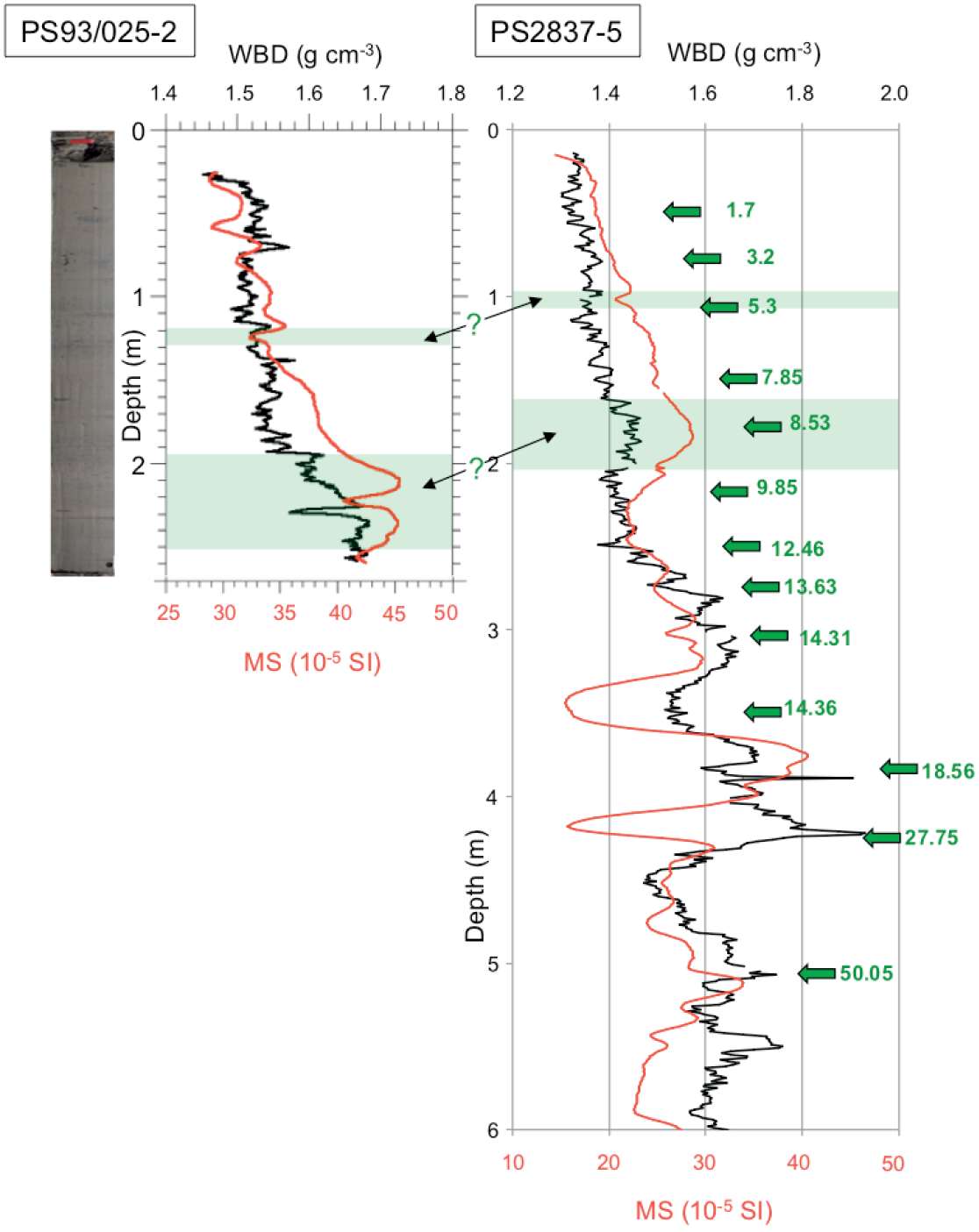

Fig. 7.16: Preliminary (Litho-) stratigraphic framework of Core PS93/025-2. Correlation of Core PS93/025-2 and Core PS2837-5 based on MSCL (WBD = wet bulk density and MS = magnetic susceptibility) data. MSCL data of Core PS2839-4 from Niessen et al. (1997). Green arrows with green numbers show AMS^{14}C ages in calendar kiloyears BP (Nørgaard-Pedersen et al. 2003). Green bars mark intervals correlated by MSCL data.

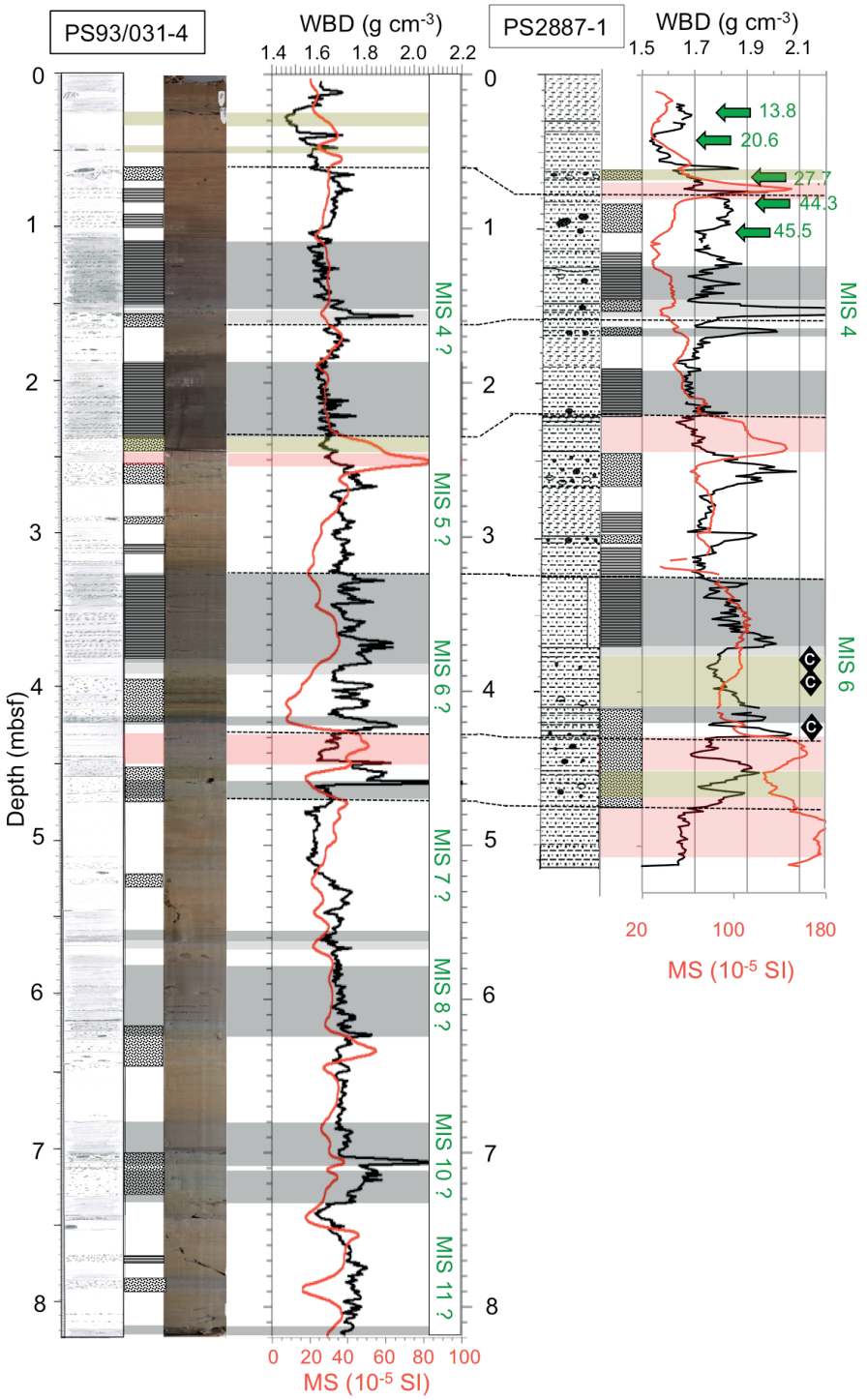

Fig. 7.17: Preliminary (litho-) stratigraphic framework of Core PS93/031-4. Correlation of Core PS93/031-4 and Core PS2887-1 based on main lithologies and MSCL (WBD = wet bulk density and MS = magnetic susceptibility) data. Lithologies and MSCL data of Core PS2839-4 from Kleiber and Swientek (1998) and Nørgaard-Pedersen (1998), respectively. (Dark) gray, light red, and olive bars mark lithologies characterized by (dark) gray, reddish and (dark) olive (gray) colors, respectively. The occurrence of coal fragments (indicative for MIS 6; cf., Bischof et al. 1990) is indicated by black rhombs. Green arrows with green numbers show AMS ^{14}C ages in calendar kiloyears BP (Nørgaard-Pedersen et al. 2003). Proposed Marine Isotope Stages (MIS - in green) are indicated for Core PS93/031-4.

Core PS93/031-4

Core PS93/031-4 (see Fig. 7.12 for location) is characterized by three main lithologies: (1) brown (10YR 4/3) grayish brown (2.5Y 5/2) and dark grayish brown (2.5Y 4/2), partly bioturbated silty clays, (2) alternations of thin silty clay/silt layers of grayish brown (10YR 5/2) and dark gray (10YR 4/1) ("laminated sediments"), and (3) more coarse-grained sandy silty clays with dropstones (Fig. 7.17). Two intervals of reddish silty clays occur at 246-254 cm and 430-440 cm core depth, suggesting periods of increased input from the Red Beds that are cropping out on NE Greenland (see Fig. 7.15). Based on the lithologies and the MSCL data, Core PS93/031-4 can be correlated very well to the near-by Core PS2887-1 (see Fig. 7.12 for location). Thus, the identification of the cold/glacial stages MIS 4 and MIS 6, characterized as prominent dark gray coarser-grained sections, is quite reliable. Below MIS 6, two more thick dark gray coarser-grained intervals occur, probably representing older glacial intervals (MIS 8 and MIS 10?). If this very tentative stratigraphy is correct, the lowermost part of the sedimentary sequence of Core PS93/031-4 may represent the interglacial MIS 11, a postulation that has to be approved by future studies.

Data management

All data (visual core description, core photographs, MSCL data etc.) will be stored in the databank PANGAEA (www.pangaea.de)

References

Bischof J, Koch J, Kubisch M, Spielhagen RF, Thiede J (1990) Nordic seas surface ice drift reconstructions: Evidence from ice-rafted coal fragments during oxygen isotope stage 6, in: Dowdeswell, J.A., Scourse, J.D. (Eds.), Glacimarine Environments: Processes and Sediments, Geol. Soc. Spec. Publ. 53, pp. 235-251.

Bond G, Kromer B, Beer J, Muscheler R, Evans MN, Showers W, Hoffmann S, Lotti-Bond R, Hajdas I, Bonani G (2001) Persistent solar influence on North Atlantic climate during the Holocene. Science 294:2130-2136.

Bond GC, Lotti R (1995) Iceberg discharges into the North Atlantic on millennial time scales during the last glaciation. Science 267, 1005-1010.

Kleiber HP, Swientek O (1998) Physical properties of sediment cores. In: Krause, G. (Ed.), 1998. The Expedition ARKTIS-XIII/3 of RV „*Polarstern*" in 1997. Rep. Pol. Res. 262, p. 23-28.

Köhler SEI, Spielhagen RF (1990) The enigma of oxygen isotope stage 5 in the central Fram Strait, in: Bleil, U., Thiede, J. (Eds.), Geological History of the Polar Oceans: Arctic versus Antarctic, Vol. 308. NATO ASI Series C, Kluwer Academic Publishers, Dordrecht, pp. 489-497.

Krause G (Ed.) (1998) The Expedition ARKTIS-XIII/3 of RV *Polarstern* in 1997. Rep. Pol. Res. 262, 93 pp.

Niessen F, Kleiber HP, Nehrke G (1997) Physical properties and core logging. In: Stein, R. and Fahl, K. (Eds.), 1997. Scientific Cruise Report oft he Arctic Expedition ARK-XIII/2 of RV „*Polarstern*" in 1997. Rep. Pol. Res. 255, p. 115-120.

Nørgaard-Pedersen N (1998) Marine geological investigations of the northern Fram Strait during ARK-XIII/3. In: Krause, G. (Ed.), 1998. The Expedition ARKTIS-XIII/3 of RV „*Polarstern*" in 1997. Rep. Pol. Res. 262, p. 17-23.

Nørgaard-Pedersen N, Spielhagen RF, Erlenkeuser H, Grootes PM, Heinemeier J, Knies J (2003) The Arctic Ocean during the Last Glacial Maximum: atlantic and polar domains of surface water mass distribution and ice cover. Paleoceanography 18:1-19.

Schubert C, Knies J, Levitan M, Musatov E, Stein R (1997) Lithostratigraphy and sediment characteristics. In: Stein, R. and Fahl, K. (Eds.), 1997. Scientific Cruise Report oft he Arctic Expedition ARK-XIII/2 of RV „*Polarstern*" in 1997. Rep. Pol. Res. 255, p. 121-135.

Stein R and Fahl K (Eds.) (1997) Scientific Cruise Report oft he Arctic Expedition ARK-XIII/2 of RV „*Polarstern*" in 1997. Rep. Pol. Res. 255, 235 pp.

8. THE “ARCTRAIN FLOATING UNIVERSITY”

Aurélie Aubry[1] , Martin Bartels[2], Amélie Bouchat[3], Tilia Breckenfelder[2], Sam Davin[1], Jade Falardeau[1], Yarisbel Garcia[4], Laura Gillard[4], Yukie Hata[3], Mathilde Jutras[3], Valerie Krillova[2], Andrea Klus[2], Annegret Krandick[2], K. Kretschmer[2], Wei Leng[2], Mathieu Plante[3], Raul Scarlat[2], Aexander Slavin[3], James Williams[3], Coralie Zorzi[1], Andre Paul[2], Ruediger Stein[5]

[1]UQAM
[2]UoB
[3]McGill
[4]UoA
[5]AWI

Grant-No. AWI-PS93.1_01

Background and objectives

Due to a complex set of feedback processes collectively known as “polar amplification”, the Arctic realm is expected to experience a greater-than-average response to global climate forcing. The cascades of feedback processes that connect the Arctic cryosphere, ocean and atmosphere remain incompletely constrained by observations and theory and are difficult to simulate in climate models. Our capacity to predict the future of the region and assess the impacts of Arctic change processes on global and regional environments hinges on the availability of interdisciplinary experts with strong international experience and understanding of the science/society interface. This is the basis of the International Research Training Group “Processes and impacts of climate change in the North Atlantic Ocean and the Canadian Arctic - ArcTrain“, which was initiated in 2013. ArcTrain aims to educate PhD students in an interdisciplinary environment that combines paleoclimatology, physical oceanography, remote sensing and glaciology with comprehensive Earth system modelling, including sea-ice and ice-sheet components. The qualification programme for the PhD students includes joint supervision, mandatory research residences at partner institutions, field courses on land and on sea (Floating University), annual meetings and training workshops and a challenging structured training in expert skills and transferrable skills. Its aim is to enhance the career prospects and employability of the graduates in a challenging international job market across academic and applied sectors.

ArcTrain is a collaborative project at the University of Bremen and the Alfred Wegener Institute Helmholtz Centre for Polar and Marine Research in Bremerhaven. The German part of the project is designed to continue for nine years and educate three cohorts of twelve PhD students each. The Canadian partners comprise a consortium of eight universities led by the GEOTOP cluster at the Université du Québec à Montréal and including Dalhousie University, McGill University, Memorial University of Newfoundland, University of Alberta, University of British Columbia, University of Calgary and Université du Québec à Rimouski.

Further details about ArcTrain are available at: *https://www.marum.de/ArcTrain.html*

Work at sea

Practical work

During the PS93.1 expedition, an "ArcTrain Floating University" was organized on board *Polarstern* to introduce one MSc student, 18 PhD students and one PostDoc with different scientific backgrounds (i.e., from physical oceanography, geosciences and numerical modelling) to the different aspects of field work in marine sciences. All participants were given the opportunity to gain a broad experience of the work on the aft deck and in the laboratories by rotating between the different working groups and signing up for the following activities for limited periods of time:

- CTD Profiling
- Mooring data analysis
- CTD Water sampling
- Hand-net/bucket sampling
- Multi-net sampling
- Box corer (GKG)
- Kastenlot (KAL)
- Gravity corer (SL)
- Parasound

ArcTrain course

A series of computer exercises was offered by André Paul (UoB) to enable the participants of the ArcTrain Floating University to visualize and analyze marine scientific data from shipboard measurements using open-source software. Examples were taken from underway weather and oceanographic data as well as bathymetric data. It was demonstrated how to plot these data in terms of maps, profiles and sections and add geographic information such as station locations, using software tools (the "Canopy" interactive data-analysis environment and Ocean Data View) that are publicly available and run on Windows, OS X and Linux:

- Extracting data from the on-board DSHIP system and using the "Canopy" environment to create a simple base map (Thursday 2. July, 14:00/Friday, 3. July, 9:30)
- Using Ocean Data View (ODV) to explore oceanographic CTD and UCTD profile data (Monday, 13 July, 12:30)
- Mapping of bathymetric data from IBCAO and the shipboard hydrosweep system (Friday, 17 July, 9:30)

ArcTrain seminar

In addition to the practical and course work, a seminar was organized. The presentations were given by senior scientists involved in the PS93.1 scientific programme, an ArcTrain PostDoc (Alexander Slavig) and an ArcTrain PhD student (Sam Davin). They were related to the work on board as well as the Arctic region in general and covered a wide range of topics from geology over oceanographic and atmospheric sciences to biology:

Monday, 6 July 2015, 16:00-17:15

- Robert Spielhagen (GEOMAR): The marine geological research programme on PS93.1 - background and objectives
- Alexander Slavig: Potential mechanism for rapid sea-ice decline in the Arctic

- Henning Bauch: Use of proxies in the Arctic

Tuesday, 7 July 2015, 16:00-17:15

- Matthias Forwick (UoT): Glaciated continental margins - morphology and sedimentary processes

Wednesday, 8 July 2015, 16:00-17:15

- Wilken-Jon von Appen (AWI): Oceanographic observations of the West Spitsbergen Current
- Jean-Louis Bonne (AWI): From source to sink: Decoding the isotopic composition of the eastern Arctic water cycle

Friday, 10 July 2015, 16:00-17:15

- Matthias Forwick (UoT): Glaciated continental margins – fjords
- Steffi Gäbler-Schwarz (AWI): Phytoplankton diversity in the Fram Strait region

Saturday, 11 July 2015, 14:00-15:30

- Raul Scarlat (UoB): Integrated retrieval of surface and atmospheric variables in the Arctic
- Lars Vaupel (HeliService): Aviation in the Arctic and Antarctic

Thursday, 16 July 2015, 19:30

- Henning Bauch (GEOMAR): The Eemian in the Arctic

Friday, 17 July 2015, 16:00

- Sam Davin (UQAM): Case study: Greenland lake sediments and life after coring

Friday, 17 July 2015, 19:00

- Audun Tholfsen (Longyearbyen): Impressions from ten months on an ice floe

In addition to the presentations, the documentary “Research Hovercraft Sabvabaa: Into the mist – Fram 2012” was shown on Sunday, 5 July 2015, 20:00 and Monday, 6 July 2015, 20:00.

Preliminary (expected) results

All participants in the ArcTrain Floating University proved to be extremely enthusiastic about the different activities on board and willing to connect to other disciplines. For example, participants who for their research mainly do theoretical or numerical modeling work were eager to gain a hands-on impression of the geological, oceanographic and biological field work. This truly interdisciplinary experience will certainly enable them to value marine observations and reconstructions and make proper use of them in their future careers.

All scientists highly appreciated the assistance of the ArcTrain participants and praised their interest and dedication. With their support, more work got done and more samples were taken than had been expected from this relatively short cruise.

Shorts reports about shipboard activities and impressions, written by the ArcTrain students, are attached to this Cruise Report (Appendix A7).

Data management

All data will be delivered to the PANGAEA database by the other PS93.1 research groups.

APPENDIX

A.1 Teilnehmende Institute / Participating Institutions

A.2 Fahrtteilnehmer / Cruise Participants

A.3 Schiffsbesatzung / Ship's Crew

A.4 Station list

A.5 Lithological Description of Giant Box Corer (GKG) Sections (R. Spielhagen, A. Quatmann-Hense)

Note: For SL and KAL cores only a limited number of sediment cores were described during the expedition, but not included in the cruise report. These core descriptions are available at the AWI (Contact: R. Stein)

A.6 Selected PARASOUND profiles across coring sites

(F. Niessen, F. Petersen)

A.7 ArcTrain Floating University onboard of Polarstern Expedition PS93.1:

- Group reports of ArcTrain students
- Group Report 1 (Laura C. Gillard, Yarisbel Garcia Quintana)
- Group Report 2 (Tilia Breckenfelder, Andrea Klus, Raul Scarlat)
- Group Report 3 (Amélie Bouchat, Yukie Hata, Mathilde Jutras, Mathieu Plante, James Williams)
- Group Report 4 (Annegret Krandick, Kerstin Kretschmer)
- Group Report 5 (Sam Davin, Coralie Zorzi, Aurélie Aubry, Jade Falardeau)
- Group Report 6 (Wei Leng, Martin Bartels, Valeriia Kirilova)

A.1 TEILNEHMENDE INSTITUTE / PARTICIPATING INSTITUTIONS

	Address
AWI	Alfred-Wegener-Institut Helmholtz-Zentrum für Polar- und Meeresforschung Postfach 120161 27515 Bremerhaven Germany
BPRC	Byrd Polar Research Center The Ohio State University, 108 Scott Hall 1090 Carmack Road, Columbus, OH 43210, USA
DWD	Deutscher Wetterdienst Geschäftsbereich Wettervorhersage Seeschifffahrtsberatung Bernhard-Nocht-Str. 76 20359 Hamburg Germany
GEOMAR	Helmholtz-Zentrum für Ozeanforschung (GEOMAR) Wischhofstr. 1-3 24148 Kiel Germany
HeliService	HeliService International GmbH Am Luneort 15 27572 Bremerhaven Germany
McGill	Department of Atmospheric and Oceanic Sciences, McGill University, 805 Sherbrooke Street West, Montreal, Quebec, H3A 0B9, Canada
KOPRI	Korea Polar Research Institute 6 Songdomirae-ro, Yeonsu-gu 406-840 Incheon Korea

	Address
UoA	Department of Earth & Atmospheric Sciences, 1-26 Earth Sciences Building University of Alberta Edmonton Edmonton, Alberta, T6G 2E3 Canada
UoB	Center for Marine Environmental Sciences (MARUM), University of Bremen Leobener Strasse, 28359 Bremen Germany
UoK	Institute for Geosciences, University of Kiel Otto-Hahn-Platz 1 24118 Kiel Germany
UoT	Institute of Geology, University of Tromsø The Arctic University of Norway Dramsveien 201 9037 Tromsø Norway
UQAM	GEOTOP & Département des sciences de la Terre et de l'atmosphère, Université du Québec à Montréal, CP 8888, succ. Centre-Ville, Montréal, Québec, H3C 3P8, Canada

A.2 FAHRTTEILNEHMER / CRUISE PARTICIPANTS

No	Name	First name	Institute	Profession	Discipline
1	Aubry	Aurélie	UQAM	PhD student	Geology
2	Bartels	Martin	UoB	PhD student	Geology
3	Bauch	Henning	GEOMAR	Scientist	Geology
4	Bonne	Jean-Louis	AWI	Scientist	Glaciology
5	Bouchat	Amélie	McGill	PhD student	Sea-ice modelling
6	Breckenfelder	Tilia	UoB	PhD student	Oceanography
7	Davin	Sam	UQAM	PhD student	Geology
8	Falardeau	Jade	UQAM	PhD student	Geology
9	Forwick	Matthias	UoT	Scientist	Geology
10	Gäbler-Schwarz	Steffi	AWI	Scientist	Biology
11	Garcia	Yarisbel	UoA	PhD student	Oceanography
12	Gillard	Laura	UoA	PhD student	Oceanography
13	Hata	Yukie	McGill	PhD student	Sea ice dynamics
14	Heckmann	Hans	HeliService	Pilot	Pilot/Technician
15	Hegstad	Sigrun	UoT	PhD student	Geology
16	Hörner	Tanja	AWI	PhD student	Geology
17	Jager	Harold	HeliService	Pilot	Pilot
18	Jutras	Mathilde	McGill	PhD student	Sea-ice modeling
19	Kirillova	Valeriia	UoB	PhD student	Geology
20	Klus	Andrea	UoB	PhD student	Modelling
21	Krandick	Annegret	UoB	PhD student	Modelling
22	Kremer	Anne	AWI	PhD student	Geology
23	Kretschmer	Kerstin	UoB	PhD student	Modelling
24	Leng	Wei	UoB	PhD student	Geology
25	Maiyegun	Babajide	AWI	Student	Bathymetry
26	Miller	Max	DWD	Scientist	Meteorology
27	Möllendorf	Carsten	HeliService	Technician	Technician
28	Niessen	Frank	AWI	Scientist	Geology
29	Olsen	Ingrid	UoT	PhD student	Geology
30	Paul	Andre	UoB	Scientist	Modelling
31	Petersen	Florian	UoK	PhD student	Geology
32	Plante	Mathieu	McGill	Student	Sea-ice modelling
33	Quatmann-Hense	Anna	UoB	Student	Geology
34	Radig	Lars	AWI	Scientist	Bathymetry

No	Name	First name	Institute	Profession	Discipline
35	Scarlat	Raul	UoB	PhD student	Sea-icedynamics
36	Schreck	Michael	KOPRI	Scientist	Geology
37	Slavin	Alexander	McGill	Scientist	Oceanography
38	Sonnabend	Hartmut	DWD	Technician	Technician
39	Spielhagen	Robert	GEOMAR	Scientist	Geology
40	Stein	Ruediger	AWI	Chief scientist	Geology
41	Strothmann	Olaf	AWI	Technician	Oceanography
42	Telesinski	Maciej	GEOMAR	PhD student	Geology
43	Vaupel	Lars	HeliService	Pilot	Pilot
44	von Appen	Wilken-Jon	AWI	Scientist	Oceanography
45	Werner	Kristin	BPRC	Scientist	Geology
46	Wildau	Antje	CAU	PhD student	Geology
47	Williams	James	McGill	PhD student	Sea ice modeling
48	Winkler	Maria	AWI	PhD student	Bathymetry
49	Zhuravleva	Anastasia	GEOMAR	PhD student	Geology
50	Zorzi	Coralie	UQAM	PhD student	Geology

A.3 SCHIFFSBESATZUNG / SHIP'S CREW

No.	Name	Rank
1	Wunderlich, Thomas	Master
2	Spilok, Norbert	Doctor
3	Lauber, Felix	Ch. Mate
4	Fallei, Holger	2nd Mate
5	Kentges, Felix	2nd Mate
6	Stolze, Henrik	2nd Mate
7	Westphal, Henning	Chief Eng.
8	Buch, Erik-Torsten	2nd Eng.
9	Rusch, Torben	2nd Eng.
10	Schnürch, Helmut	2nd Eng.
11	Brehme, Andreas	E Eng.
12	Hofmann, Jörg	Chief ELO
13	Dimmler, Werner	ELO
14	Feiertag, Thomas	ELO
15	Ganter, Armin	ELO
16	Nasis, Ilias	ELO
17	Schröter, René	Boatsw.
18	Neisner, Winfried	Carpenter
19	Burzan, Gerd-Ekkeh.	A.B.
20	Clasen, Nils	A.B.
21	Gladow, Lothar	A.B.
22	Hartwig-Lab., Andreas	A.B.
23	Kretzschmar, Uwe	A.B.
24	Leisner, Bert	A.B.
25	Müller, Steffen	A.B.
26	Schröder, Norbert	A.B.
27	Sedlak, Andreas	A.B.
28	Beth, Detlef	Storek.
29	Dinse, Horst	Mot-man
30	Klein, Gert	Mot-man
31	Krösche, Eckard	Mot-man
32	Plehn, Markus	Mot-man

No.	Name	Rank
33	Watzel, Bernhard	Mot-man
34	Meißner, Jörg	Cook
35	Golla, Gerald	Cooksmate
36	Tupy, Mario	Cooksmate
37	Wartenberg, Irina	Chief Stew.
38	Schwitzky-Schwarz, C.	Stwdss/Nurse
39	Chen, Quan Lun	2nd Stew.
40	Chen, Xiyong	2nd Stew.
41	Duka, Maribel	2nd Stew.
42	Hischke, Peggy	2nd Stew.
43	Hu, Guo Yong	2nd Stew.
44	Ruan, Hui Guang	Laundrym.

A.4 STATIONSLISTE / STATION LIST PS93.1

Station	Date	Time	Gear	Action	PositionLat	PositionLon	Depth [m]
PS93/001-1	29.06.15	22:06	HS_PS	profile start	78° 49.97‘ N	8° 0.07‘ E	1018.0
PS93/001-1	30.06.15	00:47	HS_PS	alter course	78° 58.60‘ N	5° 46.63‘ E	2202.7
PS93/001-1	30.06.15	02:30	HS_PS	alter course	78° 42.07‘ N	6° 0.01‘ E	2193.0
PS93/001-1	30.06.15	06:03	HS_PS	profile end	78° 49.77‘ N	8° 40.41‘ E	832.7
PS93/002-1	30.06.15	05:58	MOR	uptake	78° 49.51‘ N	8° 40.85‘ E	244.8
PS93/002-1	30.06.15	07:52	MOR	abort	78° 49.78‘ N	8° 41.49‘ E	0.0
PS93/002-2	30.06.15	08:02	MOR	positioning	78° 49.80‘ N	8° 40.26‘ E	0.0
PS93/002-2	30.06.15	08:05	MOR	positioning	78° 49.80‘ N	8° 40.11‘ E	0.0
PS93/003-1	30.06.15	08:55	MOR	on ground/ max depth	78° 49.67‘ N	8° 0.20‘ E	0.0
PS93/003-1	30.06.15	09:37	MOR	on deck	78° 49.95‘ N	7° 58.97‘ E	1027.9
PS93/003-1	30.06.15	09:52	MOR	on deck	78° 49.94‘ N	7° 58.31‘ E	1032.0
PS93/003-1	30.06.15	10:04	MOR	on deck	78° 49.94‘ N	7° 57.79‘ E	1035.3
PS93/003-1	30.06.15	10:13	MOR	on deck	78° 49.94‘ N	7° 57.37‘ E	1040.8
PS93/003-1	30.06.15	10:28	MOR	on deck	78° 49.82‘ N	7° 56.91‘ E	1040.8
PS93/004-1	30.06.15	11:34	MOR	on ground/ max depth	78° 49.80‘ N	7° 0.35‘ E	1457.9
PS93/004-1	30.06.15	12:07	MOR	on deck	78° 50.06‘ N	6° 59.03‘ E	1468.4
PS93/004-1	30.06.15	12:13	MOR	on deck	78° 50.04‘ N	6° 58.93‘ E	1471.2
PS93/004-1	30.06.15	12:36	MOR	on deck	78° 50.08‘ N	6° 58.17‘ E	1484.0
PS93/004-1	30.06.15	12:42	MOR	on deck	78° 50.05‘ N	6° 58.22‘ E	1484.9
PS93/004-1	30.06.15	13:00	MOR	on deck	78° 50.05‘ N	6° 57.64‘ E	1495.5
PS93/004-1	30.06.15	13:07	MOR	on deck	78° 50.05‘ N	6° 57.44‘ E	1498.5
PS93/005-1	30.06.15	14:13	MOR	in the water	78° 49.70‘ N	6° 0.60‘ E	0.0
PS93/005-1	30.06.15	16:38	MOR	on deck	78° 49.90‘ N	6° 0.00‘ E	0.0
PS93/005-1	30.06.15	16:44	MOR	on deck	78° 49.80‘ N	5° 59.80‘ E	0.0
PS93/005-1	30.06.15	17:02	MOR	on deck	78° 49.90‘ N	5° 59.90‘ E	0.0
PS93/005-1	30.06.15	17:45	MOR	on deck	78° 49.60‘ N	5° 59.95‘ E	2448.4
PS93/005-1	30.06.15	17:50	MOR	on deck	78° 49.58‘ N	5° 59.94‘ E	2448.3
PS93/006-1	30.06.15	22:16	KAL	on ground/ max depth	79° 12.22‘ N	4° 40.13‘ E	1593.3
PS93/006-2	01.07.15	00:46	GKG	on ground/ max depth	79° 12.20‘ N	4° 40.08‘ E	1605.2
PS93/007-1	01.07.15	05:03	HN	on ground/ max depth	79° 22.90‘ N	2° 29.73‘ E	3180.4
PS93/008-1	01.07.15	18:23	HN	on ground/ max depth	79° 46.53‘ N	1° 37.65‘ W	2718.6
PS93/009-1	01.07.15	21:56	HS_PS	profile start	79° 44.93‘ N	3° 0.55‘ W	2496.5
PS93/009-1	02.07.15	11:01	HS_PS	profile end	80° 22.40‘ N	6° 59.67‘ W	255.2

Station	Date	Time	Gear	Action	PositionLat	PositionLon	Depth [m]
PS93/010-1	02.07.15	07:22	HN	on ground/ max depth	80° 17.09‘ N	6°20.34‘ W	317.4
PS93/011-1	02.07.15	11:18	CTD/RO	on ground/ max depth	80° 22.56‘ N	6° 59.83‘ W	255.0
PS93/011-2	02.07.15	11:51	HN	on ground/ max depth	80° 22.77‘ N	6° 59.62‘ W	256.5
PS93/011-3	02.07.15	12:22	MN	on ground/ max depth	80° 22.91‘ N	6° 57.76‘ W	261.1
PS93/011-4	02.07.15	12:57	MUC	on ground/ max depth	80° 23.13‘ N	6° 56.49‘ W	258.4
PS93/012-1	02.07.15	16:17	GKG	on ground/ max depth	80° 27.88‘ N	8° 26.33‘ W	295.4
PS93/012-2	02.07.15	17:26	GC	on ground/ max depth	80° 27.37‘ N	8° 25.83‘ W	296.9
PS93/013-1	03.07.15	02:17	GC	on ground/ max depth	80° 50.81‘ N	9° 6.17‘ W	58.8
PS93/014-1	03.07.15	03:03	GC	on ground/ max depth	80° 51.27‘ N	9° 11.44‘ W	56.7
PS93/015-1	03.07.15	04:34	GC	on ground/ max depth	80° 52.83‘ N	9° 2.95‘ W	74.9
PS93/016-1	03.07.15	12:33	CTD/RO	on ground/ max depth	81° 13.04‘ N	7° 20.53‘ W	1549.3
PS93/016-2	03.07.15	13:28	HN	on ground/ max depth	81° 13.03‘ N	7° 20.52‘ W	1549.4
PS93/016-3	03.07.15	14:13	MN	on ground/ max depth	81° 13.03‘ N	7° 20.48‘ W	1549.5
PS93/016-4	03.07.15	15:34	GKG	on ground/ max depth	81° 13.02‘ N	7° 20.44‘ W	1549.8
PS93/016-5	03.07.15	16:57	MUC	on ground/ max depth	81° 13.04‘ N	7° 20.48‘ W	1568.9
PS93/016-6	03.07.15	18:52	KAL	on ground/ max depth	81° 13.01‘ N	7° 20.46‘ W	1548.3
PS93/017-1	03.07.15	23:26	CTD/RO	in the water	81° 35.66‘ N	6° 34.99‘ W	3339.3
PS93/017-2	03.07.15	23:49	HN	on ground/ max depth	81° 35.68‘ N	6° 35.22‘ W	3341
PS93/017-1	04.07.15	00:41	CTD/RO	on ground/ max depth	81° 35.69‘ N	6° 35.19‘ W	3379.1
PS93/017-3	04.07.15	02:46	MN	on ground/ max depth	81° 35.68‘ N	6° 35.20‘ W	3351.8
PS93/017-4	04.07.15	04:30	GKG	on ground/ max depth	81° 35.69‘ N	6° 35.17‘ W	3351.1
PS93/017-5	04.07.15	07:00	MUC	on ground/ max depth	81° 35.71‘ N	6° 35.22‘ W	3344.8
PS93/017-6	04.07.15	09:30	GC	on ground/ max depth	81° 35.52‘ N	6° 35.64‘ W	3333.7

Station	Date	Time	Gear	Action	PositionLat	PositionLon	Depth [m]
PS93/018-1	04.07.15	13:06	HN	on ground/ max depth	81° 44.15‘ N	8° 8.62‘ W	2505.2
PS93/018-6	04.07.15	13:22	ZODIAK	on ground/ max depth	81° 44.15‘ N	8° 8.42‘ W	2502.6
PS93/018-2	04.07.15	13:59	GKG	on ground/ max depth	81° 44.16‘ N	8° 8.37‘ W	2520.7
PS93/018-3	04.07.15	15:15	GKG	on ground/ max depth	81° 44.15‘ N	8° 8.53‘ W	2475
PS93/018-4	04.07.15	17:09	MUC	on ground/ max depth	81° 44.16‘ N	8° 8.51‘ W	2504.6
PS93/018-5	04.07.15	19:27	GC	on ground/ max depth	81° 44.19‘ N	8° 8.39‘ W	2561.4
PS93/019-1	04.07.15	21:46	HN	on ground/ max depth	81° 45.14‘ N	9° 7.64‘ W	2055.4
PS93/019-2	04.07.15	22:30	GC	on ground/ max depth	81° 45.10‘ N	9° 8.53‘ W	2033.9
PS93/019-3	04.07.15	23:44	GKG	on ground/ max depth	81° 45.09‘ N	9° 8.51‘ W	2036.1
PS93/019-3	05.07.15	00:47	GKG	on ground/ max depth	81° 45.08‘ N	9° 8.29‘ W	2030.9
PS93/019-3	05.07.15	01:49	GKG	on ground/ max depth	81° 45.08‘ N	9° 8.45‘ W	2032.9
PS93/020-1	05.07.15	07:50	HN	on ground/ max depth	82° 6.47‘ N	8° 58.93‘ W	2847.9
PS93/020-2	05.07.15	09:48	CTD/RO	on ground/ max depth	82° 6.02‘ N	8° 55.89‘ W	2859
PS93/020-7	05.07.15	10:56	ZODIAK	on ground/ max depth	82° 5.85‘ N	8° 54.86‘ W	2803
PS93/020-8	05.07.15	11:10	HN	on ground/ max depth	82° 5.82‘ N	8° 54.62‘ W	2861.2
PS93/020-3	05.07.15	11:43	MN	on ground/ max depth	82° 5.75‘ N	8° 54.05‘ W	2857.9
PS93/020-4	05.07.15	13:25	GC	on ground/ max depth	82° 5.51‘ N	8° 52.20‘ W	2844.7
PS93/020-5	05.07.15	15:31	MUC	on ground/ max depth	82° 5.28‘ N	8° 50.25‘ W	2872.5
PS93/020-6	05.07.15	17:43	GKG	on ground/ max depth	82° 5.17‘ N	8° 48.84‘ W	2877.7
PS93/020-6	05.07.15	19:20	GKG	on ground/ max depth	82° 5.14‘ N	8° 47.92‘ W	2800.2
PS93/021-1	06.07.15	04:18	HS_PS	profile start	81° 54.53‘ N	9° 52.41‘ W	2414.2
PS93/021-1	06.07.15	06:27	HS_PS	alter course	81° 46.17‘ N	10° 37.65‘ W	202.6
PS93/021-1	06.07.15	07:38	HS_PS	alter course	81° 50.62‘ N	11° 16.37‘ W	197.1
PS93/021-1	06.07.15	09:37	HS_PS	alter course	82° 0.76‘ N	11° 26.92‘ W	239.2

Station	Date	Time	Gear	Action	PositionLat	PositionLon	Depth [m]
PS93/021-1	06.07.15	11:08	HS_PS	alter course	82° 5.42‘ N	12° 0.64‘ W	227
PS93/021-1	06.07.15	13:13	HS_PS	alter course	82° 2.54‘ N	11° 26.65‘ W	255.2
PS93/021-1	06.07.15	13:48	HS_PS	alter course	82° 2.01‘ N	11° 28.22‘ W	252.4
PS93/021-1	06.07.15	14:01	HS_PS	alter course	82° 2.99‘ N	11° 36.38‘ W	243.3
PS93/021-1	06.07.15	14:53	HS_PS	alter course	82° 4.65‘ N	12° 1.83‘ W	215.4
PS93/021-1	06.07.15	15:04	HS_PS	profile end	82° 4.16‘ N	11° 58.26‘ W	213.1
PS93/022-1	06.07.15	15:23	GKG	on ground/ max depth	82° 4.12‘ N	11° 57.72‘ W	217.6
PS93/022-2	06.07.15	15:55	GKG	on ground/ max depth	82° 4.02‘ N	11° 57.15‘ W	216.5
PS93/023-1	07.07.15	02:28	HN	on ground/ max depth	81° 15.81‘ N	7° 14.66‘ W	1501.1
PS93/023-2	07.07.15	02:53	GKG	on ground/ max depth	81° 15.79‘ N	7° 14.68‘ W	1500.9
PS93/023-3	07.07.15	07:53	GKG	on ground/ max depth	81° 15.43‘ N	7° 11.37‘ W	1505
PS93/023-4	07.07.15	05:01	MUC	on ground/ max depth	81° 15.96‘ N	7° 12.60‘ W	1509
PS93/023-5	07.07.15	09:27	GC	on ground/ max depth	81° 15.11‘ N	7° 14.79‘ W	1508.2
PS93/024-1	07.07.15	14:09	CTD/RO	on ground/ max depth	80° 54.88‘ N	6° 22.35‘ W	1314.3
PS93/024-3	07.07.15	15:08	HN	on ground/ max depth	80° 54.82‘ N	6° 21.90‘ W	1317.6
PS93/024-7	07.07.15	15:11	ZODIAK	on ground/ max depth	80° 54.82‘ N	6° 21.90‘ W	1317.7
PS93/024-2	07.07.15	15:21	MN	on ground/ max depth	80° 54.79‘ N	6° 21.90‘ W	1317.8
PS93/024-4	07.07.15	16:30	GKG	on ground/ max depth	80° 54.62‘ N	6° 23.43‘ W	1307.3
PS93/024-5	07.07.15	17:30	GKG	on ground/ max depth	80° 54.49‘ N	6° 25.09‘ W	1295.8
PS93/024-6	07.07.15	18:50	MUC	on ground/ max depth	80° 54.58‘ N	6° 22.90‘ W	1308.3
PS93/025-1	08.07.15	01:10	GKG	on ground/ max depth	80° 28.84‘ N	8° 29.24‘ W	291.3
PS93/025-3	08.07.15	01:19	HN	on ground/ max depth	80° 28.82‘ N	8° 29.40‘ W	291.2
PS93/025-2	08.07.15	02:20	KAL	on ground/ max depth	80° 28.90‘ N	8° 29.40‘ W	290.2
PS93/026-1	08.07.15	06:49	GC	on ground/ max depth	80° 26.42‘ N	10° 13.36‘ W	292.5
PS93/027-1	08.07.15	07:37	GC	on ground/ max depth	80° 25.64‘ N	10° 16.64‘ W	284.7

Station	Date	Time	Gear	Action	PositionLat	PositionLon	Depth [m]
PS93/028-1	08.07.15	08:41	GC	on ground/ max depth	80° 26.27‘ N	10° 40.64‘ W	289.3
PS93/029-1	08.07.15	10:42	GC	on ground/ max depth	80° 22.19‘ N	9° 58.50‘ W	307.6
PS93/029-2	08.07.15	11:20	GKG	on ground/ max depth	80° 22.19‘ N	9° 58.54‘ W	318.2
PS93/029-3	08.07.15	11:53	GKG	on ground/ max depth	80° 22.18‘ N	9° 58.62‘ W	318.2
PS93/030-2	08.07.15	22:51	HN	on ground/ max depth	79° 33.21‘ N	4° 50.66‘ W	1282.3
PS93/030-1	08.07.15	23:15	CTD/RO	on ground/ max depth	79° 33.23‘ N	4° 50.29‘ W	1288.9
PS93/030-3	09.07.15	00:50	MN	on ground/ max depth	79° 33.52‘ N	4° 48.84‘ W	1305.9
PS93/030-4	09.07.15	02:04	MUC	on ground/ max depth	79° 33.66‘ N	4° 48.84‘ W	1305.7
PS93/030-5	09.07.15	03:09	GKG	on ground/ max depth	79° 33.83‘ N	4° 49.36‘ W	1294.9
PS93/030-6	09.07.15	04:17	GC	on ground/ max depth	79° 33.99‘ N	4° 50.54‘ W	1277.5
PS93/031-1	09.07.15	12:27	GKG	on ground/ max depth	79° 21.10‘ N	3° 28.39‘ W	2145.7
PS93/031-2	09.07.15	10:38	MUC	on ground/ max depth	79° 20.63‘ N	3° 32.03‘ W	2123.8
PS93/031-3	09.07.15	13:40	GKG	on ground/ max depth	79° 21.09‘ N	3° 28.36‘ W	2144.0
PS93/031-4	09.07.15	15:03	KAL	on ground/ max depth	79° 21.08‘ N	3° 28.24‘ W	2147.3
PS93/031-5	09.07.15	16:50	GKG	on ground/ max depth	79° 20.97‘ N	3° 31.43‘ W	2134.5
PS93/032-1	10.07.15	08:47	CTD/UW	on ground/ max depth	78° 39.41‘ N	1° 16.76‘ W	2744.9
PS93/032-1	10.07.15	08:48	CTD/UW	profile start	78° 39.44‘ N	1° 15.78‘ W	2744.3
PS93/032-1	10.07.15	09:24	CTD/UW	profile start	78° 40.62‘ N	0° 40.18‘ W	2661.8
PS93/032-1	10.07.15	09:56	CTD/UW	profile start	78° 41.64‘ N	0° 8.36‘ W	1893.7
PS93/032-1	10.07.15	10:46	CTD/UW	profile start	78° 43.31‘ N	0° 42.19‘ E	2477.2
PS93/032-1	10.07.15	12:07	CTD/UW	profile start	78° 45.85‘ N	2° 0.67‘ E	2512.2
PS93/032-1	10.07.15	12:20	CTD/UW	profile start	78° 46.27‘ N	2° 13.17‘ E	2504.6
PS93/032-1	10.07.15	12:36	CTD/UW	profile start	78° 46.75‘ N	2° 28.45‘ E	2499.6
PS93/032-1	10.07.15	12:56	CTD/UW	profile start	78° 47.36‘ N	2° 47.58‘ E	2453.0
PS93/032-1	10.07.15	13:17	CTD/UW	profile start	78° 48.04‘ N	3° 8.16‘ E	2413.4
PS93/032-1	10.07.15	13:37	CTD/UW	profile start	78° 48.67‘ N	3° 27.61‘ E	2313.3
PS93/033-1	10.07.15	15:35	MOR	on deck	78° 49.77‘ N	3° 58.51‘ E	2274.7
PS93/033-1	10.07.15	15:38	MOR	on deck	78° 49.77‘ N	3° 58.16‘ E	2272.2

Station	Date	Time	Gear	Action	PositionLat	PositionLon	Depth [m]
PS93/033-1	10.07.15	15:49	MOR	on deck	78° 49.78‘ N	3° 57.01‘ E	2273.5
PS93/033-1	10.07.15	16:00	MOR	on deck	78° 49.77‘ N	3° 55.79‘ E	2264.4
PS93/033-1	10.07.15	16:21	MOR	on deck	78° 49.82‘ N	3° 53.62‘ E	2269.1
PS93/033-1	10.07.15	16:38	MOR	on deck	78° 49.92‘ N	3° 52.45‘ E	2264.6
PS93/033-1	10.07.15	16:45	MOR	on deck	78° 49.95‘ N	3° 51.93‘ E	2262.1
PS93/034-1	10.07.15	19:36	MOR	on deck	78° 49.99‘ N	4° 59.42‘ E	0.0
PS93/035-1	10.07.15	20:58	MOR	positioning	78° 45.00‘ N	5° 30.02‘ E	2482.4
PS93/035-1	10.07.15	21:55	MOR	in the water	78° 45.01‘ N	5° 29.98‘ E	2345.9
PS93/035-1	10.07.15	22:10	MOR	in the water	78° 44.99‘ N	5° 29.99‘ E	2407.1
PS93/035-1	10.07.15	22:17	MOR	on ground/ max depth	78° 44.99‘ N	5° 29.98‘ E	2403.5
PS93/036-1	10.07.15	23:08	CTD/UW	in the water	78° 44.39‘ N	5° 21.78‘ E	2273.9
PS93/036-1	10.07.15	23:08	CTD/UW	profile start	78° 44.39‘ N	5° 21.78‘ E	2273.9
PS93/036-2	10.07.15	23:15	CTD/UW	profile start	78° 43.99‘ N	5° 16.79‘ E	2297.5
PS93/036-3	10.07.15	23:20	CTD/UW	profile start	78° 43.72‘ N	5° 13.52‘ E	2309.2
PS93/036-4	10.07.15	23:26	CTD/UW	profile start	78° 43.45‘ N	5° 9.71‘ E	2331.0
PS93/036-5	10.07.15	23:32	CTD/UW	profile start	78° 43.12‘ N	5° 5.83‘ E	2334.9
PS93/036-6	10.07.15	23:37	CTD/UW	profile start	78° 42.87‘ N	5° 2.54‘ E	2345.2
PS93/036-7	10.07.15	23:43	CTD/UW	profile start	78° 42.58‘ N	4° 58.60‘ E	2299.2
PS93/036-8	10.07.15	23:49	CTD/UW	profile start	78° 42.27‘ N	4° 54.78‘ E	2334.3
PS93/036-9	10.07.15	23:54	CTD/UW	profile start	78° 42.03‘ N	4° 51.53‘ E	2338.5
PS93/036-10	11.07.15	00:00	CTD/UW	profile start	78° 41.73‘ N	4° 47.74‘ E	2341.5
PS93/036-11	11.07.15	00:05	CTD/UW	profile start	78° 41.47‘ N	4° 44.54‘ E	2349.3
PS93/036-12	11.07.15	00:11	CTD/UW	profile start	78° 41.18‘ N	4° 40.65‘ E	2352.6
PS93/036-13	11.07.15	00:17	CTD/UW	profile start	78° 40.89‘ N	4° 36.72‘ E	2357.8
PS93/036-14	11.07.15	00:22	CTD/UW	profile start	78° 40.62‘ N	4° 33.45‘ E	2359.3
PS93/036-15	11.07.15	00:28	CTD/UW	profile start	78° 40.32‘ N	4° 29.44‘ E	2361.1
PS93/036-16	11.07.15	00:33	CTD/UW	profile start	78° 40.05‘ N	4° 26.16‘ E	2358.9
PS93/036-17	11.07.15	00:40	CTD/UW	profile start	78° 39.69‘ N	4° 21.49‘ E	2361.8
PS93/036-18	11.07.15	00:45	CTD/UW	profile start	78° 39.44‘ N	4° 18.14‘ E	2358.3
PS93/036-19	11.07.15	00:50	CTD/UW	profile start	78° 39.19‘ N	4° 14.77‘ E	2359.1
PS93/036-20	11.07.15	00:56	CTD/UW	profile start	78° 38.86‘ N	4° 10.81‘ E	2349.5
PS93/036-21	11.07.15	01:02	CTD/UW	profile start	78° 38.56‘ N	4° 6.77‘ E	2343.4
PS93/036-22	11.07.15	01:07	CTD/UW	profile start	78° 38.29‘ N	4° 3.53‘ E	2345.3
PS93/036-23	11.07.15	01:12	CTD/UW	profile start	78° 38.04‘ N	4° 0.29‘ E	2302.3
PS93/036-24	11.07.15	01:17	CTD/UW	profile start	78° 37.80‘ N	3° 56.99‘ E	2315.9
PS93/036-25	11.07.15	01:23	CTD/UW	profile start	78° 37.49‘ N	3° 52.99‘ E	2294.6
PS93/036-26	11.07.15	01:28	CTD/UW	profile start	78° 37.24‘ N	3° 49.77‘ E	2282.3
PS93/036-27	11.07.15	01:33	CTD/UW	profile start	78° 36.99‘ N	3° 46.64‘ E	2289.2
PS93/036-28	11.07.15	01:46	CTD/UW	profile start	78° 36.36‘ N	3° 38.64‘ E	2386.0
PS93/036-29	11.07.15	01:53	CTD/UW	profile start	78° 36.03‘ N	3° 34.31‘ E	2420.7

Station	Date	Time	Gear	Action	PositionLat	PositionLon	Depth [m]
PS93/036-30	11.07.15	01:59	CTD/UW	profile start	78° 35.74‘ N	3° 30.58‘ E	2432.9
PS93/036-31	11.07.15	02:06	CTD/UW	profile start	78° 35.39‘ N	3° 26.31‘ E	2456.6
PS93/036-32	11.07.15	02:11	CTD/UW	profile start	78° 35.14‘ N	3° 23.23‘ E	2466.5
PS93/036-33	11.07.15	02:17	CTD/UW	profile start	78° 34.85‘ N	3° 19.54‘ E	2466.6
PS93/036-34	11.07.15	02:22	CTD/UW	profile start	78° 34.63‘ N	3° 16.40‘ E	2480.3
PS93/036-35	11.07.15	02:28	CTD/UW	profile start	78° 34.33‘ N	3° 12.68‘ E	2487.4
PS93/036-36	11.07.15	02:34	CTD/UW	profile start	78° 34.03‘ N	3° 9.00‘ E	2498.0
PS93/036-37	11.07.15	02:43	CTD/UW	profile start	78° 33.61‘ N	3° 3.47‘ E	2504.9
PS93/036-38	11.07.15	02:48	CTD/UW	profile start	78° 33.36‘ N	3° 0.41‘ E	2499.7
PS93/036-39	11.07.15	02:54	CTD/UW	profile start	78° 33.07‘ N	2° 56.78‘ E	2489.8
PS93/036-40	11.07.15	02:59	CTD/UW	profile start	78° 32.84‘ N	2° 53.76‘ E	2480.6
PS93/036-41	11.07.15	03:04	CTD/UW	profile start	78° 32.62‘ N	2° 50.63‘ E	2456.8
PS93/036-42	11.07.15	03:10	CTD/UW	profile start	78° 32.31‘ N	2° 46.97‘ E	2449.7
PS93/036-43	11.07.15	03:16	CTD/UW	profile start	78° 32.03‘ N	2° 43.23‘ E	2454.6
PS93/036-44	11.07.15	03:22	CTD/UW	profile start	78° 31.71‘ N	2° 39.54‘ E	2435.5
PS93/036-45	11.07.15	03:29	CTD/UW	profile start	78° 31.38‘ N	2° 35.11‘ E	2430.3
PS93/036-46	11.07.15	03:36	CTD/UW	profile start	78° 31.02‘ N	2° 30.69‘ E	2407.5
PS93/036-47	11.07.15	03:41	CTD/UW	profile start	78° 30.79‘ N	2° 27.46‘ E	2380.2
PS93/036-48	11.07.15	03:47	CTD/UW	profile start	78° 30.47‘ N	2° 23.60‘ E	2389.4
PS93/036-49	11.07.15	03:52	CTD/UW	profile start	78° 30.23‘ N	2° 20.36‘ E	2372.2
PS93/036-50	11.07.15	03:58	CTD/UW	profile start	78° 29.90‘ N	2° 16.56‘ E	2245.7
PS93/036-51	11.07.15	04:05	CTD/UW	profile start	78° 29.55‘ N	2° 12.10‘ E	2273.2
PS93/036-52	11.07.15	04:21	CTD/UW	profile start	78° 28.76‘ N	2° 2.06‘ E	2482.0
PS93/036-53	11.07.15	04:27	CTD/UW	profile start	78° 28.48‘ N	1° 58.27‘ E	2464.9
PS93/036-54	11.07.15	04:33	CTD/UW	profile start	78° 28.17‘ N	1° 54.57‘ E	2450.3
PS93/036-55	11.07.15	04:39	CTD/UW	profile start	78° 27.90‘ N	1° 50.80‘ E	2572.1
PS93/036-56	11.07.15	04:45	CTD/UW	profile start	78° 27.58‘ N	1° 47.07‘ E	2573.2
PS93/036-57	11.07.15	04:51	CTD/UW	profile start	78° 27.30‘ N	1° 43.25‘ E	2561.0
PS93/036-58	11.07.15	04:57	CTD/UW	profile start	78° 26.98‘ N	1° 39.66‘ E	2569.5
PS93/036-59	11.07.15	05:02	CTD/UW	profile start	78° 26.75‘ N	1° 36.53‘ E	2482.3
PS93/036-60	11.07.15	05:09	CTD/UW	profile start	78° 26.40‘ N	1° 32.10‘ E	2180.4
PS93/036-61	11.07.15	05:14	CTD/UW	profile start	78° 26.14‘ N	1° 28.91‘ E	1814.3
PS93/036-62	11.07.15	05:20	CTD/UW	profile start	78° 25.85‘ N	1° 25.04‘ E	1587.4
PS93/036-63	11.07.15	05:26	CTD/UW	profile start	78° 25.54‘ N	1° 21.28‘ E	1438.9
PS93/036-64	11.07.15	05:32	CTD/UW	profile start	78° 25.24‘ N	1° 17.47‘ E	1301.6
PS93/036-65	11.07.15	05:37	CTD/UW	profile start	78° 25.00‘ N	1° 14.27‘ E	1250.4
PS93/036-65	11.07.15	05:45	CTD/UW	on deck	78° 24.57‘ N	1° 9.02‘ E	1183.9
PS93/037-1	11.07.15	06:57	GC	on ground/ max depth	78° 24.09‘ N	1° 2.78‘ E	1168.9
PS93/038-1	11.07.15	07:45	CTD/UW	profile start	78° 23.78‘ N	0° 54.61‘ E	1246.1
PS93/038-2	11.07.15	07:51	CTD/UW	profile start	78° 23.83‘ N	0° 49.52‘ E	1496.8

Station	Date	Time	Gear	Action	PositionLat	PositionLon	Depth [m]
PS93/038-3	11.07.15	07:56	CTD/UW	profile start	78° 23.86‘ N	0° 45.29‘ E	1716.4
PS93/038-4	11.07.15	08:03	CTD/UW	profile start	78° 23.78‘ N	0° 39.41‘ E	2236.2
PS93/038-5	11.07.15	08:08	CTD/UW	profile start	78° 23.71‘ N	0° 35.26‘ E	2472.8
PS93/038-6	11.07.15	08:13	CTD/UW	profile start	78° 23.72‘ N	0° 31.16‘ E	2735.4
PS93/038-7	11.07.15	08:18	CTD/UW	profile start	78° 23.83‘ N	0° 27.14‘ E	2796.4
PS93/038-8	11.07.15	08:23	CTD/UW	profile start	78° 23.98‘ N	0° 23.15‘ E	2808.7
PS93/038-9	11.07.15	08:28	CTD/UW	profile start	78° 24.11‘ N	0° 19.14‘ E	2825.7
PS93/038-10	11.07.15	08:33	CTD/UW	profile start	78° 24.23‘ N	0° 15.06‘ E	2863.1
PS93/038-11	11.07.15	08:38	CTD/UW	profile start	78° 24.36‘ N	0° 11.00‘ E	2894.9
PS93/038-12	11.07.15	08:43	CTD/UW	profile start	78° 24.50‘ N	0° 6.93‘ E	2894.0
PS93/038-13	11.07.15	08:47	CTD/UW	profile start	78° 24.59‘ N	0° 3.66‘ E	2902.3
PS93/038-14	11.07.15	08:52	CTD/UW	profile start	78° 24.74‘ N	0° 0.44‘ W	2892.3
PS93/038-15	11.07.15	08:57	CTD/UW	profile start	78° 24.85‘ N	0° 4.58‘ W	2798.1
PS93/038-16	11.07.15	09:03	CTD/UW	profile start	78° 24.91‘ N	0° 9.67‘ W	2867.6
PS93/038-17	11.07.15	09:07	CTD/UW	profile start	78° 24.93‘ N	0° 13.09‘ W	2853.4
PS93/038-18	11.07.15	09:12	CTD/UW	profile start	78° 24.99‘ N	0° 17.34‘ W	2849.9
PS93/038-19	11.07.15	09:17	CTD/UW	profile start	78° 25.06‘ N	0° 21.54‘ W	2838.1
PS93/038-20	11.07.15	09:22	CTD/UW	profile start	78° 25.08‘ N	0° 25.70‘ W	2894.6
PS93/038-21	11.07.15	09:27	CTD/UW	profile start	78° 25.15‘ N	0° 29.81‘ W	2819.9
PS93/038-22	11.07.15	09:32	CTD/UW	profile start	78° 25.18‘ N	0° 33.87‘ W	2817.9
PS93/038-23	11.07.15	09:37	CTD/UW	profile start	78° 25.24‘ N	0° 37.95‘ W	2825.0
PS93/038-24	11.07.15	09:42	CTD/UW	profile start	78° 25.29‘ N	0° 42.12‘ W	2821.1
PS93/038-25	11.07.15	09:46	CTD/UW	profile start	78° 25.33‘ N	0° 45.43‘ W	2834.3
PS93/038-26	11.07.15	09:52	CTD/UW	profile start	78° 25.36‘ N	0° 50.35‘ W	2927.2
PS93/038-27	11.07.15	10:03	CTD/UW	profile start	78° 25.49‘ N	0° 59.29‘ W	2819.4
PS93/038-28	11.07.15	10:07	CTD/UW	profile start	78° 25.53‘ N	1° 2.52‘ W	2815.8
PS93/038-29	11.07.15	10:16	CTD/UW	profile start	78° 25.60‘ N	1° 9.81‘ W	2729.0
PS93/038-30	11.07.15	10:21	CTD/UW	profile start	78° 25.66‘ N	1° 13.84‘ W	2824.1
PS93/038-31	11.07.15	10:27	CTD/UW	profile start	78° 25.69‘ N	1° 18.69‘ W	2817.8
PS93/038-32	11.07.15	10:32	CTD/UW	profile start	78° 25.74‘ N	1° 22.72‘ W	2816.0
PS93/038-33	11.07.15	10:38	CTD/UW	profile start	78° 25.81‘ N	1° 27.52‘ W	2814.3
PS93/038-34	11.07.15	10:44	CTD/UW	profile start	78° 25.85‘ N	1° 32.25‘ W	2833.4
PS93/038-35	11.07.15	10:50	CTD/UW	profile start	78° 25.92‘ N	1° 36.97‘ W	2833.6
PS93/038-36	11.07.15	10:56	CTD/UW	profile start	78° 25.96‘ N	1° 41.68‘ W	2854.3
PS93/038-37	11.07.15	11:01	CTD/UW	profile start	78° 25.99‘ N	1° 45.58‘ W	2801.2
PS93/038-38	11.07.15	11:05	CTD/UW	profile start	78° 25.85‘ N	1° 48.64‘ W	2837.7
PS93/038-39	11.07.15	11:11	CTD/UW	profile start	78° 25.64‘ N	1° 53.29‘ W	2849.3
PS93/038-40	11.07.15	11:16	CTD/UW	profile start	78° 25.48‘ N	1° 57.20‘ W	2892.9
PS93/038-41	11.07.15	11:22	CTD/UW	profile start	78° 25.27‘ N	2° 1.86‘ W	2840.1
PS93/038-42	11.07.15	11:27	CTD/UW	profile start	78° 25.08‘ N	2° 5.77‘ W	2829.6

Station	Date	Time	Gear	Action	PositionLat	PositionLon	Depth [m]
PS93/038-43	11.07.15	11:33	CTD/UW	profile start	78° 24.90‘ N	2° 10.47‘ W	2820.4
PS93/038-44	11.07.15	11:39	CTD/UW	profile start	78° 24.70‘ N	2° 15.23‘ W	2809.4
PS93/038-45	11.07.15	11:45	CTD/UW	profile start	78° 24.47‘ N	2° 20.00‘ W	2796.8
PS93/038-46	11.07.15	11:50	CTD/UW	profile start	78° 24.31‘ N	2° 24.02‘ W	2807.8
PS93/038-47	11.07.15	11:56	CTD/UW	profile start	78° 24.11‘ N	2° 28.79‘ W	2776.1
PS93/038-48	11.07.15	12:02	CTD/UW	profile start	78° 24.01‘ N	2° 33.54‘ W	2758.7
PS93/038-49	11.07.15	12:08	CTD/UW	profile start	78° 23.99‘ N	2° 38.36‘ W	2735.8
PS93/038-50	11.07.15	12:13	CTD/UW	profile start	78° 23.99‘ N	2° 42.36‘ W	2712.1
PS93/038-51	11.07.15	12:19	CTD/UW	profile start	78° 23.99‘ N	2° 47.12‘ W	2682.5
PS93/038-52	11.07.15	12:25	CTD/UW	profile start	78° 23.99‘ N	2° 51.88‘ W	2658.5
PS93/038-53	11.07.15	12:40	CTD/UW	profile start	78° 24.01‘ N	3° 3.83‘ W	2550.1
PS93/038-54	11.07.15	12:46	CTD/UW	profile start	78° 24.00‘ N	3° 8.66‘ W	2513.2
PS93/038-55	11.07.15	12:51	CTD/UW	profile start	78° 23.99‘ N	3° 12.72‘ W	2473.0
PS93/038-54	11.07.15	12:51	CTD/UW	profile end	78° 23.99‘ N	3° 12.72‘ W	2473.0
PS93/038-56	11.07.15	12:57	CTD/UW	profile start	78° 23.99‘ N	3° 17.67‘ W	2423.0
PS93/038-57	11.07.15	13:02	CTD/UW	profile start	78° 24.01‘ N	3° 21.81‘ W	2378.0
PS93/038-58	11.07.15	13:08	CTD/UW	profile start	78° 24.01‘ N	3° 26.65‘ W	2324.0
PS93/038-59	11.07.15	13:13	CTD/UW	profile start	78° 23.95‘ N	3° 30.63‘ W	2293.6
PS93/038-60	11.07.15	13:18	CTD/UW	profile start	78° 23.62‘ N	3° 34.26‘ W	2233.1
PS93/038-61	11.07.15	13:23	CTD/UW	profile start	78° 23.30‘ N	3° 37.89‘ W	2185.5
PS93/038-62	11.07.15	13:29	CTD/UW	profile start	78° 22.88‘ N	3° 42.16‘ W	2138.4
PS93/038-63	11.07.15	13:34	CTD/UW	profile start	78° 22.58‘ N	3° 45.76‘ W	2099.8
PS93/038-64	11.07.15	13:39	CTD/UW	profile start	78° 22.25‘ N	3° 49.29‘ W	2047.0
PS93/038-65	11.07.15	13:44	CTD/UW	profile start	78° 21.92‘ N	3° 52.80‘ W	1989.2
PS93/039-1	12.07.15	12:42	CTD/RO	on ground/ max depth	78° 44.76‘ N	9° 37.84‘ W	398.8
PS93/039-2	12.07.15	12:44	HN	on ground/ max depth	78° 44.76‘ N	9° 37.77‘ W	399.7
PS93/039-9	12.07.15	13:16	ZODIAK	on ground/ max depth	78° 44.88‘ N	9° 37.15‘ W	400.4
PS93/039-3	12.07.15	13:35	MN	on ground/ max depth	78° 44.90‘ N	9° 36.71‘ W	399.1
PS93/039-4	12.07.15	14:16	GKG	on ground/ max depth	78° 44.91‘ N	9° 35.73‘ W	400.3
PS93/039-5	12.07.15	14:40	GKG	on ground/ max depth	78° 44.92‘ N	9° 35.53‘ W	401
PS93/039-6	12.07.15	15:20	GKG	on ground/ max depth	78° 44.94‘ N	9° 35.35‘ W	402.4
PS93/039-7	12.07.15	16:13	MUC	on ground/ max depth	78° 44.97‘ N	9° 35.30‘ W	403.3
PS93/039-8	12.07.15	17:02	GC	on ground/ max depth	78° 44.97‘ N	9° 35.12‘ W	402.8

Station	Date	Time	Gear	Action	PositionLat	PositionLon	Depth [m]
PS93/039-10	12.07.15	18:19	GC	on ground/ max depth	78° 45.08‘ N	9° 35.23‘ W	403.4
PS93/039-11	12.07.15	19:26	GC	on ground/ max depth	78° 45.31‘ N	9° 34.95‘ W	400.9
PS93/040-1	13.07.15	17:03	CTD/UW	profile start	77° 19.63‘ N	5° 51.00‘ W	326.3
PS93/040-2	13.07.15	17:12	CTD/UW	profile start	0° 0.00‘ N	0° 0.00‘ E	0.0
PS93/040-3	13.07.15	17:18	CTD/UW	profile start	77° 17.59‘ N	5° 45.08‘ W	425.0
PS93/040-4	13.07.15	17:23	CTD/UW	profile start	77° 16.90‘ N	5° 43.07‘ W	389.3
PS93/040-5	13.07.15	17:29	CTD/UW	profile start	77° 16.08‘ N	5° 40.78‘ W	552.9
PS93/040-6	13.07.15	17:34	CTD/UW	profile start	77° 15.38‘ N	5° 38.97‘ W	607.9
PS93/040-7	13.07.15	17:40	CTD/UW	profile start	77° 14.56‘ N	5° 36.81‘ W	660.0
PS93/040-8	13.07.15	17:45	CTD/UW	profile start	77° 13.88‘ N	5° 34.97‘ W	714.4
PS93/040-9	13.07.15	17:51	CTD/UW	profile start	77° 13.06‘ N	5° 32.74‘ W	774.7
PS93/040-10	13.07.15	17:56	CTD/UW	profile start	77° 12.37‘ N	5° 30.91‘ W	819.9
PS93/040-11	13.07.15	18:01	CTD/UW	profile start	77° 11.82‘ N	5° 28.54‘ W	869.5
PS93/040-12	13.07.15	18:06	CTD/UW	profile start	77° 11.46‘ N	5° 25.36‘ W	929.8
PS93/040-13	13.07.15	18:11	CTD/UW	profile start	77° 11.10‘ N	5° 22.17‘ W	981.5
PS93/040-14	13.07.15	18:16	CTD/UW	profile start	77° 10.75‘ N	5° 18.99‘ W	1037.4
PS93/040-15	13.07.15	18:22	CTD/UW	profile start	77° 10.31‘ N	5° 15.20‘ W	1101.1
PS93/040-16	13.07.15	18:27	CTD/UW	profile start	77° 9.93‘ N	5° 12.07‘ W	1151.9
PS93/040-17	13.07.15	18:33	CTD/UW	profile start	77° 9.50‘ N	5° 8.27‘ W	1201.5
PS93/040-18	13.07.15	18:38	CTD/UW	profile start	77° 9.14‘ N	5° 5.11‘ W	1246.5
PS93/040-19	13.07.15	18:48	CTD/UW	profile start	77° 8.43‘ N	4° 58.78‘ W	1315.0
PS93/040-20	13.07.15	18:53	CTD/UW	profile start	77° 8.06‘ N	4° 55.66‘ W	1346.7
PS93/040-21	13.07.15	18:59	CTD/UW	profile start	77° 7.61‘ N	4° 51.85‘ W	1379.6
PS93/040-22	13.07.15	19:02	CTD/UW	profile start	77° 7.40‘ N	4° 49.95‘ W	1381.4
PS93/040-23	13.07.15	19:08	CTD/UW	profile start	77° 6.96‘ N	4° 46.17‘ W	1406.0
PS93/040-24	13.07.15	19:12	CTD/UW	profile start	77° 6.67‘ N	4° 43.65‘ W	1460.0
PS93/040-25	13.07.15	19:18	CTD/UW	profile start	77° 6.23‘ N	4° 39.83‘ W	1513.7
PS93/040-26	13.07.15	19:23	CTD/UW	profile start	77° 5.88‘ N	4° 36.66‘ W	1543.7
PS93/040-27	13.07.15	19:28	CTD/UW	profile start	77° 5.52‘ N	4° 33.50‘ W	1573.5
PS93/040-28	13.07.15	19:32	CTD/UW	profile start	77° 5.23‘ N	4° 30.99‘ W	1595.4
PS93/040-29	13.07.15	19:37	CTD/UW	profile start	77° 4.86‘ N	4° 27.87‘ W	1619.2
PS93/040-30	13.07.15	19:42	CTD/UW	profile start	77° 4.49‘ N	4° 24.75‘ W	1643.4
PS93/040-31	13.07.15	19:47	CTD/UW	profile start	77° 4.14‘ N	4° 21.62‘ W	1666.0
PS93/040-32	13.07.15	19:51	CTD/UW	profile start	77° 3.86‘ N	4° 19.11‘ W	1682.2
PS93/040-33	13.07.15	19:56	CTD/UW	profile start	77° 3.50‘ N	4° 15.96‘ W	1707.6
PS93/040-34	13.07.15	20:00	CTD/UW	profile start	77° 3.20‘ N	4° 13.46‘ W	1724.0
PS93/040-35	13.07.15	20:05	CTD/UW	profile start	77° 2.84‘ N	4° 10.30‘ W	1740.6
PS93/040-36	13.07.15	20:12	CTD/UW	profile start	77° 2.31‘ N	4° 5.86‘ W	1771.2

Station	Date	Time	Gear	Action	PositionLat	PositionLon	Depth [m]
PS93/040-37	13.07.15	20:17	CTD/UW	profile start	77° 1.94‘ N	4° 2.69‘ W	1788.1
PS93/040-38	13.07.15	20:22	CTD/UW	profile start	77° 1.58‘ N	3° 59.54‘ W	1804.0
PS93/040-39	13.07.15	20:27	CTD/UW	profile start	77° 1.24‘ N	3° 56.33‘ W	1819.7
PS93/040-40	13.07.15	20:32	CTD/UW	profile start	77° 0.85‘ N	3° 53.23‘ W	1838.2
PS93/040-41	13.07.15	20:41	CTD/UW	profile start	77° 0.21‘ N	3° 47.47‘ W	1860.0
PS93/040-42	13.07.15	20:46	CTD/UW	profile start	76° 59.81‘ N	3° 44.29‘ W	1875.8
PS93/040-43	13.07.15	20:51	CTD/UW	profile start	76° 59.44‘ N	3° 41.07‘ W	1887.3
PS93/040-44	13.07.15	20:55	CTD/UW	profile start	76° 59.13‘ N	3° 38.50‘ W	1868.9
PS93/041-1	13.07.15	22:07	GKG	on ground/ max depth	76° 57.79‘ N	3° 26.85‘ W	1768.3
PS93/041-2	13.07.15	23:44	MUC	on ground/ max depth	76° 57.81‘ N	3° 26.94‘ W	1746.8
PS93/041-3	14.07.15	01:15	GC	on ground/ max depth	76° 57.81‘ N	3° 26.92‘ W	1718.3
PS93/042-4	14.07.15	11:20	ZODIAK	on ground/ max depth	75° 44.39‘ N	3° 9.00‘ W	3612.2
PS93/042-1	14.07.15	11:39	GKG	on ground/ max depth	75° 44.39‘ N	3° 9.05‘ W	3625.8
PS93/042-3	14.07.15	12:30	ZODIAK	on ground/ max depth	75° 44.40‘ N	3° 9.05‘ W	3467.9
PS93/042-2	14.07.15	14:00	GC	on ground/ max depth	75° 44.39‘ N	3° 9.03‘ W	3622.3
PS93/043-1	14.07.15	16:40	GC	on ground/ max depth	75° 40.20‘ N	3° 16.32‘ W	3614.3
PS93/043-2	14.07.15	18:07	ZODIAK	on ground/ max depth	75° 40.17‘ N	3° 16.29‘ W	3616.2
PS93/043-3	14.07.15	18:50	FLOAT	on ground/ max depth	75° 40.27‘ N	3° 16.11‘ W	3614.7
PS93/044-1	14.07.15	20:14	GC	on ground/ max depth	75° 39.48‘ N	3° 31.52‘ W	3605.8
PS93/044-2	14.07.15	21:24	FLOAT	on ground/ max depth	75° 39.54‘ N	3° 32.07‘ W	3611.1
PS93/045-1	14.07.15	21:29	CTD/UW	profile start	75° 39.87‘ N	3° 33.72‘ W	3603.9
PS93/045-2	14.07.15	21:37	CTD/UW	profile start	75° 40.50‘ N	3° 38.10‘ W	3594.5
PS93/045-3	14.07.15	21:43	CTD/UW	profile start	75° 41.02‘ N	3° 41.34‘ W	3588.8
PS93/045-4	14.07.15	21:50	CTD/UW	profile start	75° 41.59‘ N	3° 45.25‘ W	3582.4
PS93/045-5	14.07.15	21:57	CTD/UW	profile start	75° 42.20‘ N	3° 49.09‘ W	3576.1
PS93/045-6	14.07.15	22:04	CTD/UW	profile start	75° 42.77‘ N	3° 53.01‘ W	3567.7
PS93/045-7	14.07.15	22:10	CTD/UW	profile start	75° 43.29‘ N	3° 56.30‘ W	3568.4
PS93/045-7	14.07.15	22:16	CTD/UW	profile start	75° 43.81‘ N	3° 59.63‘ W	3548.6
PS93/045-8	14.07.15	22:23	CTD/UW	profile start	75° 44.34‘ N	4° 3.63‘ W	3535.1
PS93/045-9	14.07.15	22:29	CTD/UW	profile start	75° 44.63‘ N	4° 7.40‘ W	3522.4
PS93/045-10	14.07.15	22:38	CTD/UW	profile start	75° 45.06‘ N	4° 13.03‘ W	3502.5

Station	Date	Time	Gear	Action	PositionLat	PositionLon	Depth [m]
PS93/045-11	14.07.15	22:44	CTD/UW	profile start	75° 45.32‘ N	4° 16.80‘ W	3487.2
PS93/045-12	14.07.15	22:50	CTD/UW	profile start	75° 45.62‘ N	4° 20.57‘ W	3473.1
PS93/045-13	14.07.15	22:57	CTD/UW	profile start	75° 45.97‘ N	4° 25.00‘ W	3457.1
PS93/045-14	14.07.15	23:03	CTD/UW	profile start	75° 46.24‘ N	4° 28.82‘ W	3443.8
PS93/045-15	14.07.15	23:10	CTD/UW	profile start	75° 46.59‘ N	4° 33.22‘ W	3422.5
PS93/045-16	14.07.15	23:16	CTD/UW	profile start	75° 46.88‘ N	4° 36.98‘ W	3404.4
PS93/045-17	14.07.15	23:21	CTD/UW	profile start	75° 47.12‘ N	4° 40.14‘ W	3432.1
PS93/045-17	14.07.15	23:24	CTD/UW	alter course	75° 47.26‘ N	4° 42.03‘ W	3403.9
PS93/045-18	14.07.15	23:27	CTD/UW	profile start	75° 47.40‘ N	4° 43.92‘ W	3388.6
PS93/045-19	14.07.15	23:34	CTD/UW	profile start	75° 47.84‘ N	4° 48.16‘ W	3365.5
PS93/045-20	14.07.15	23:39	CTD/UW	profile start	75° 48.15‘ N	4° 51.16‘ W	3349.5
PS93/045-21	14.07.15	23:44	CTD/UW	profile start	75° 48.43‘ N	4° 54.19‘ W	3333
PS93/045-22	14.07.15	23:52	CTD/UW	profile start	75° 48.93‘ N	4° 59.00‘ W	3306.4
PS93/045-23	15.07.15	00:05	CTD/UW	profile start	75° 49.71‘ N	5° 6.93‘ W	3253.4
PS93/045-24	15.07.15	00:10	CTD/UW	profile start	75° 50.01‘ N	5° 10.01‘ W	3231.9
PS93/045-25	15.07.15	00:16	CTD/UW	profile start	75° 50.40‘ N	5° 13.71‘ W	3200.8
PS93/045-26	15.07.15	00:22	CTD/UW	profile start	75° 50.77‘ N	5° 17.44‘ W	3180.9
PS93/045-27	15.07.15	00:29	CTD/UW	profile start	75° 51.20‘ N	5° 21.75‘ W	3175.8
PS93/045-28	15.07.15	00:49	CTD/UW	profile start	75° 52.41‘ N	5° 34.18‘ W	3106.2
PS93/045-29	15.07.15	00:54	CTD/UW	profile start	75° 52.74‘ N	5° 37.27‘ W	3087.9
PS93/045-30	15.07.15	00:59	CTD/UW	profile start	75° 53.05‘ N	5° 40.38‘ W	3017.9
PS93/045-31	15.07.15	01:12	CTD/UW	profile start	75° 53.85‘ N	5° 48.52‘ W	3023.4
PS93/045-32	15.07.15	01:17	CTD/UW	profile start	75° 54.17‘ N	5° 51.60‘ W	3030.7
PS93/045-33	15.07.15	01:23	CTD/UW	profile start	75° 54.52‘ N	5° 55.35‘ W	3006
PS93/045-34	15.07.15	01:28	CTD/UW	profile start	75° 54.84‘ N	5° 58.45‘ W	2971.2
PS93/045-35	15.07.15	01:34	CTD/UW	profile start	75° 55.22‘ N	6° 2.16‘ W	2915.8
PS93/045-36	15.07.15	01:39	CTD/UW	profile start	75° 55.53‘ N	6° 5.26‘ W	2917.8
PS93/045-37	15.07.15	01:44	CTD/UW	profile start	75° 55.83‘ N	6° 8.41‘ W	2898.2
PS93/045-37	15.07.15	01:45	CTD/UW	alter course	75° 55.89‘ N	6° 9.04‘ W	2892.3
PS93/045-38	15.07.15	01:49	CTD/UW	profile start	75° 56.18‘ N	6° 11.45‘ W	2877.4
PS93/046-1	15.07.15	04:19	CTD/RO	on ground/ max depth	76° 5.11‘ N	6° 48.71‘ W	2456.1
PS93/046-2	15.07.15	06:03	MN	on ground/ max depth	76° 5.10‘ N	6° 48.71‘ W	2456
PS93/046-3	15.07.15	07:18	GKG	on ground/ max depth	76° 5.08‘ N	6° 48.72‘ W	2457.2
PS93/046-4	15.07.15	09:17	MUC	on ground/ max depth	76° 5.10‘ N	6° 48.76‘ W	2457.9
PS93/046-5	15.07.15	11:07	GC	on ground/ max depth	76° 4.33‘ N	6° 49.07‘ W	2461.7
PS93/047-1	15.07.15	13:27	HS_PS	profile start	76° 4.82‘ N	6° 48.22‘ W	2464.2

Station	Date	Time	Gear	Action	PositionLat	PositionLon	Depth [m]
PS93/047-1	15.07.15	14:12	HS_PS	alter course	76° 6.42‘ N	6° 18.66‘ W	2672.9
PS93/047-1	15.07.15	16:04	HS_PS	alter course	75° 58.93‘ N	4° 53.43‘ W	3212.1
PS93/047-1	15.07.15	17:33	HS_PS	alter course	75° 52.78‘ N	3° 38.65‘ W	3530.1
PS93/047-1	15.07.15	18:59	HS_PS	alter course	75° 35.66‘ N	3° 8.80‘ W	3638.8
PS93/047-1	15.07.15	20:52	HS_PS	alter course	75° 13.79‘ N	2° 46.76‘ W	3642.4
PS93/047-1	15.07.15	21:21	HS_PS	alter course	75° 16.98‘ N	2° 30.56‘ W	3654.1
PS93/047-1	15.07.15	23:00	HS_PS	alter course	75° 36.32‘ N	2° 44.23‘ W	3650.4
PS93/047-1	15.07.15	23:28	HS_PS	alter course	75° 37.81‘ N	2° 23.41‘ W	3666.3
PS93/047-1	16.07.15	00:54	HS_PS	profile end	75° 21.19‘ N	2° 13.51‘ W	3665.2